ISTANBUL TECHNICAL UNIVERSITY ★ GRADUATE SCHOOL OF SCIENCE ENGINEERING AND TECHNOLOGY

A NEW APPROACH FOR ESTIMATING THE GEOTHERMAL GRADIENT AND DEEP SUBSURFACE TEMPERATURE DISTRIBUTION IN TURKEY

M.Sc. THESIS

Daniel Nlimah NJOLNBI

Department of Petroleum and Natural Gas Engineering

Petroleum and Natural Gas Engineering Programme

JANUARY 2015

ISTANBUL TECHNICAL UNIVERSITY ★ GRADUATE SCHOOL OF SCIENCE ENGINEERING AND TECHNOLOGY

A NEW APPROACH FOR ESTIMATING THE GEOTHERMAL GRADIENT AND DEEP SUBSURFACE TEMPERATURE DISTRIBUTION IN TURKEY

M.Sc. THESIS

Daniel Nlimah NJOLNBI
(505111504)

Department of Petroleum and Natural Gas Engineering

Petroleum and Natural Gas Engineering Programme

Thesis Advisor: Asst. Prof. Dr. İbrahim Metin MIHÇAKAN

JANUARY 2015

Daniel Nlimah NJOLNBI, a **M.Sc.** student of ITU **Graduate School of Science Engineering and Technology** student ID **505111504**, successfully defended the **thesis** entitled **"A NEW APPROACH FOR ESTIMATING THE GEOTHERMAL GRADIENT AND DEEP SUBSURFACE TEMPERATURE DISTRIBUTION IN TURKEY"**, which he prepared after fulfilling the requirements specified in the associated legislations, before the jury whose signatures are below.

Thesis Advisor :	**Asst. Prof. Dr. İbrahim Metin MIHÇAKAN** İstanbul Technical University	.....
Jury Members :	**Prof. Dr. Abdurrahman SATMAN** İstanbul Technical University	.....
	Asst. Prof. Dr. Halit Tuğrul GENÇ İstanbul Technical University	.....

Date of Submission : 16 December 2014
Date of Defense : 21 January 2015

To my parents and siblings,

FOREWORD

I would like to express my sincerest gratitude to Asst. Prof. Dr. İ. Metin Mıhçakan, my teacher and supervisor, and Asst. Prof. Dr. H. Tuğrul Genç. I have benefited immensely from their great kindness, guidance and motivation accorded me during my studies. For this I say a heartfelt thank you. To my beloved parents, Jacob Njolnbi Tabasun Gaala and Ichiin Kubaja Gaala, I owe a huge dept of gratitude for their invaluable contributions to my life. My special thanks also goes to my siblings and uncles for their unflinching support and words of encouragement during the entire period of my studies.

January 2015 Daniel Nlimah NJOLNBI

TABLE OF CONTENTS

Page

FOREWORD ..... **ix**
ABBREVIATIONS ..... **xiii**
LIST OF TABLES ..... **xv**
LIST OF FIGURES ..... **xvii**
SUMMARY ..... **xix**
1. INTRODUCTION **1**
1.1 Purpose of Thesis 1
1.2 Structure of Thesis 3
2. LITERATURE REVIEW **5**
2.1 Sources of Heat Flow 7
2.2 Heat Flow Mechanisms 12
2.3 Heat Flow Measurement Techniques 13
2.4 Geology of Turkey 16
2.5 Neotectonics of Turkey 23
2.6 Crustal Structure of Turkey 27
2.7 Curie-point Depth and Curie Temperature Estimates in Turkey 30
2.8 Geothermal Potential and Heat Flow Measurement in Turkey 34
2.9 Radiogenic Heat Production in Turkey 38
3. DATA AND TECHNIQUES OF HEAT FLOW GENERATION **41**
3.1 Regeneration of Curie Depth Map of Turkey 41
3.2 Re-evaluation of Deep Well Temperature Measurement Data 43
3.3 Deep-subsurface-thermal Gradient Estimation 47
3.4 Deep-subsurface Temperature Estimation 56
4. DISCUSSION OF THE RESULTS **65**
5. CONCLUSIONS AND FUTURE WORK **67**
REFERENCES **69**
APPENDICES **83**
CURRICULUM VITAE **95**

ABBREVIATIONS

AD : Ağrı Dağı (Mount Ararat)
AL : Alaşehir
AY : Aydın
BZSZ : Bitlis-Zagros suture zone
BHT : Bottom-hole temperatures
CACC : Central Anatolian Crystalline Complex
CPD : Curie-point depth
DOE : (United States) Department of Energy
DST : Drill stem test
DSTFZ : Dead Sea transform fault zone
EAFZ : East Anatolian fault zone
EFZ : Ecemiş fault zone
FBFZ : Fethiye Burdur fault zone
GH : Gümüşhane
GMT : Generic Mapping Tools
GPS : Global Positioning System
HP/LT : high pressure/low temperature
IAES : Izmir-Ankara-Erzincan suture
MM : Menderes Massif
MTA : General Directorate of Mineral Research and Exploration, Turkey
NAFZ : North Anatolian fault zone
TAP : Tauride-Anatolide platform
TGFZ : Tuz Gölü fault zone
SK : Şırnak
USGS : United States Geological Survey

LIST OF TABLES

Page

Table 2. 1: Continental heat flow as a function of surface geology and age. 12
Table 2. 2: Continental and oceanic mean heat flow and global heat loss..... 16
Table 2. 3: Plate motions in the Mediterranean and south-west Asia. 26
Table 2. 4: Motions along faults and deformation zones. 27
Table 2. 5: Moho depth in different parts of Turkey. 29
Table 2. 6: CPD of some areas in Turkey. 33
Table 2. 7: Curie temperature of some lithology or rock samples. 35
Table 2. 8: Curie temperature of some minerals. 36
Table 2. 9: Stored heat beneath Turkey to 10 km depth (Basel et al, 2009, 2010). .. 38
Table 2. 10: Conductivity values of lithology samples in Turkey. 39

LIST OF FIGURES

Page

Figure 2. 1: Tectonic map of Turkey showing major neotectonic structures and provinces (Bozkurt, 2001)..... 24
Figure 3. 1: Curie-point depth map of Turkey (modified after MTA, 2007). 42
Figure 3. 2: Topography map of Turkey (digital elevetion model data taken from the USGS). 44
Figure 3. 3: CPD map of Turkey from ground level (modified after MTA, 2007). 45
Figure 3. 4: Subsurface geothermal gradient map of Turkey to depth of ~5 km (modified after Mıhçakan et al, 2006). 46
Figure 3. 5: Gradient profile analysis of field data. 50
Figure 3. 6: Deep subsurface temperature gradient map of Turkey between depths of ~5 km to ~30 km for a Curie isotherm of 560 ºC. 54
Figure 3. 7: Deep subsurface temperature gradient map of Turkey between depths of ~5 km to ~30 km for a Curie isotherm of 580 ºC. 55
Figure 3. 8: Sample graphs of exponential function. 58
Figure 3. 9: Map of coefficient "a" distribution. 60
Figure 3. 10: Map of coefficient "b" distribution. . 61
Figure 3. 11: Map of deep-subsurface temperature distribution beneath Turkey at 2 km depth. 62
Figure 3. 12: Map of deep-subsurface temperature distribution beneath Turkey at 5 km depth. 63
Figure A. 1: Tectonic map of North-eastern Mediterranean region showing the major sutures and continental blocks (Okay, 2008). 87
Figure A. 2: Distribution of different basement types and accretionary complexes in Turkey (Okay, 2008). 89
Figure B: Curie-point depth map of Turkey (MTA, 2007)..... 93

A NEW APPROACH FOR ESTIMATING THE GEOTHERMAL GRADIENT AND DEEP SUBSURFACE TEMPERATURE DISTRIBUTION IN TURKEY

SUMMARY

A deep subsurface-temperature gradient distribution map of Turkey is generated by a never before applied approach, in which the Curie-Point-Depth (CPD) temperature data and the available deep well temperature measurements across the country are utilized. All the maps in the present work are generated using the Generic Mapping Tools (GMT) software. The CPD values are obtained by digitizing the contours of the Curie-Point Depth Map of Turkey, published by the MTA (General Directorate of Mineral Research and Exploration), Turkey. The contour digitization is performed with the 500-meter intervals between the depths from 6000 to 27500 meters, below the reference of MSL (mean sea level). In this study, the Curie isotherm of 560 ºC at CPDs, where crustal rocks lose permanent magnetization, is assumed beneath Turkey.

The CPD data and its subsequent contours from the ground level (GL) are obtained by combining the digitized CPD data and the surface topography data of Turkey, the latter of which is above the reference of MSL. The exact coordinates for CPDs that correspond to those for the deep wells, for which the temperature data are available, are determined using the GMT software. Then, the depth interval and temperature difference for each pair of CPD and deep-well are used to calculate the subsurface temperature gradient at the coordinate of each pair. Subsequently, the temperature gradient data are mapped and the deep subsurface-temperature gradient distribution map of Turkey is generated. Since, the Curie isotherm of 580 ºC is also considered for the continents by some researchers in the literature, another deep subsurface gradient distribution map of Turkey is also generated based on the Curie isotherm of 580 ºC. In between the both maps a detectable or significant difference is not observed.

If the deep subsurface temperatures are assumed to vary linearly with depth, the estimates of deep-subsurface-temperature gradients are found to be in between 2.28 to 11.10 °C/100m, based on the Curie isotherm of 560 °C, and are found to be in between 2.37 to 11.56 °C/100m, based on the Curie isotherm of 580 °C. The highest values of the deep-subsurface-temperature gradient are concentrated in the area between Mardin and Şırnak, in the Southeastern region of Turkey. On the other hand, the lowest values of the deep-subsurface-temperature gradient are located in the area of Şebinkarahisar, Reşadiye, Alurca and Gümüşhane, in the eastern Pontides Mountain regions. The highest value of the deep-subsurface-temperature gradient in the Western Anatolia is about 8.33 ºC/100 m in the area around Alaşehir, Baklacı, Akkeçili and Erenköy.

When the variation of the deep subsurface-temperatures from the measurement point in wells to the corresponding CPDs is fit with exponential function, the resultant exponential temperature gradients yielded the estimate of subsurface temperatures

that vary of from 20 to 265 ºC at 2-km depth and that vary of from 40 to 455 ºC at 5-km depth beneath Turkey. Based on the subsurface temperature gradients with exponential behavior, the extensional region of Western Anatolia has the highest subsurface temperature estimates. In Mardin-Şırnak region, however, the subsurface temperatures may be as low as has 58 ºC in average at 2-km depth and may go up to 193 ºC in average at 5-km depth. At an average depth of 7654 meters in this region, the subsurface temperature is expected to reach 560 ºC. Thus it may be said that the Mardin-Şırnak area has low temperatures to depths of about 4 km but experiences a high gradient change at depths beyond about 5 km.

A very important feature of the deep subsurface temperature gradient and the subsurface temperature distribution maps is the indication of potential hot dry rock resources in the active extensional province of Western Anatolian, portions of Central Turkey, Southeastern region of Turkey, and the Central Pontic belts of the NAFZ (North Anatolian Fault Zone). These resources may also lie within reach (at about 5 km depth in Western Anatolia and Central Turkey) of the current drilling technology and could be exploited to augment the energy budget of the country if the enhanced geothermal systems (EGS) technology is given serious attention.

TÜRKİYE DERİN YERALTI SICAKLIĞI VE SICAKLIK GRADYANI DAĞILIMININ BELİRLENMESİNE YENİ BİR YAKLAŞIM

ÖZET

Türkiye'nin derin yeraltı sıcaklık gradyanı dağılımı haritası daha önce uygulanmamış ve Curie Noktası Derinliği (CND) Sıcaklığı verileri ile elde bulunan derin kuyu sıcaklık ölçümlerinin kullanıldığı bir yaklaşımla türetilmiştir. Bu çalışmadaki tüm haritalar Generic Mapping Tools (GMT) yazılımı kullanılarak oluşturulmuşlardır. CND değerleri MTA (Maden Tetkik ve Arama) Genel Müdürlüğü'nün yayınlamış olduğu Türkiye Curie Noktası Derinliği Haritası eş-derinlik konturlarının sayısal hale getirilmesi ile elde edilmiştir. Konturların sayısallaştırılması, ODD (Ortalama Deniz Düzeyi) baz alınmak üzere, 6000 metre ile 27500 metre arası derinlikte ve 500 metre aralıklarla gerçekleştirilmiştir. Yer kabuğunu oluşturan kayaçlarının magnetik özelik kazanmaya başladıkları sıcaklık olarak tanımlanan Curie izoterminin (eşsıcaklığının) bu çalışmada Türkiye altında 560 ºC olduğu varsayılmıştır.

Sayısallaştırılan CND verileri ile, ODD'ni baz alan Türkiye yüzey topoğrafya verileri birleştirilmiştir ve böylece yeryüzü düzeyini (YD) baz alan CND verileri ve bunlara ait konturlar elde edilmiştir. Sıcaklık ölçüm verisi bulunan kuyulara karşılık gelen ve aynı koordinatlarda bulunan CND değerleri, GMT yazılımı yardımı ile kesin olarak saptanmıştır. Sonra, her derin kuyu ve buna karşılık gelen CND çiftinin derinlik ve sıcaklık aralıkları kullanılarak, o çiftin koordinatlarında bulunan derin yeraltı sıcaklık gradyanları hesaplanmıştır. Sonuçta, hesaplanmış sıcaklık gradyanları haritalanarak, Türkiye derin yeraltı sıcaklık gradyanı dağılımı haritası oluşturulmuştur. Yazında bazı araştırmacıların kıtalar için Curie eş-sıcaklığını 580 ºC kabul etmeleri nedeni ile, Türkiye derin yeraltı sıcaklık gradyanı dağılımı haritası 580 ºC Curie sıcaklığı baz alınarak da oluşturulmuştur. Oluşturulan iki harita arasında saptanabilecek veya önemli bir fark görülmemiştir.

Eğer derin yeraltı sıcaklıklarının derinlikle doğrusal değiştiği varsayılırsa, kestirilen derin yeraltı sıcaklık gradyanlarının 560 °C Curie izotermi baz alındığında 2.28 ile 11.10 °C/100m arasında ve 580 °C Curie izotermi baz alındığında ise 2.37 ile 11.56 °C/100m arasında değiştiği bulunmuştur. Derin yeraltı sıcaklık gradyanlarının en yüksek değerleri Türkiye'nin Güneydoğu bölgesinde Mardin ile Şırnak arasındaki alanda yoğunlaşmaktadır. Buna karşılık, derin yeraltı sıcaklık gradyanının en düşük değerleri Doğu Pontid yöresinde Şebinkarahisar, Reşadiye, Alurca ve Gümüşhane'yi kapsayan alandadır. Batı Anadolu'daki en yüksek derin yeraltı sıcaklık gradyanı 8.33 ºC/100 m olup, Alaşehir, Baklacı, Akkeçili ve Erenköy cıvarındadır.

Derin yeraltı sıcaklıklarının kuyulardaki ölçüm derinlikleri ile bunlara karşılık gelen CND arasındaki değişimlerine exponansiyel fonksiyon uyumlandığında, elde edilen exponansiyel sıcaklık gradyanları yeraltı sıcaklıklarının 2-km derinlikte 20 ile 265 ºC arasında ve 5-km derinlikte 40 ile 455 ºC arasında kestirilmesini sağlamışlardır. Yer-altı sıcaklık gradyanlarının exponansiyel davranışlı olması halinde, Batı Anadolu'nun

açılımsal bölgesi en yüksek yeraltı sıcaklık kestirimlerine sahiptir. Buna karşılık, yeraltı sıcaklıkları Mardin-Şırnak bölgesinde 2-km derinlikte ortalama 58 ºC kadar düşük olduğu gibi, 5-km derinlikte ortalama 193 ºC'ye kadar çıkabilmektedir. Bu bölgede ortalama 7654 metre derinlikte, yeraltı sıcaklığının 560 ºC düzeyine erişmesi beklenir. Dolayısı ile, Mardin-Şırnak bölgesinin 4-km derinliğe kadar görece düşük sıcaklıklara ve 5-km derinlik ve ötesinde görece daha yüksek sıcaklıklara yol açan sıcaklık gradyanlarına sahip olduğuı söylenebilir.

Derin yeraltı sıcaklık gradyanı dağılımının ve ısı akışı örüntüsünün çok önemli bir özeliği, Türkiye'nin Güneydoğu ve Batı Anadolu bölgesi ile, Orta Anadolu'nun Tuz Gölü ve Kuzey Anadolu Fayının Orta Pontid kuşağı yöresinde potansiyel sıcak kuru kayaç kaynaklarının varlığına işaret etmesidir. Gelişkin jeotermal sistemlere gerekli ilgi gösterildiği takdirde, bu kaynaklar günümüz teknolojisi ile yapılacak sondajların erişimi içindedir ve ülkenin enerji bütçesini artırmak üzere bunlardan yararlanılabilir.

1. INTRODUCTION

That towards the Earth's interior, temperature increases with depth is a knowledge of antiquity, especially for dwellers in areas replete with volcanoes, hot springs and other thermal phenomena cannot be overemphasized (Pollack, 1982; Beardsmore and Cull, 2001; UNESCO, 2003; Jaupart and Mareschal, 2011). Thus, the relevance and exploitability of this prodigious reservoir of heat only assumed much importance between the sixteenth and nineteenth century following excavations in mines and the subsequent advances in physics regarding the development of the theory of heat conduction and of thermodynamics (UNESCO, 2003; Jaupart and Mareschal 2011). However, in spite of the advances in technology and increased understanding of the internal structure and evolution of the Earth, the manner and means of measuring, assessing and interpreting the Earth's (geo) thermal (heat) flux potential or heat flux data are still poorly understood, even among specialist whose job it is to manipulate such data (Beardsmore and Cull, 2001). By the very nature of heat flux estimation, researchers at various points in time have relied on different approaches and sometimes combining data from varied sources to establish meaningful heat-flux data or construct heat-flux distribution maps. Over the years, there has been tremendous improvement in knowledge and understanding of heat transport in the Earth, however, the availability information on heat flow is still very limited to selected few areas of interest. Economic and technological challenges are the major factors hampering the attainment of very representative and robust heat flow measurements, especially from direct readings in deep boreholes. This has necessitated a combination of the most reliable and other indirect, but scientifically reliable approaches in estimating surface heat flux.

1.1 Purpose of Thesis

In a new approach, the study seeks to establish a toward surface thermal gradient and subsurface temperature distribution using the Curie depth-temperature pair data and temperature data from 318 deep oil and gas wells (carefully selected using gradient

profile analysis from a total of 530 deep oil and gas well temperature measurements). In this research, the Curie depth-temperature pair data is used as the base for the estimation of thermal gradient and consequently, the construction of upward successive subsurface temperature distribution maps at reachable depths and then compare these maps with the deep wells' thermal gradient distribution map and other surface geothermal menifestations.

The study is underpinned by the fact that until such a time that very representative and robust estimates of heat flux distribution is achieved, the need to continuously update previous works and as well explore new techniques of estimating geothermal gradient and subsurface temperature distributions still remains very relevant; especially in geothermally endowed regions. According to Mertoglu et al. (2010), the Alpine-Himalayan orogenic activities, which directly controls the present distribution of the Turkish terranes, holds enormous geothermal potential and Turkey is no exception. The Turkish terranes remains one of the most tectonically active regions of the world and the western part abounds geothermal activities similar to that of the Great Basin of the USA (Basel et al, 2010). This potential places Turkey as the 7th richest geothermally endowed region in the world, with 186 geothermal fields discovered so far by the General Directorate of Mineral Research and Exploration (MTA) and about 1500 hot and mineral water resources which has surface temperatures ranging from 20 $^{\circ}$C to 242 $^{\circ}$C (Mertoglu et al, 2010).

As indicated by Basel et al. (2009), the electricity and energy demands of Turkey increases at about 7.5% and 4.5% per annum, respectively. To be able to exploit these resources (both hydrothermal and hot dry rock) to augment the energy budget of the country, there is the need for a comprehensive deep-subsurface temperature and heat flow study on both regional and countrywide scales. To study heat flow distribution of a given area in the context envisaged, there is the need to correlate surface geothermal manifestations with other deep-seated geophysical features with the aid of deep well temperature measurements. Therefore, to enable this comparison, the construction of deep thermal gradient, subsurface temperature and surface heat-flux distribution maps is necessary to determine hot regions since crustal heat distribution is not uniform. According to DOE (2008), fluids or "water is not nearly ubiquitous in the Earth as heat" and therefore, the natural coincidence of heat, water and permeable rock forming naturally occurring vast hydrothermal systems at

depths less than 5 km is not a common place in the earth. However, geothermal exploitation and heat flux studies is often concentrated on just the focal points of observed surface geological or geophysical manifestations (usually hydrothermal) to the neglect of other potential regions.

For instance, the exploration and development activities in Turkey are focused largely on such hydrothermal resource systems (Basel et al., 2009), without much attention to the hot dry-rock potential. The research therefore, seeks to expand the scope and conduct a study on a national scale, and with a different approach, determine the geothermal gradient distribution and subsurface temperature distribution at different depths beneath Turkey using 318 temperature data points from the deep wells database of Mihcakan et al. (2006), and the Curie depth-temperature pair data (Curie isotherms) digitized from the Curie-depth map of Turkey prepared by MTA (2007).

1.2 Structure of Thesis

The research work is organized into five chapters. The first chapter covers the introduction, purpose and structure of the work. The second chapter contains the literature review on heat flow measurement from general to specifics, with emphasis on the Turkish terranes. Chapter 3 covers a systematic approach to obtaining data and the methodology used in computations. The fourth chapter presents the data analysis and discussions, whereas Chapter 5 covers the findings and conclusions, and future work we intend to carry out in furtherance of deep-subsurface temperature distribution and surface heat-flux update of the Turkish terranes.

2. LITERATURE REVIEW

Heat flux, also commonly referred to as terrestrial heat flow in geophysics literature is a measure of conductive heat flow through the crust since heat loss through the Earth's surface in all but a few regions is mostly by conduction (Artemieva, 2011). In much simpler terms, Pollack (1982) described terrestrial heat flow (heat flux) as "the quantity of heat escaping per unit time from the Earth's interior across each unit area of the Earth's solid surface". According to Fourier (1955), an empirical relationship between the conduction rate in a material and temperature gradient in the direction of energy flow was first formulated by Fourier in 1822. The empirical relation is commonly referred to as Fourier's law. Fourier concluded that "the heat flux, q(W/m^2), resulting from thermal conduction is proportional to the magnitude of the temperature gradient and opposite to it in sign". For an isotropic medium, a generallized three-dimension Fourier's law between heat flux and temperature can be expressed as:

$$q = -\lambda \nabla T = -\lambda \left(\frac{\partial T}{\partial x} + \frac{\partial T}{\partial y} + \frac{\partial T}{\partial z} \right) \qquad \textbf{(2.1)}$$

Where q is heat flux in power per unit area (watts per square meter, W/m^2 or milliwatts per square meter mW/m^2), λ as the thermal conductivity coefficient of the medium, in W/m ºC or W/mK, and T being the temperature distribution function in three dimensions along the axes x, y, and z. One key parameter in equation 2.1 above is the thermal (or geothermal) gradient. Thermal gradient is a physical quantity that expresses the rate of increase in temperature per unit depth in the Earth (UNESCO, 2003). It has units of temperature per unit distance (degrees Kelvin per meters, K/m, or degrees Celsius per meter, ºC/m, or degrees Celsius per kilometer, ºC/km). Both heat flux and thermal gradient are vector quantities having both magnitude and direction. As a vector quantity, thermal gradient is dependent on distribution of temperature in three dimensions. The magnitude and direction or the orientation of maximum thermal gradient are obtained using the following equation.

$$\nabla T = \frac{\partial T}{\partial x}\vec{i} + \frac{\partial T}{\partial y}\vec{j} + \frac{\partial T}{\partial z}\vec{k} \qquad \textbf{(2.2)}$$

Where **i, j**, and **k** are unit vectors along x, y, and z-axes (z is the direction of vertical temperature profile). Conventionally, it is invariably assumed that the direction of maximum gradient in the upper crust is vertical (Beardsmore and Cull, 2001). This assumption is valid if the Earth's surface forms approximately a horizontal, constant temperature boundary, which tends to minimize lateral temperature variations (Beardsmore and Cull, 2001). Thus, the thermal gradient is then expressed in one dimension as

$$\nabla T = \frac{\partial T}{\partial z}\vec{k} \qquad \textbf{(2.3)}$$

Therefore, the surface heat-flow equation also takes the form

$$q = -\lambda \frac{\partial T}{\partial z} \qquad \textbf{(2.4)}$$

and the thermal gradient is defined as

$$\frac{\partial T}{\partial z} \cong \frac{\Delta T}{\Delta Z} = \frac{(T_2 - T_1)}{(Z_2 - Z_1)} \qquad \textbf{(2.5)}$$

Where T_1 and T_2 are temperatures of two points separated by a distance, Δz. As a practice, a positive gradient is in the direction of increasing temperature whereas positive heat flow is in the direction of decreasing temperature, which is the opposite of the gradient and hence the reason for the negative sign in equation (2.4). Down to depth limits accessible by drilling with current drilling technology (over 10 000 m or 10 km), the mean thermal gradient is about 2.5 to 3 K/100m or 30 ºC/km (UNESCO, 2003). Stein (1995), suggest the value of vertical temperature gradient is between an approximate range of 10 to 80 ºC/km. However, no matter the degree of certainty of these global mean values, the use of locally obtained values is the most appropriate for any research. There are areas with thermal gradients lower than 1 K/100m whiles there are other gradient profiles more than 10 times the average value. Thus, at depths of about 3 to 4 km, it would not be strange to find temperatures of about 100ºC (UNESCO, 2003). Another important parameter is the thermal conductivity tensor, a proportionality constant that relates the heat flow vector to the thermal gradient vector. Thermal conductivity is a measure of ease of heat transmission

through a medium. It has units of power per unit distance per unit temperature (W/mK). Thermal conductivity is usually estimated along the same profile that thermal gradient and heat production are known. According to Pollack and Chapman (1977a), there exist adequate experimental data showing temperature dependence of conductivity. Like temperature, thermal conductivity in the Earth varies from point to point because of the heterogeneity of crustal composition. For instance, Stein (1995) gives approximate ranges of 0.6 – 1.2 W/mK and 1 – 5 W/mK for marine sediments and continental sediments, respectively. However, there are instances where approximate mean values have been used as crustal thermal conductivity for modeling thermal effects, calculating heat flux and other important physical changes within the Earth. In stating the properties used in modeling upper mantle temperature calculations, Schatz and Simmon (1972) used a value of 2.5 W/mK for crustal conductivity. Pollack and Chapman (1977a) also used this same value of 2.5 W/mK as thermal conductivity throughout the crust to determine regional geotherms and subsequently the lithospheric thickness. For the Turkish terranes, Tezcan (1979) after obtaining gradient data from four major geothermal provinces settled on a constant thermal conductivity value of 2.1 W/mK of Neogene Clayey formations to generate heat flow data and map. Similarly, Dolmaz et al. (2005) calculated an average thermal conductivity value of 2.127 W/mK for Western Anatolia (based on data from Yemen, 1999).

2.1 Sources of Heat Flow

Generally, sources of crustal heat flow include radiogenic heat production, heat flux from the mantle below (including the lower crust below the enriched radiogenic zone), tectonic setting (for example, history of thermal events and frictional heating along faults, subduction zones, intraplate strain and plate motions) and exothermic metamorphic reaction (Beardsmore and Cull, 2001). However, the dominant sources of heat flow on the continental crust are the radiogenic heat production, tectonic setting and mantle heat flux (Stein, 1995). According to Sclater and Francheteau (1970), continental heat flux is a function of the age of latest thermal activity, its magnitude and the concentration of radioactive elements in the crust. Thus, the contribution of metamorphism to contineantal heat flux is negligible, whereas that of

frictional heating along faults or subduction zones should be evaluated based on the prevailing local environment.

Since the Turkish terranes are seismically active and beset with subduction zones and continental collisions along faulting lines and plate margins (Anatolia, Arabia, Africa, Aegean and Eurasia), the case of shear (or frictional) heating contribution to surface heat flux of the local environment (though beyond the scope of this research) is worth discussing in brief. Although, little or no data exist regarding frictional stress (σ_f) acting along faults and frictional heat (Q_f) generated by slow-creeping fault effect, however, there are data on slip rate (u) of faults and plate motions. One prominent example of such active regions within Turkey is the North Anatolian Fault Zone (NAFZ). Its slip rate according to three separate studies are 24 ± 1 mm/yr, 40 mm/yr and 110 mm/yr by McClusky et al. (2000), McKenzie (1972) and Brune (1968), repectively. According to Beardsmopre and Cull (2001), the frictional heat generated by slow-creeping fault and dissipated into the surrounding rocks as heat is proportional to the distance from top to bottom of fault (d), rate of slip and frictional stress along fault. A mathematical expression for this relationship is given below.

$$Q_f = d \times u \times \sigma_f \qquad \textbf{(2.6)}$$

In search of heat flow anomaly over San Andreas Fault, California, Brune et al. (1969) modelled the fault as a vertical plane 20 km ($d = 2 \times 10^4$ m) high with a slip rate of 50 mm/yr (u = 5 cm/yr = 1.58×10^{-9} m/s). They investigated different stress models including depth-constant and and depth-varying stress and then determined the theoretical surface heat flow anomaly for each model. The results indicated no heat flow anomaly over the fault. A heat flux anomaly of about 12.56 mW/m^2 (0.3 μcal/s-cm^2) or more will be generated by a steady-state creep of 5 cm/yr at a stress of about 100 bars (10 MPa). Brune et al. (1969) concluded that the average shear stress must be less than 10 MPa. Drawing from the study, equation (2.6) indicates that a fault may only cause significant changes on surface heat flow if either the slip-rate is > 10 cm/yr or shear stress is > 20 MPa (Beardsmore and Cull, 2001). The debate over heat generation by faulting activities on nearby regions remain inconclusive. In the the case of the NAFZ, there is no much study undertaken in this regard, but the regions of the NAFZ is regarded as one of the areas with great geothermal potential (Basel et al, 2010; Mertoglu et al, 2010).

Although sources of surface heat flux must be evaluated based on each local terrane, but, in general, radiogenic sources are dominant (Beardsmore and Cull, 2001). The natural abundance of the radioactive elements of uranium (U), thorium (Th) and potassium (K) in a rock determines the level of radiogenic heat production. According to Malamud and Turcotte (1999), radiogenic heat production within the crust and mantle account for 80% of the heat source and 20% due to circular cooling of the Earth (primordial heat – including latent heat from solidification of the core and magmatic intrusions). It is estimated that 98% of the geothermal radiogenic heat originates from the decay of single isotopes of ^{238}U, ^{232}Th and ^{40}K. Other uranium isotopes of ^{235}U (0.74%) and ^{234}U (0.01%) have very minimal contribution due to their short half-lives and limited natural abundance (Beardsmore and Cull, 2001; Pasquale et al, 2014). Research has shown that rocks of the continental crust are by far the most naturally enriched, in terms of heat-producing radioactive isotopes. A work by Pollack and Chapman (1977b), with limited surface heat-flux data then, modelled heat flux from the mantle at the crust-mantle boundary and then compared the two. The mantle heat flux showed a marked contrast between continents and oceans, which did not appear same in surface heat flux. The near equality in average continental and oceanic surface heat flux (continents, 53 mW/m^2; oceans, 62 mW/m^2) is altered to a higher contrast in the mantle heat flux (continents, 28 mW/m^2; oceans, 57 mW/m^2). The contrast is attributed to the continental crust being both thicker and more radioactive than the oceanic crust. The continents contain sialic or more silica rich rocks (known to have high heat production) than the simatic rocks underlying the ocean floors (Kennedy, 1959). On a continental scale, the mean crustal heat production is between 0.79 – 0.95 $\mu W/m^3$, representing 32 – 38 mW/m^2 of surface heat flux. The value from published literature vary by a factor > 2 between 0.55 $\mu W/m^3$ and 1.31 $\mu W/m^3$ (Jaupart and Mareschal, 2003). The upper crust, which has a high and more variable heat generation, is usually assigned a mean value between 2 – 3 $\mu W/m^3$ whiles the lower crust between 0.2 – 0.6 $\mu W/m^3$ as observed in the literature of continental heat production models (for example, Pollack and Chapman, 1977a, 1977b, and Drury, 1989).

The enrichment of the crust with U, Th, K and other depleted radiogenic elements is supposed to have occurred by differentiation during the Earth's formative years. Just as the continental rocks differentiation from the underlying mantle, so were the

isotopes selectively removed from the mantle and concentrated in the crust by magnetism (Sclater and Francheteau, 1970). Attempts at estimating crustal heat generation led to the development of an empirical linear relationship between the local surface heat-flux (Q) and local crustal heat generation (A_o). The proponents, Lacherbruch (1968) and Birch et al. (1968) defined the relationship of heat flow province as follows.

$$Q = q_r + A_o D \qquad \textbf{(2.7)}$$

Where D is the depth scale related to the vertical distribution of the radiogenic enriched layer of the crust, and q_r is called the reduced heat flux, representing the heat contribution from the mantle and crust below the enriched zone. The concept of heat flow province refers to "a region of common tectonothermal history within which consistent values of q_r and D are obtained" (Beardsmore and Cull, 2001). The relationship partitions the observed surface heat flux, with 40% attributed to the upper crustal radiogenic source and 60% from deeper mantle and lower crust (Pollack and Chapman, 1977a; Vitorello and Pollack, 1980). The trend revealed by heat flow – heat production relationship indicates a decrease in crustal heat radioactivity (heat production) with depth. However, some researchers have vigorously challenged this proposal. For instance, Jaupart et al. (2007), and Jaupart and Mareschal (2003) argues that measurement of heat production in super deep boreholes (for example, the German Continental Deep Drilling – KTB, Kola and Russia) does not show that the concentration of heat sources systematically decrease with depth as expected by the linear relationship. They state that at KTB, heat production actually decreases with depth at shallow levels, reaches a minimum between 3 – 8 km and then increases again for the deepest part of the borehole. They concluded that with enough data, such relation might only hold for areas of exposed plutons enriched with radioactive elemenets, and that the vertical distribution of heat production of the entire Earth cannot be described by a single universal function within a province. From published literature, the thickness of the crustal radiogenic zone estaimated from the linear relationship is within 7 – 15 km with very few cases outside this range. A 10 km approximate depth dominates the literetaure as an average value. The pioneering work of Roy et al. (1968) estimates indicate a 7 – 11 km range. However, Drury (1989) gives the range as 10 to 15 km.

Generally, younger or recently active regions (during the past 200 Ma) exhibit higher heat flux than stable continental regions (ages greater than 500 Ma). Stable continental regions have surface heat flux ≤ 55 mW/m^2, arising mostly from crustal heat production. The value is in between 30 – 40 mW/m^2 in continental shields (Jaupart et al, 2007; Pasquale et al, 2014). According to Sclater et al. (1980), mean heat flow decreases from a value of 77 mW/m^2 for the youngest province to a constant value of about 46 mW/m^2 (1.1 μcal $cm^{-2}s^{-1}$) after 800 Ma. Recently active or active region such as compressional orogens, continental margins and zones of extension are not in thermal steady state. These regions are characterized by higher heat flow than the continental average. In compressional orogens, e.g., in the Eastern part of the over thrust belt in Southeastern Turkey, an extensional shortening could cause crustal and lithospheric thickening, so that the subsequent reduction in heat flow and temperature gradient are compensated for the presence of total heat content in the resultant thick crust. The interplay of these two competing effects may lead to a complex transient thermal structure with heat flux in some cases > 100 mW/m^2 (Janpart et al, 2007). In transient regimes such as zones of extension (the case of N-S extension in Western Turkey), surface heat flux exceeds 75 mW/m^2 with an average of about 105 mW/m^2. The contribution includes crustal radioactivity source of about 30 mW/m^2 and the mantle in transient component (Jaupart et al, 2007). Thin crust at margins of continents are also points of higher heat flow. Mean surface heat flux in these regions is about 80 mW/m^2. On oceanic scale, heat flux in older oceanic floors (> 80 Ma) is approximetly 48 ± 3 mW/m^2 and > 150 mW/m^2 in the youngest floors, and the heat contribution from these regions (younger seafloors) dominates the oceanic heat flow (Pasquale et al, 2014).

Whether the heat source is radiogenic, tectonic or as a result of circular cooling (of the core and magmatic emplacement), the decay of heat flow is a function of age. Literature credits Kraskovski (1961), Lee and Uyede (1965) and Polyak and Smirnov (1968) with the delineation of heat flow with age. The time scale for the thermal decay of heat flux differ in continents and oceans. It takes billion of years for continents to reach a constant value of 41.87 mW/m^2 (1.00 μ cal cm^{-2} s^{-1}), whereas the oceans after 100 Ma reach a constant value of about 46.05 mW/m^2 or 1.1 μ cal cm^{-2} s^{-1} (Slater and Francheteau, 1970). In Table 2.1 shows the relationship between age and heat flow.

Table 2. 1: Continental heat flow as a function of surface geology and age**.**

Description	No. Data	Area of the Earth, %	Age (Ma)	Mean heat flux [mW/m^2]
Undifferentiated subaqueous	295	9.1		77.7 ± 53.6
Cenozoic: igneous	3705	1.1	0 – 65	97.0 ± 66.9
sed & met [a]	2912	8.1	0 – 65	63.9 ± 27.5
Mesozoic: igneous	1591	1.6	65 – 251	64.2 ± 28.8
sed & met	1359	4.5	65 – 251	63.7 ± 28.2
Paleozoic: igneous	1810	0.4	251 – 545	57.7 ± 20.5
sed & met	403	5.9	251 – 545	61.0 ± 30.2
Proterozoic	260	6.2	545 – 2500	58.3 ± 23.6
Archean	963	2.5	2500 - 3800	51.5 ± 25.6

[a] sed – sedimentary, met – metamorphic. Source: Pollack et al. (1993).

2.2 Heat Flow Mechanisms

Within the Earth, all heat transfer mechanisms, conduction, convection, advection (forced convection) and radiation play various roles at different depths. However, the influence of heat transfer by radiation (heat transfer in a vacuum) within the solid Earth is minor or the heating effect is limited to few meters from the surface. The magnitude and depth of perturbation is dependent on the magnitude and duration of surface temperature changes. For this reason, it is important that the depth of measurement be greater than 300 meters for continental regions (Stein, 1995). Principally, heat transfer from interior to the surface of the Earth is by the interplay of conduction, convection and advection. Conduction is the transfer of heat from a region of higher to one of lower temperature in a continuous object or materials in direct contact with each other due to the exchange of energy by adjacent molecules. Heat flow to the surface of the Earth is primarily by convection in the mantle, conduction dominating in the crust and a combination of these three processes at near-surface or in the lower crust (Artemieva, 2011; Jaupart and Mareschal 2011; Beardsmore and Cull, 2001; Zhao et al, 2008). It is worth noting that the role of convection (free convection or temperature gradient convection) and advection (heat transport by a moving mass of fluid or rock during deformation) is of little effect on a lithospheric scale but of great importance at shallow environments where heat flux measurements are taken (Jaupart and Mareschal, 2011; Zhao et al, 2008). For instance, in localized measurements, heat transport by advection is crucial especially in volcanic regions, mid-ocean ridges and regions of hydraulic crustal permeability

such as sedimentary basins whereas free convection due to water circulation in the oceanic crust can also not be neglected (Artemieva, 2011). Therefore, heat transfer by advection as described in the context above refers to the contribution of pore-fluid pressure gradient driven flow to heat flux, whiles convection refers to the contribution of pore-fluid buoyancy driven flow to heat flux in a fluid-saturated porous medium (Zhoa et al, 2008).

The contribution of convective and/or advective processes as observed is very pronounced in marine heat flow measurements. Stein and Stein (1994) demonstrated that the significant discrepancy between predicted and observed average heat fluxes (from 0 -70 Ma) by cooling plate models is due to hydrothermal heat flux. They concluded that on a global scale, the cumulative effect of hydrothermal heat flux increases steadily until a sealing age of 65 ± 10Ma. That is, where the observed and predicted heat fluxes are approximately equal. Stein and Stein (1994) attributed the decrease in hydrothermal heat flux largely to aging of the crust with consequential reduction in crustal porosity and permeability, and to a lesser extent, the effect of covering by sedimentation (about 150-200 meters as proposed by Anderson and Hobart, 1976).

2.3 Heat Flow Measurement Techniques

Geothermal flux or heat flux determination is fraught with many difficulties. The investigations involve answering many geoscience questions, spanning from the physical state of the Earth, tectonics, seismicity and volcanism to practical issues in drilling, geothermal resources and techniques used in geothermal exploration, mining and environmental geophysics (Schön, 1998). In carrying out heat flow measurements, data often sought after include sub-surface temperature, geothermal gradient, thermal conductivity, thermal diffusivity, heat capacity, specific/relative heat capacity, and heat generation. Geothermal flux may be conceived as a sum of three main components; heat generated by radioactive isotopes in the lithosphere, transient component controlled by tectonothermal processes and heat flow from the asthenosphere (Pasquale et al, 2014). Thus, heat flow estimation also requires the knowledge of some physical parameters and thermal activities beyond direct measurement. Limitation to local and global heat flow measurement (economics, technology, and accessibility) has led to the use of different models based on

observations and data from few direct measurements and indirect geological and petrological arguments.

The conduction theory is the bases of models to the base of the lithosphere. The steady-state conduction and the transient cooling or conductive cooling models are used for the continental and oceanic lithospheres, respectively. On a global scale, the use of models fairly achieve representativeness, especially for inaccessible terrains of Antarctica, Greenland, South America, large areas of Africa and high-latitude oceans where there are inadequate direct measurements. The scientific modelling approach takes into cognizance the geology, age, heat generation, tectonic activities and the interaction of heat transport mechanisms among other factors in achieving representative estimates. The essence of representativeness in heat-flux data is specifically important when stating heat flux as mean values on regional or global scale. For instance, continental heat flux averaged over $1^o \times 1^o$ windows yielded a mean of 65.3 mW/m^2, whereas taking out the USA values reduced the mean to 61.1 mW/m^2 (Jaupart et al, 2007). For robust heat-flux estimates, one hurdle to overcome is reliable temperature data or thermal gradient. There are direct and indirect ways of obtaining temperature data. Temperature data from different wells are used to confirm the validity of each other and are projected into a single well to obtain a common thermal profile for a particular field, where these wells are located.

Although the technique used may be based on the nature of the research in question, but data sources for heat flow estimation is ranked on the order of decreasing accuracy, with data from the least accurate technique given lowest priority. As expected, direct temperature measurement techniques are preferred to indirect approaches. However, some indirect approaches are proven to give as much as accurate temperature estimates just as using direct techniques. This is especially necessary in cases where temperature values beyond 10 km depths are needed (depth at which current drilling technology barely reach). The following are both direct and indirect techniques used in obtaining temperature data for heat flux estimation.

i. Direct techniques

- Precision temperature logs
- Drill stem tests
- Corrected bottom-hole temperatures (BHTs)

ii. Indirect techniques

- Ground water geochemistry
- Curie point
- Mantle resistivity temperature correlation
- Xenolith equilibrium point

For the purposes of this research, only the techniques (temperature logs and Curie point) by which data has been obtained for this research shall be discussed (see Sections 2.7 and 3.2). For most direct techniques, often relied on, as the primary source of data for heat flow estimations, data obtained from the fields is generally bedeviled with deviations in measurement from the actual values. There is the need for correction or removal of such effects before the data can be used. Some local factors that may cause deviations in actual temperature values include the following.

i. Water circulation (near-surface hydrothermal circulation)

ii. Sedimentation

iii. Erosion

iv. Topography or relief

v. Climate variability or near-surface temperature perturbations

vi. Borehole inclination

vii. Variations in radioactive heat production (negligible for terrains > 50 Ma – reaches a steady-state or when measurement is over hundreds of meters)

From published literature (including data from observed and conductive models), refined estimates of average continental heat flux is between 55 – 66 mW/m^2. For instance, after compiling heat flow measurements from 24 774 observation points at 20 201 sites. Pollack et al. (1993) estimated mean heat flows from the continents and oceans as 65 and 101 mW/m^2, respectively. Weighting the data areally yield a global mean of 87 mW/m^2 or a global heat loss of 44.2 TW. The estimates indicate a heat loss of 70% from the oceans and 30% from the continents. In Table 2.2 below are averages of continental and oceanic heat-flux estimates on a global scale.

Table 2. 2: Continental and oceanic mean heat flow and global heat loss.

Reference	Heat Flux, mW/m^2			Global Heat Loss, TW
	Continental	Oceanic	Global	
WVH [1974]*	61	93	84	42.7
Davies [1980]	55 ± 5	95 ± 10	80 ± 8	41 ± 4
Sclater et al. [1980]	57	99	82	42.0
Pollack et al. [1993]	65 ± 1.6	101 ± 2.2	87 ± 2	44.2 ± 1
Jaupart et al. [2007]	65	94		46.0
Davıes & Davies [2010]	70.9	105.4	91.6	46.7

* WVH – Williams and von Herzen

2.4 Geology of Turkey

Anatolian geocientists regard the landmass of Turkey (Asia Minor) as a complex and fascinnating geological puzzle. Anatolia is viwed as a superb natural laboratory for the study of obduction, ophiolite obduction, continent-continent collision, metamorphism, the relationship between lithospheric deformation and magmatism, post-collisional intra-continental convergence and tectonic escape-related deformations and the consequent structures thereof (Bozkurt and Mittwede, 2001). A geologic event, known as the Alpide (or Alpine) orogeny or the Alps, considered the last major orogenic event related to the closure of the Neotethyan branches, is said to have directly influenced the present day distribution of the Turkish terranes (Goncuoglu, 2010). Thus, the geological framework of Turkey is a mosaic of several terranes or continenetal fragments that were derived from the megacontinental margins and oceanic fragments and then almagated in the Late Crataceous-Tertiary period during the Alpide orogeny (Sengor and Yilmaz, 1981; Okay and Tuysuz, 1999; Bozkurt and Mittwede, 2001; Moix et al, 2008; Okay, 2008; Goncuoglu, 2010). The landmass of Turkey (presently situated within the Alpine-Himalayan orogenic belt near the Arabian-African-Eurasian plates junction) was once situated at the collision boundary of two megacontinents – Gondwana in the south and Laurasia in the North. The Turkish landmass has been divided into many units based on particular geologic interest. One of such early divisions based on orogeny or geography was conducted by Ketin (1966). These divisions include the Pontides (Laurasian realm), the Anatolides, the Taurides and the Border folds (Gondwana realm). Other ealier divisions of the orogeny of Anatolia and its tectonic units include works by Arni (1939), Blumenthal (1946), Ergeran (1947) and many others.

Recent geologic divisions have been made by Okay and Tuysuz (1999), Bozkurt and Mittwede (2001), Okay (2008), Miox et al. (2008) and Goncuoglu (2010) based on the concept of plate tectonics and on the paleogeographic framework of five major Neotethyan suture zones (Izmir-Ankara-Erzincan or IAE, Intra-Pontide, Inner Tauride, Antalya and Southeast Anatolian) that are marked by complete or partial ophiolite complexes and ophiolitic melanges. These new divisions gives detailed geologic discriptions of the microcontinental blocks, sutures and their respective lithologies. Based on these divisions, a careful delineation of sutures (boundaries of former lithospheric plates) indicates the landmass of Turkey consist of six major lithospheric fragments: the Strandja/Stranca zone, the Istanbul and Sarkaya zones, the Anatolide-Tauride block, the Kirsehir Massif and the Arabian platform (Sengor and Yilmaz, 1981; Okay and Tuysuz, 1999). These fragments are further regrouped into three main geologic-tectonic units. The first three zones, which show Laurasian affinities are classically reffered to as the Pontides, whereas the the Kirsehir massif is subsumed under one block called the Anatolide-Tauride and the third being the Arabian Platform (Okay, 2008). The description of these geologic units and their lithological compsition here is largely on the account outlined in Okay (2008) and Bozkurt and Mittwede (2001).

The Pontides comprise the territories north of the IAE suture. These are folded and thrusts faulted in the Alpine orogeny but were not metamorphosed. The terranes here bear avidence of Hercynian or Variscan (Carboniferous) and Cimmeride (Triassic) orogenies (Okay, 2008). The three terranes comprising the region are the Stranca/Strandja, Istanbul and Sarkaya. Some other similar subdivisions with little difference in nomenclature of the Pontides include the Sarkaya, Rhodope-Strandja and the composite Istanbul-Zonguldak (sometimes separated as Istanbul and Zonguldak) zones. All but Zonguldak zone, belongs to the Laurasia, and were affected by the Variscan metamorphic-plutonic events (Moix et al, 2008). The Stranca massif is part of the large crystalline terrane in the southern Balkans. It includes the Rhodope and serbo-Mecedonian massifs. It is composed of a Hercynian crystalline basement which is overlain by a Triassic-Jurasic continental to marine metasediments. Stratigraphically, the highly deformed and metamorphesed basement is predominantly quartzo-feldispathic gneisses intruded by Late Carboniferous and Early Permian (257 ± 6 Ma) granitoids (Okay et al, 2001; Sunal et al, 2006).

The Istanbul terrane is a continental unit (400 km long and 55 km wide) on the south-western margin of the Black sea. The unit unit is a precambrian crystalline basement composed of gneiss, amphibolite, metavolcanic rocks, metaophiolite and voluminous Late Precambrian granitoids (Chen et al, 2002; Yiğitbaş et al, 2004; Ustaömer et al, 2005). The basement is exposed in the north of Bolu in the Bolu Massif and is unconformably overlying Ordovician to Eocene sediments (Görür et al, 1997; Dean et al, 2000).

The Sarkaya terrane is an east-west trending continental unit from the Aegean in the west to the eastern Pontides in the east. It is bordered on the northwest by the Rhodope-Strandja, Istanbul and Zonguldak terranes along the Intra-Pontides Suture/North Anatolian Fault system and to the northeast by the Black sea. It is bounded on the south by the composite Anatolide-Tauride block along the melanges and ophiolites of IAE zone (Moix et al, 2008). This crystalline complex is further divided into three types. They include; (i) A high-grade Carboniferous (330 – 310 Ma) Variscan metamorphic sequence of gneiss, amphibolite marble and scarce metaperidotite (Okay et al, 2006; Topuz et al, 2004, 2007). (ii) Paleozoic (or Palaeozoic) granitoids of Dovonian, Carboniferous and Permian crystallization periods which are unconformably overlain by Jurassic and younger sediments (Delayoye and Bingöl, 2000; Okay et al 2002, 2006; Topuz et al, 2007). (iii) The Karakaya low metamorphic complex, extensively composed of the Permo-Triassic metabasite and lesser amounts of phyllite and marble (Okay et al, 2002; Okay, 2008).

The composite Anatolide-Tauride terrane also called the Tauride-Anatolide platform or TAP by Sengör and Yilmaz (1981), and sometimes decoupled in litereture as the Anatolides and Taurides terranes refers to the landmass of southern Turkey between the Neotethyan IAE ocean to the north and the southern branch of Neotethys. It is supposed that the TAP was the hard-hit during the obduction, subduction and continental collision episodes in the Late Cretaceous and Early Tertiary (Paleocene) period. The region underwent much severer Alpine deformation and regional metamorphism than the northern Pontic belts (Okay, 2008). In the context of decoupled terranes, the Anatolides represent the metamorphic northern margin of the TAP, separated from the Sarkaya terrane by the Izmir-Ankara suture. The Anatolides is composed of four zones, namely (i) the Bornova Flysch zone, (ii) the Tavşanlı zone, (iii) the Afyon zone and (iv) the Menderes Massif (MM) and the Central

Anatolian Crystalline Complex (CACC) (Bozkurt and Mittwede, 2001; Göncüoğlu, 2010). On the other hand, the Taurides consist of a stockpile of unmetamorphosed (except the Alanya nappes which experienced high pressure/low temperature – HP/LT metamorphism; Okay and Özgür, 1984; Okay, 1989) thrust sheets or nappes composed of paleozoic to Early Tertairy sedimentary rocks such as carbonates, turbidites and continental clastic rocks.

In the contetext of Anatolide-Tauride or TAP single paleogeographic entity, the different types and ages of the Alpide metamorphism has resulted in subdivisions of the TAP into zones with different metamorphic features. There are three main regional metamorphic zones in the TAP in Western Turkey. They are; (i) the Tavşanlı zone in the north; (ii) the Afyon zone in the center; and (iii) the Barrovian-type metamorphic region called the Menderes Massif in the south. The other zones of the TAP are (iv) the Bornova Flysch zone located northeast of the MM; (v) the Taurides (including the Bitlis Massif in southeast Anatolia) located south of the metamorphic regions and (vi) the Central Anatolian Crystalline Complex (CACC) situated north of the Taurides' region.

The Tavşanlı zone is a blueschist belt in northwest Turkey, approxiamtely 50 km wide and 250 km long. The belt is comoposed of deformed volcano-sedimenetry rocks affected by HP/LT metamorphism in the Campanian or Late Cretaceous (80 ± 5 Ma). The blueschist series is tectonically overlain by a Cretaceous accretionary complex of basalt, radiolarian chert and pelagic shale (Harris et al, 1994; Okay, 1984, 1986, 1996, 2008; Okay et al, 1998; Sherlock et al, 1999).

The Afyon zone is located in the region between the MM and the Tavşanlı zone. The zone consist of a Paleozoic (Dovinian-Permian) to Mesozoic (Triassic-Maastrichtian) sedimentary series composed mainly of metaclastics and thick carbonate platforms with interspersed Paleozoic greenschist facies (Özcan et al, 1988; Okay, 1984; Göncüoğlu et al, 1997; Bozkurt and Mittwede, 2001).

The Menderes Massif is a large crystalline metamorphic unit in Western Turkey, with a complex Alpine and partly Pan-African matamorphic and igneous structural history (Bozkurt et al, 1993). The metamorphic complex is estimated as belonging to the Precambrian and Eocene metamorphic and deformationary events (Şengör et al, 1984; Bozkurt and Oberhansli, 2001). The MM is composed of Precambrian

micaschists, gneiss and minor granulite and eclogite intruded by large metagranites with latest Precambrian (~550 Ma) intrusion ages (Candan et al, 2001). The east-west trending Neogene grabens (the Gediz Graben and the Büyük Menderes Graben) subdivides the MM into three major horst units which includes the Southern Menderes, Central Menderes and Northern Menderes submassifs (Okay, 2008; Erkan, 2014).

The Bonova Flysch zone is a large scale (50 to 90 km wide and about 230 km long) tectonic unit between the MM and the IAE suture. It is a chaotically deformed belt made up of upper Maasstrichtian-Lower Paleocene graywacke, shale and extensive blocks of Mesozoic limestone, mafic volcanic rocks, radiolarian chert and sepentinite (Erdoğan, 1990; Erdoğan et al, 1990; Okay et al, 1996).

The Central Anatolian Crystalline Complex is an extensive area of metamorphic and granitic rocks of Cretaceous period. Large Neogene sedimentary and metamorphic cover has resulted in further subdivision of the CACC into submassifs, and these include very important units such as the Kırşehir, Akdağ and Niğde massifs (Okay, 2008).

The Tauride belt consist of a Neoproterozoic basement (composed of metaclastic rocks - slates, conglomerates and greywackes; stromatolithic limestones and lydites together with meta-rhyolites and quartz-porphyries) and non-metamorphic Paleozoic-Mesozoic cover of platformal sediments (Göncüoğlu, 2010). The topmost nappe consist of ophiolite and/or ophilitic melange which forms large isolated bodies throught the Taurides (Özgül, 1984; Gürsu et al, 2004; Okay, 2008). In the eastern Taurides is an important geologic feature known as the Bitlis massif. The Bitlis massif is a 30 km wide and 500 km long metamorphic belt in southeast Turkey separated from the Arabian platform by a narrow upper Cretaceous to Eocene flysch and ophilitic melange. The Bitlis massif is divided into two units composed of a Precambrian basement (Lower Unit – made of gneiss, amphibolite, micaschist and eclogite) and Phanerozoic sequence as the Upper Unit consisting of schist, phyllite, marble and metavolcanic rocks (Göncüoğlu and Turhan, 1984; Çağlayan et al, 1984; Okay, 2008).

The Arabian platform is the northernmost extension of the Arabian platform in Southeast Turkey separated from the TAP by the southern branch of Neotethys,

which is evident today as Assyrian suture (Şengör and Yılmaz, 1981, Okay, 2008). The platfaorm has a Pan-African crystalline basement covered by a Paleozoic to Tertiary sedimentary series. The allochthonous units, Bitlis massifs and the underlying melange units is said to to have been placed on the Arabian platform during the continental collision with the TAP in Miocene (Okay, 2008). The allochthonous regions are subdivided into three important areas, namely; the Hakkari and Maden Complexes, the Yüksekova Complex and the Cretaceous-Tertiary Basin – Fore-Arc to Fore-Deep region.

Bozkurt and Mittwede (2001) also provided a further paleogeographic discription of the Turkish terranes in details, whereby the terranes are identified and grouped or subdivided into Metamorphic Belts, Cenozoic Volcanism, Sedimentary Basins, Ophilitic Belts, Orogenic Belts (as described above) and Neotectonic belts.

The Metamorphic Belts: The metamorphic regions of Anatolia are classified into three major groups based their ages and degree of metamorphism (latest event) as Hercynian (or Variscan), Cimmerian and Alpine. The Hercynian metamorphics occur only in the Pontides and generally comprise Precambrian greenschist to amphibolite facies rocks. They are exposed only in the western Pontides as basement to Paleozoic rocks of the Istanbul zone known as the Bolu Massif (Ustaömer and Rogers, 1999; Yiğitbas et al, 1999). Hercynian continental units of high-grade metamorphic rocks such as the gneiss-amphibolite alternations forms tectonic windows in the core of the Kazdağı (mount Ida) and Uludağ massifs, and the exposed Pulur Massif in eastern Pontıdes (Okay, 1996; Okay and Leven, 1996). The Cimmerian (Triassic) metamorphic units underlie terranes mainly in the Pontides and are put into three belts, namely (i) the Southern belt (north of IAE suture) which include the Karakaya complex, the Uludağ and Pulur massifs (Okay, 1996; Okay et al, 1996; Göncüoglu et al, 2000); (ii) the northern belt exposures of the Amutlu Peninsula called the Pamukova and Iznik metamorphics (Göncüoglu and Erendil, 1990); (iii) the eastern belt, which includes the Kırşehir Massif in central Pontides, and the eastern Pontide massifs of Tokat and Agvanis (Bozkurt and Mittwede, 2001).

The Alpine metamorphics is divided into four belts. They are, (i) the Cretaceous blue schist- to eclogite-facies, (ii) the Cretaceous green schist- to amphibolite-facies rocks that form two major metamorphic zones known as the CACC and the Bitlis and Pötürge massifs of southern Anatolia; (iii) the Paleocene-Eocene greenschist- to

eclogite-facies rocks that occur only in Western Anatolia in the Afyon zone and the MM; and (iv) the Oligocene amphibolite-facies metamorphic rocks, some of which are exposed in Kazdağ massif related to the extensional exhumation (Okay and Satir, 2000b). The Cretaceous blueschist- to eclogite-facies is subdivided into three groups, namely the Tavşanlı and Çamlıca metamorphics in Western Turkey and the Alanya Massif in western Taurides (Harris et al, 1994; Okay, 1984; Okay et al, 1998; Sherlock et al, 1999; Okay and Satir, 2000a). The Cretaceous greenschist- to amphibolite-facies rocks form two major metamorphic zones known as the CACC and the Bitlis and Pötürge massifs of southern Anatolia.

Cenozoic Volcanism: Vast volcanic belts, related to the closure of the Tethyan oceans and other Neotectonic activities, underlie several Anatolian terranes. There are five major Tertiary – Quaternary volcanic provinces in Turkey, namely:

(i) The Western Anatolia Volcanics;

(ii) Galatia Volcanics - occurred between the Early and Late Miocene (23 – 5 Ma; Wilson et al., 1997; Tankut et al, 1998);

(iii) Central Anatolian Volcanics – a calc-alkaline province composed of an early phase basaltic-andesitic lava flows (13.5 – 8.5 Ma) underlying voluminous rhyolitic ignimbrite ejection with interbedded Plinian pumice-fall deposits (9.5-9 to 2.7 Ma; Pasquare et al, 1988; Le Pennec et al, 1994; Schumacher and Mues-Schumacher, 1996; Temel et al, 1998);

(iv) Eastern Anatolian Volcanics – Miocene-Pliocene collision-related volcanic rocks (11 ± 2.7 Ma; Keskin et al, 1998) and the last eruption in the region is said to have occurred at Nemrut Dagı in 1441 (Tchalenko, 1977); and

(v) The Karacadağ Volcanics – Volcanic activities of the Nemrut Dağı in Eastern Anatolia, Erciyes and Hasan Dağı in central Anatolia, and the Kula region are regarded geologically very young and may be considered as dormant volcanoes (Bozkurt and Mittwede, 2001). The ancient cave dwellings (monuments) carved out of young volcanic rocks in Cappadocia and Afyon territories are testaments of a historically unstable region (Topal and Sözmen, 2001; Bozkurt and Mittwede, 2001).

Sedimentary Basins: The Mesozoic – Lower Tertiary deformed Neotethyan regions of Turkey are unconformable overlain by Neogene basins. The basins occupy vast areas of land and are mostly filled with Miocene fluvial-lacustrine sediments (Görür et al, 1998). For instance, the East-West trending grabens of the Gökova, Büyük

Menderes, Gediz and Simav in Western Anatolia are filled with Miocene sediments, and so are the North-South trending basins of Soma, Uşak – Selendi, Gördes and Emet. Other basins where Miocene sedimentation has occurred include the Adana, Aksu, Köpru, Manavgat and Mut foreland basins along the Taurides; Beypazari basin in Central Anatolia; the collision related Thrace basin of the Pontides and the Çankırı, Tuzgölü, Haymana and Sivas basins in the Anatolides (Hayward, 1984; Robertson et al., 1991; Flecker et al, 1995, Williams et al, 1995; Yetis et al., 1995; Karabiyikoglu et al, 2000; Robertson, 2000; Helvaci et al, 1989; Inci, 1991; Görür and Okay, 1996; Çiner et al, 1996; Görür et al, 1998; Kaymakçi et al, 2000; Ocakoğlu, 2001). The map of Appendix A.1 shows the tectonics of North-Eastern Mediterranean region indicating the major sutures and continental blocks of Turkey, and in Appendix A.2, the distribution of different basement types and accretionary complexes in Turkey.

2.5 Neotectonics of Turkey

Detailed schematic and dynamics of the relative motions of major plates in the Mediterranean-Middle East section of the Alpine-Himalayan Belt suggest that the region's tectonic activities is dominated by the collision of African and Arabian plates with Eurasia (McKenzie 1970, 1972; Jackson and McKenzie 1984, 1988; McClusky et al. 2000). Tectonic activities in the region were identified and put into different categories. These categories include (i) the different stages of continental collision (Zagros/Caucasus/Black Sea), (ii) subduction of oceanic lithosphere and the associated back arc spreading (Cyprus/Hellenic/Calabrian arcs, Aegean and Tyrrhenian Seas), (iii) continental extension in Western Turkey/Marmara Sea/Gulf of Corinth), (iv) the continental "escape" (Anatolian block), (v) major continental strike-slip faults (North and East Anatolian and Dead Sea faults), and a variety of small-scale processes associated with the African-Arabian-Eurasian plate interactions as shown in Figure 2.1. The portion of Turkey herein referred to as the Anatolian plate (or Anatolian block) denotes the region of Turkey in the west of Karliova triple junction trapped between the right-lateral North Anatolian and left-lateral East Anatolian strike-slip faults.

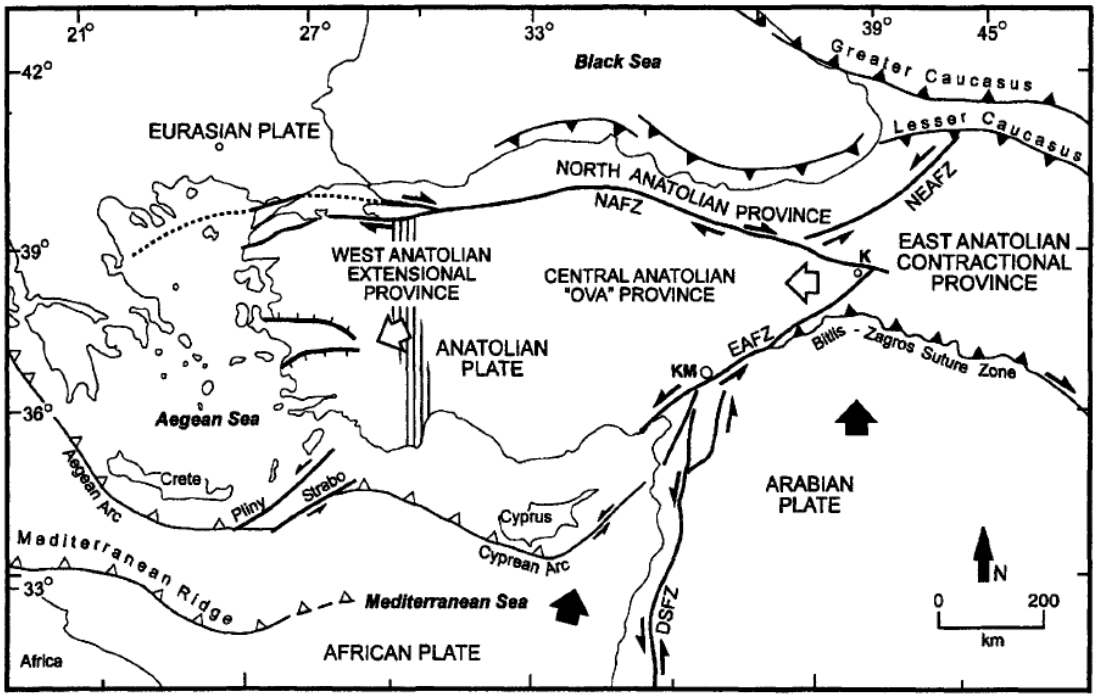

Figure 2. 1: Tectonic map of Turkey showing major neotectonic structures and provinces (Bozkurt, 2001).

In Figure 2.1 above,the abbreviations: K - Karliova; KM - Kahramanmaras; DSFZ - Dead Sea fault zone; EAFZ - East Anatolian fault zone, NAFZ - North Anatolian fault zone; NEAFZ - Northeast Anatolian fault zone. Heavy lines with half arrows are strike-slip faults. Half arrows show relative movement sense. Heavy lines with filled triangles show major fold and thrust belt; tips of the small triangles indicate direction of vergence. Heavy lines with open triangles indicate an active subduction zone; tips of the small triangles indicate polarity. The heavy hachured lines show normal faults; hachure indicates downthrown side. Bold filled arrows indicate relative movement direction of African and Arabian plates; open arrows indicate relative motion of Anatolian Plate. The hatched area shows the transition zone between the western Anatolian extensional province and the central Anatolian "ova" province (Sengör et al., 1985).

Based on the Global Positioning System (GPS) measurement of crustal motions for a period of 9 years, McClusky et al. (2000) conducted out a thorough analysis of plate (major and minor) kinematics and dynamics in the region. Generally, the study indicates northward motions of northeastern Africa as well as the northern part of the Arabian plate, a coherent plate motion (internal deformation of < 2mm/yr) involving westward displacement and a counterclockwise rotation of much of Central/Western

Turkey (Anatolian plate) and the Southern Aegean/Peloponnesus. The NAFZ provides a break on Anatolia in the north and as well decouples it from Eurasia. This facilitates the westward-counterclockwise motion of Anatolia whiles aided by another strike-slip fault, the East Anatolian Fault (EAF) zone on the Southeastern part. The continental land mass north of the Arabian-Anatolian plate collision zone (Bitlis suture) is thought to move around and between the oceanic lithosphere of the Black and Caspian seas, whereas the Caucasus/Eastern Turkey moves around the eastern side of the Black Sea.

The tectonic analyses (using seafloor spreading, fault systems, earthquake slip vectors and GPS measurements) of plate motions indicate Arabia is moving North-Northwest relative to Eurasia at an estimated rate of 18-25 mm/yr (averaged over 3Ma). The African plate is moving in the northerly direction relative to Eurasia at a rate between 5-6 ± 2 mm/yr (GPS based data) or 10mm/yr based on global model NUVEL-1A. The African plate is said to be subduction along the Hellenic arc at a rate higher than its northward relative motion whereas a similar subduction of the plate may be occurring along the Cyprean arc and /or the Florence rise south of Turkey. The estimated differential motions between Africa and Arabia vary between 10-15mm/yr and may be accountable for the left-lateral motion along the Dead Sea Transform Fault zone (DSTFZ).

Furthermore, opposed to the theory of a single plate deformation in Western Turkey is the two-plate model, which suggests that the relative motion of Anatolia and Aegean is distributed and not confined to a single fault (McKenzie, 1970, 1972). McClusky et al. (2000) also added that the GPS velocity field confirms the southward motion of the Aegean plate relative to Anatolia in favor of the two-plate model. The Aegean-Anatolian differential motions vary between 10-15mm/yr, consistent with a rough estimate of the average geological extension rate 6-18mm/yr across south-west Turkey (36.5ºto 38.5ºN). The motion is accommodated by the major East-West oriented normal faults associated with the horst and graben features controlling the active deformation in Western Turkey (Büyük Menderes and Gediz grabens). The two-plate model further relies on the coherent, plate-like motions of Anatolia and the Southern Aegean, separated by the North-South (36.5º to 38.5ºN) extension in Western Turkey. That is, the bulk motion of Aegean/Hellenic arc appears to be associated with a coherent rotation of the Southern Aegean plate and

probably bounded by the South-West striking, right-lateral strike-slip and North-West oriented normal faults in north Aegean Sea. It is estimated that the Central and Southern Aegean is involved in a coherent motion (internal deformation < 2mm/yr) towards south-west at 30 ± 1 mm/yr relative to Eurasia. The vector triangles approximation by McKenzie (1972) yielded 20 mm/yr and 35 mm/yr for the relative motion of Aegean to Eurasia and Africa, respectively.

Other seismically active areas of interest are the NAFZ, EAFZ and the Southeast orogenic belt (Border Zone) herein referred to us the Bitlis Zagros Suture Zone (BZSZ). The GPS upper bounds on fault slip rates are estimated to be 24 ± 1 mm/yr for the NAFZ and 9 ± 1 mm/yr for the EAF. Relying on the assumption that the active zones are strike slip faults, similar slip rates using the vector triangles approach by McKenzie (1972) on the NAFZ and the Border Zone produced 40 mm/yr and 50 mm/yr, respectively. Based on earthquakes data, Brune (1968) also estimated a slip rate of 110 mm/yr for the NAF. A summary of the relative motions of plates and active zones in the region related to the study is provided in Tables 2.3 and 2.4. Associated with plates kinematics in the region are also numerous small-scale activities such as the Fethiye Burdur fault zone (FBFZ), Ecemiş fault zone (EFZ), and the Tuz Gölü fault zone (TGFZ) (Aydin et al, 2005, Figure 1).

Table 2. 3: Plate motions in the Mediterranean and south-west Asia.

Fixed	Moving	Rate, mm/yr	Direction	Reference
Eurasia	Arabia	18-25	NNW	MCEL[2000]
Eurasia	Africa	5-6 ± 2 (GPS)	N	MCEL[2000]
Eurasia	Africa	10 (NUVEL-1A)	N	MCEL[2000]
Eurasia	Aegean [Central/Southern]	30 ± 1	Coherent &SW	MCEL[2000]
Eurasia	Aegean	20	SW	MK[1972]
Africa	Aegean	35		MK[1972]
Africa- Arabia	DM	10	N	MK[1972]
Aegean-Anatolia	DM	10 -15		MCEL[2000]

MCEL - McClusky et al., MK - McKenzie and DM – Differential motion.

Table 2. 4: Motions along faults and deformation zones.

Region	Slip Rate/Deformation, mm/yr	Reference
NAFZ	24 ± 1	MCEL[2000]
NAFZ	40	MK[1972]
NAFZ	110	Brune [1968]
EAF	9 ± 1	MCEL[2000]
Border Zone [BZSZ]	50	MK[1972]
NS-SW Extension [36.5^o to 38.5^{o}N]	6 - 18	MCEL[2000]
Central Anatolia	< 2 deformation	MCEL[2000]

2.6 Crustal Structure of Turkey

The crustal structure of Turkey is a product of the continent-continent collision of African, Arabian and Eurasian plates as expressed by the post-collisional intra-continental convergence and tectonic excape-related deformations from the Late Miocene – Pliocene epochs (Bozkurt and Mittwede, 2001). The Anatolian terranes are still considered very active and the August 17, 1999 Kocaeli (also known as the İzmit or Gölcük earthquake with a moment magnatude of 7.4) and November 12, 1999 Düzce (M = 7.2) devastating earthquake events are testaments (Barka, 1999; Bozkurt and Mittwede, 2001). According to Ates et al. (2012), these destructive seismic activities occur at very shallow depths of about 8 to 10 km and are therefore fault controlled. The terranes of Turkey are thought to have undergone an initial N-S shortening and some relics of this event are the Miocene sedimentations of Western Anatolia in the east-west trending grabens and the approximately north-south trending basins which are supposed to have been occasioned by orogenic collapse (Bozkurt and Mittwede, 2001; Şengör and Yılmaz, 1981). Presently, the intra-continental convergence and North-South compression is said to have ceased in Western Anatolia but subsist in Eastern Turkey. It is thought that at the end of intra-continental collision, the early compressional–contractional tectonic regime of Eastern Anatolia got replaced by a new compressional – extensional regime – the neotectonic regime (with tectonic escape/extrusion tectonics) of the Early Pliocene (Bozkurt and Mittwede, 2001).

As indicated in Section 2.5 (also Figure 2.1), neotectonic activities of Turkey is controlled by three major structures: the intracontinental transform faults, which include the dextral NAFZ and the sinistral EAFZ, and the Aegean – Cyprian Arc (a

convergent plate boundary where the African plate to the south is subducting beneath the Anatolian plate at the north; Bozkurt and Mittwede, 2001). In addtion to these three structures is the sinistral DSTFZ which also has very significant role in the neotectonic Turkish terranes. Four distinct neotectonic provinces have been devised alongside the continous deformational activities of NAFZ, EAFZ and the westward extrusion of Anatolia, which has been ocassioned to accommodate the internal deformation. The divisions include the East Anatolian contractional, the North Anatolian, the Central Anatolian "Ova", and the West Anatolian extentional provinces (Sengör et al, 1985). Over the years, numerous studies have been undertaken to determine the crustal structure of these terranes on both regional and countrywide bases. Some of the most recent studies include Tezel et al. (2007, 2013), Zor et al. (2003, 2006), Ates et al. (2012), Bekler and Gurbuz (2008) and Karabulut et al. (2013). In these investigations, several methodologies such as gravity data, receiver function, seismic wave velocity, surface wave dispersion and seismological records among others were used to determine the crustal thickness or the Moho (Mohorovicic) discontinuity.

As expected, the results come with some degree of variations but generally agree on a trend of increasing Moho depths from Western Turkey towards the east. The thinnest Mohorovicic discontinuity is observed in the coastal areas of Western Turkey and the deepest in Eastern Turkey, through the Iranian border. For instance, from the west to east of Turkey, crustal thickness estimates are given as 25 – 40 km, 28 – 42 km averages, 24 – 48 km and 31 – 50 km by Tezel et al. (2007), Ates et al. (2012), Tezel et al. (2013) and Arslan et al. (2010), respectively. Ates et al. (2012) divided Turkey into three blocks, namely the West, the Central and the East and estimated the respective crustal thicknes. In the West, from the shorelines to the hinterland of Aegean grabens, the thickness varies from 26 to 34 km, respectively. In the Central block from the Black sea to the Mediterranean sea, the thickness is 28 km for coastal regions and between 34 – 38 km inland (mean range of 33 – 35 km) and in the East (from the Black Sea to the Arabian block) between 30 – 33 km, but incraeses up to 43 km in the Turkish – Iranian border areas. Furthermore, an average value of 28 km across Western Anatolia at 28^{o} E longitude (from the Black Sea to the Mediterranean sea) by Karabulut et al. (2013) agrees with estimates of the West

block. A summary of the Moho depth estimates of Turkey and some important zones are given in Table 2.5 below.

Table 2. 5: Moho depth in different parts of Turkey.

Area/Location	Moho depth, km	Method	Reference
West to East Turkey	25 - 40	SWDA	Tezel et al. [2007]
West to East Turkey	28 – 42^{av}	GD	Ates et al. [2012]
West to East Turkey	24 - 48	RF	Tezel et al. [2013]
West to East Turkey	31 - 50	GD	Arslan et al. [2010]
Western Turkey	25 - 32	SWV	Necioglu et al. [1981]
Western Turkey [coast to hinterland – Aegean grabens]	26 - 34	GD	Ates et al. [2012]
Western Turkey	20 - 35	RF	Tezel et al. [2010]
Western Turkey [Aegean region]	25 - 34	RF	Zhu et al. [2006]
Western Turkey [N-S at 28ºE longitude]	27^{av}	RF	Karabulut et al. [2013]
W-SW Turkey	23 - 41	RF	Tezel et al. [2013]
Western Turkey [Kula – Uşak]	30 - 34	RF	Saunders et al. [1998]
Central Turkey/Anatolia	38	RF	Saunders et al. [1998]
Central Turkey/Anatolia	38	P&S-WRF	Çakır and Eduran [2011]
Central block/Turkey [coast – inland]	28 - 38	GD	Ates et al. [2012]
Eastern Turkey	30 - 55	S-WRF	Angus et al. [2006]
Eastern Turkey [Black sea to Iraian border]	30 - 43	GD	Ates et al. [2012]
East Anatolian plateau	45^{av}	RF	Zor et el. [2003]
Eastern Marmara [W – E along NAFZ]	29 – 35 [31±2^{av}]	RF	Zor et el. [2006]
Eastern Marmara [N-S beneath central Amutlu]	24 - 34	SWV	Bekler and Gurbuz [2008]

SWDA – Surface wave dispersion analysis, GD – Gravity data, RF – Receiver function, SWV – Seismic wave velocity, P&S-WRF – P and S-wave receiver function, S-WRF – S-wave receiver function, SR – Seismological records, av – Average value.

Table 2.5 (continued): Moho depth in different parts of Turkey.

Area/Location	Moho depth (crustal thickness), km	Method	Reference
Menderes Massif	25	RF	Karabulut et al. [2013]
Borno Flysch	31.5	RF	Karabulut et al. [2013]
Anatolian plateau	37	RF	Karabulut et al. [2013]
Thrace Basin	31	RF	Karabulut et al. [2013]
Izmir-Ankara suture	32	RF	Karabulut et al. [2013]
Rhodos Island & Mediterranean coast	20	RF	Karabulut et al. [2013]
Marmara Sea	25	RF	Karabulut et al. [2013]
Arabian platform	36^{av}	SR	Gök et al. [2007]
Anatolian block	44^{av}	SR	Gök et al. [2007]
Anatolian plateau	48^{av} [40 - 52]	SR	Gök et al. [2007]
Central MM	28 - 30	RF	Zhu et al. [2006]
Aegean Sea	25	RF	Zhu et al. [2006]
Central Anatolia	36	RF	Zhu et al. [2006]
Cycladic Massif	25 - 26	RF	Zhu et al. [2006]

SWDA – Surface wave dispersion analysis, GD – Gravity data, RF – Receiver function, SWV – Seismic wave velocity, P&S-WRF – P and S-wave receiver function, S-WRF – S-wave receiver function, SR – Seismological records, av – Average value.

2.7 Curie-point Depth and Curie Temperature Estimates in Turkey

As stated by Pollack and Chapman (1977a), the idea that depth to important changes or transitions in physical properties within the Earth depends on temperature is not new; Kennedy (1959) speculated that the variations in Moho depth underneath the continents, oceans and mountain ranges was linked to variations in heat flux and geotherms between these regions. Furthermore, the concept that ferromagnetic substances exhibited a critical temperature transition, above which a mineral loses its ferromagnetic property, known as the Curie point was discovered by Pierre Curie in 1895. Thus within the Earth, the depth at which substances (rocks and/or minerals) passes from ferromagnetic state to paramagnetic state under the effect of increasing temperature is called Curie-Point Depth (CPD), and this depth is calculated to the basal (bottom) of the magnetized bodies in the crust (Beardsmore and Cull, 2001; Aydin et al, 2005; Şalk et al, 2005). Simlarly, Curie-point temperature or Curie

temperature refers to the measure of temperature at which minerals loses their ferromagnetic behavior.

The Curie temperature varies from place to place depending on the geology, mineral content of the rocks and prevailing presure condtions. Through out Turkey, CPD maps have been prepared on both countrywide and on regional bases by several researchers. Some these include works done by the General Directorate of Mineral Reasearch and Exploration or MTA (2007), Aydin et al. (2005), Şalk et al. (2005), Ates et al. (2005), Dolmaz et al. (2005), Bektaş et al. (2007) and Maden (2009, 2010). Most of the CPD maps have been prepared from aeromagnetic survey data which was conducted by the MTA between 1978 – 1989 and also a couple of maps from the Magsat data of the British geological survey (for example, Şalk et al, 2005). An aeromagnetic survey is usually carried out by an aircraft with a magnetometer mounted to measure and record the total intensity of the magnetic field. The total intensity of the magnetic field recorded is composed of the desired magnetic field generated in the Earth (local effect of the magnetic minerals and regional magentic field) as well as the temporal effects of solar wind and the magnetic field of the aircraft. The data is then refined, such as subtracting the regional, solar and aircraft effects among others, resulting in an aeromagnetic data or map that shows spatial distribution and relative abundance of magnetic minerals (iron oxide bearing minerals such as magnetite) in the Earth's crust.

The variety in rock types and different magnetic mineral content enables the interpretation of these magnetic maps. These magnetic maps or data enables a visualization of the geological structure in the crust such as the saptial geometries of bodies of rocks, faults, folds and the aeromagentic anomalies (hills, ridges and valleys,) which are then interpreted by geophysicist using mathematical models to calculate depth, shape and properties of the rocks causing these anomalies. Such surveys are also carried out to determine mineral, geothermal and other natural resource potentials. The CPD is determined based on Fourier analysis of aeromagnetic data. The approach involves a rigorous statistical method known as the Power Spectrum, developed by Spector and Grant in 1970. There are other simplified forms of calculating the CPD based on the power spectrum approach. For example, Curie isotherm depth investagations by researchers mentioned aboved were mostly estimated using the spectrum (spectral) analysis developed by Okubo et al (1985)

and Tanaka et al (1999); all developed on the bases of Spector and Grant (1970) technique.

The determined CPD or basal depths of the magnetized bodies responsible for the magnetic anomalies may not necessarily represent the CPD isotherm in all cases. As noted earlier, the Earth's crust is not homgeneous and the different rock types exhibit varying Curie temperatures, therefore, the CPD could also correspeond to a composition boundary (Beardsmore and Cull, 2001). For this reason, it is important to corrrelate CPD with deep seismic or garvity models to determine which of the two cases (a Curie isotherm or a compositioanl boundary) is prevailing. If the CPD matches with the inferred velocity or density boundary, it is most likely to be a change in composition, especially, where stratigraphy data indicate intermediate to mafic rocks underlying accidic rocks. On the other hand, if CPD does not match the density or velocity boundary, it can be interpreted as the Curie isotherm, which is about 580 ^{o}C in most continental regions (Beardsmore and Cull, 2001).

In the published litertature, the basal depths (CPDs of Turkey) of the magnetized bodies agree on a particular trend over the country. For instance, shallow CPDs (between 6 – 10 km) are associated with crustal thinning in the Aegean area and young volcanic regions. These areas have positive correlation with geothermic activities whereas the orogenic belts with some nappe structures such as the Taurides, Pontides and suture zones have the deepest CPDs greater than 20 km (Aydin et al. 2005; Şalk et al, 2005; Dolmaz et al, 2005). In Table.2.6 below are CPDs range of Turkey and some other few areas. It must however, be noted that these depths are below sea level and topography data must be added to obtain measurements to the surface or ground level.

As noted by Beardsmore and Cull (2001), the Curie depth-temperature pair constitute an excellent deep datum for modelling thermal gradient. This datum can therefore be used as a base for the estimation of upward successive subsurface temperature dsitribution at reachable depths and consequently compare such maps with deep well geothermal gradients. From published literature of CPD and corresponding thermal gradient or heat flux maps of the study areas (for example, Ates et al, 2005; Maden, 2010; Hisarli et al, 2012), a Curie-point temperature of 580°C has been used for thermal gradient (λ = 580 °C/CPD) calculation and between 2 – 2.5 W/m°C conductivity value for heat flux estimation. However, Şalk et al. (2005) estimated a

Curie temperature of 560 °C for Western Anatolia using both the moving windows spectrum and spectral analysis.

Table 2. 6: CPD of some areas in Turkey**.**

Area	CPD, km	Method	Reference
Turkey	6 - 29	SA	MTA [2007]
Turkey	6 - 30	SA	Aydin et al. [2005]
Western Anatolia	6 - 22	SA	Şalk et al. [2005]
Western Anatolia	4 - 14	MWSA	Şalk et al. [2005]
Western Anatolia	10 - 15	SA	Gökturkler et al. [2003]
Western Anatolia	8.2 – 19.9	SA	Dolmaz et al. [2005]
Central Anatolia	7.9 – 22.6	SA	Ates et al. [2005]
Eastern Anatolia	13 - 23	SA	Bekteş et al. [2007]
Cappadocia & Erciyes volcanic complexes	7.9	SA	Ates et al. [2005]
Erciyes region	13.7	SA	Maden [2010]
Erciyes region	11.4	gT	Maden [2010]
Horst & grabens of Aegean region	8.2 – 12.4	SA	Dolmaz et al. [2005]
Horst & grabens of Aegean region	6 - 10	SA	Aydin et al. [2005]
Bolu district	8 - 14	SA	Aydin et al. [2005]
Gönen, Yalova & Bursa	10 - 12	SA	Aydin et al. [2005]
Balikşehir area	8 - 12	SA	Aydin et al. [2005]
Karacadağ volcanism	7	SA	Aydin et al. [2005]
Ponttides, W-Taurides & eastern plateaus	20 - 29	SA	Aydin et al. [2005]
Thrace region	17 - 18	SA	Aydin et al. [2005]
Central Pontides [South to North]	14.8 - 21.8	SA	Maden [2009]

SA – Spectral analysis, MWSA – Moving windows spectrum analysis, and gT – Geothermal gradient.

Similarly, Aydin et al. (2005) observed that some of the CPDs do not reflect depths at which temperature reaches 580 °C (a generally accepted value for the magnetic crust). For instance, Haggerty (1978) pointed out that the magnetic anomally model should not be constrained by a Curie isotherm of 580 °C limit. He argued that the source of crustal magentic anomalies can extend to limits whcih exceed the conventionally held Curie isotherm (580 °C). For example, the range in temperature

may extend to 680 °C if the magnetic source mineral is Hematite (α Fe_2O_3) and the body is weakly magnetic, or could be reduce to 300 °C if the source mineral is is Maghemite (γFe_2O_3) and the body is strongly magnetic. Assuming an average thermal gradient of 3 °C/100m (30 °C/km), a Curie isotherm of a magnetite dominant crust is at a depth of 19 km. Howerever, he indicated that there are variations about this average depending on the tectonic setting of the area under investigation. The Curie isotherm could also be raised to very shallow depths in high thermal gradient provinces (as in the horst and grabens and young volcanic regions of Turkey). Thus the Curie isotherm need not be constrained by 580 °C value if the mineral invoked is not magnetite (Haggerty, 1978; Smith 1973).

In determinig the magnetic carrier in deep crust and consequently, the Curie temperature, one obvious way is the study of rocks that are presently exposed but were once buried deep in the crust or at lower crustal depths. This may include rocks from categories such as xenoliths, general plutonic and high-grade metamorphic terrains and obducted cross-sections from lower continental crust (Frost and Shieve, 1986). Experimantal results of Curie temperature of minerals and rock samples from such terrains are given in Table 2.7 and 2.8 below.

2.8 Geothermal Potential and Heat Flow Measurement in Turkey

The Alpine-Himalayan orogenic belt on which Turkey is located holds enomous geothermal potential (Mertoglu et al, 2010). The estimatimation of Turkey's geothermal potential in the form of geothermal gradients, temperature, surface and subsurface heat flow maps have been conducted using three main techniques. They include (i) the conventional approach (based on temperature data from logs, equilibrium/corrected BHTs from both shallow and deep boreholes/wells and thermal conductivity data), (ii) groundwater/springs geochemistry and (iii) the out of reach deep Curie isotherm. Explorationa activities by the state agency (MTA), alongside reasearch is yielding results in the geothermal energy subsector. According to Tureyen and Satman (2013), nearly 300 geothermal resource areas have been identified and current geothermal power and direct use installations are over 110 MWe and 2100 MWt, respectively. These figures are expected to reach 550MWe of power and 4000 MWt of direct use system in 2015 (Mertoglu et al, 2010). According to Parlaktuna et al. (2013), total installed capacity as of 2013 was 162.2 MWe, and

estimated projections of geothermal power and total direct use by the year 2018 are 750 MWe and 8340 MWt, respectively.

Table 2. 7: Curie temperature of some lithology or rock samples.

Description	Curie Temperature, ºC	Reference
Western Anatolia	560	Şalk et al. [2005]
56 samples [31 metamorphic grade from greenschist to granulite, 22 silicic plutonic rocks & 3 mafic supra continental samples containing pyrrohotite]	560 - 580	Williams et al. [1985]
4 samples [mafic-ultramafic granulite facies rocks & amphibolites]	570 - 580	Wasilewski and Fountain [1982]
45 samples [intrusions & gneisses of both granulite & amphibolite facies]	550 - 575	Schlinger [1985]
Continental/magnetic crust	580	Schlinger [1985], Frost and Shieve [1986] & Ross et al. [2006]
Continental/magnetic crust	520 - 560	Mayhew [1982]
Granulite xenolith	560 - 570	Wasilewski and Mayhew [1982]
Acidic rocks	> 500	Gasparini et al. [1979]
Ferromagnetic minerals in alkali-basalts & andesitic rocks	100 - 300	Gasparini et al. [1979]
Intermediate [andesitic] to mafic compositions	300 - 450	Gasparini et al. [1979]
Serpentinized mafic & ultramafic rocks [Fe-Ni-Co-Cu alloys]	620 - 1100	Haggerty [1978]

Apart from power generation, direct geothermal use of geothermal energy in Turkey is focused on individual space and district heating, greenhouse applications, balneology (estimated 260 to 400 thermal tourism facilities,) and bathing pools/spas (Basel et al, 2010; Mertoglu et al, 2010; Parlaktuna et al, 2013).

Turkey's geothermal resources are of two main categories; namely hydrothermal and hot rock (EGS - enhanced geothermal systems) resources. Most of these geothermal resources are located along the major grabens of Western Anatolia, the NAFZ and the Central and Eastern Anatolian volcanic regions (Basel et al, 2010; Mertoglu et al, 2010). For a better appreciation of the geothermal potential and results of heat flow

measurements, the concept of heat flow maps, in the form of geothermal gradients and subsuraface/surface temperature distribution is very necessary.

Table 2. 8: Curie temperature of some minerals.

Description	Curie Temperature, ºC	Reference
Pure magnetite [Fe_3O_4]	580	Gasparini et al. [1979], Dunlop & Özdemir [2001]
Hematite [αFe_2O_3]	860	Gasparini et al. [1979
Hematite [αFe_2O_3]	680	Haggerty [1978]
Hematite [αFe_2O_3]	675	Dunlop & Özdemir [2001]
Titanifrous hematite	600 - 645	Schlinger [1985]
Titanifrous magnetite	> 300	Gasparini et al. [1979]
Titanifrous magnetite	< 250	Haggerty [1978]
Titanomagnetite	150	Dunlop & Özdemir [2001]
Maghemite [γFe_2O_3]	590 - 675	Dunlop & Özdemir [2001]
Maghemite [γFe_2O_3]	545	Haggerty [1978]
Maghemite [γFe_2O_3]	545	Gasparini et al. [1979]
Iron [Fe]	765	Dunlop & Özdemir [2001]
Iron [Fe]	770	Haggerty [1978]
Pyrrhotite [Fe_7S_8]	320	Haggerty [1978], Dunlop & Özdemir [2001]
Goethite [$\alpha FeOOH$]	120	Dunlop & Özdemir [2001]
Stoichiometric [$Fe_2Ti_{0.6}O_4$]	150 - 200	Dunlop & Özdemir [2001]
Wairauite [CoFe]	986	Haggerty [1978]
Awaruite [Ni_3Fe]	620	Haggerty [1978]
Ilmentite-hematite	50 - 300	Haggerty [1978]
Copper [Cu]	1084	Haggerty [1978]
Cobalt [Co]	1123	Haggerty [1978]
Nickel [Ni]	358	Haggerty [1978]

For this reason, heat flow maps have been prepared covering Turkey on both regional and countrywide bases. For instance, heat flow maps of Turkey has been prepared by Tezcan (1979, 1995) using gradient data from at least 176 boreholes, İlkişik (1995) using silica geothermometer heat flow values estimated from 187

springs, Turkey's tempearature gradient distribution from deep wells measurement by Mihçakan et al. (2006), regional and countrywide subsuraface temperature distribution between 500 and 1000 meters by Basel et.al. (2010), Başel et.al. (2010) and other selective regional investigations such as Pfister et al. (1998) in the Northwestern Turkey based on borehole temperature and conductivity data.

In these investigations, high heat flow is observed in Western, Central and Northeastern Turkey. Temperature distribution map of Tezcan (1995) indicates approximate values of 50 - 140 mWm^{-2} over the entire country with Western, Central and Northeastern Turkey on the high side (Western Anatolia shows most areas > 100 mW/m^2 and Central Anatolia between 70 - 100 mW/m^2). Similarly, based on silica data, İlkişik (1995) conluded on a mean value of 107 ± 45 mW/m^2 for Western Turkey (Anatolia) after investigating 187 thermal springs and a mean value of 97 ± 27 mW/m^2 using the conventional heat flow data. These values are approximately 50 – 60 % above the world continental average of about 65 mW/m^2. Pfister et al. (1998) also estimated mean surface heat flux of 60 mW/m^2 for the Marmara sea region (Northwestern Turkey) with the heat flux varying between 50 – 115 mW/m^2.

The geothermally endowed region of Western Anatolia has been divided into about 10 geothermal provinces, namely (i) the Menderes Massif, (ii) İzmir, (iii) Balıkesir-Gediz, (iv) Manyas-Apolyont-Bursa, (v) Afyon, (vi) Kızılcahamam-Bolu, (vii) Ankara-Haymana, (viii) Eskişehir, (ix) Beyşehir-Konya, and (x) Kayseri-Kozakli geothermal provinces (Dam and Khrebtov, 1970). Of the nearly 300 geothermal ocurences 17 fields have reservoir temperatures above 120 ºC with almost all located in Western Anatolia (Mertoglu et al, 2010; Basel et al, 2010). Applying the Monte-Carlo simulation technique of reserve (potential) estimation over the 17 fields at a reference temperature of 100 ºC, a P10 power generation and thermal energy are given as 710 MWe and 20313 MWt, respectively (Basel et al, 2010). In totality, they analyzed 55 field and estimated a combined thermal power value of 23 556 MWt for P10 at a reference temperature of 15 ºC. In addition, using subsurface temperature distribution data and thermal gradient map of Turkey prepared by Mıhçakan et al. (2006), Basel et al. (2009) and Basel et al. (2010) estimated stored thermal energy to 10 km depth beneath Turkey at a reference temperature of 15 ºC. For instance, to a depth of 3 km, stored thermal energy beneath Turkey is estimated at an average value of $3 \pm 1 \times 10^{23}$ J. This value is nearly 67 000 times greater than Turkey's annual

energy consumption (106 million tones of oil = 4.45×10^{18}J) (Basel et al, 2009). In Table 2.9 below is a break down of thermal energy stored beaneth Turkey to 10 km.

Table 2. 9: Stored heat beneath Turkey to 10 km depth (Basel et al, 2009, 2010).

Depth Interval, km	Stored Heat, 10^{23}J
0 - 3	3.97
3 - 5	7.04
0 - 5	11.01
5 - 10	33.07
0 - 10	44.01

The conventional technique of heat flux or geothermal assesment require two most important paramenters, they include reliable temperature and thermal conductivuty. For better heat flux estimates, temperature data should be taken from boreholes or wells deeper than and the necessary corrections applied to refine the values. The second parameter, thermal conductivity is very important. Assigning a wrong thermal cocductivity value to a different lithology can lead to misleading heat flow results. The measurement of rocks or lithology conductivity are of two categories; the steady state and transients methods (Pasquale et al, 2014). The steady-state (temperature does not vary with time) approach is the method often used for heat flow calculations and involves measurement taken along the same lithology profile of temperature data. However, in the literture, most coductivity values used for heat flow estimation are assigned values based on reliable information about lithology profiles. In Table 2.10 are some conductivity values measured from lithologies or rock samples of the Turkish terranes.

2.9 Radiogenic Heat Production in Turkey

The extent of radiogenic heat (heat generated from radioactive isotopic decay) contribution to surface heat flow in Turkey has aslo been investigated in some regions, and the linear relationship between local surface heat flow and heat production analyzed. For example, Akin and Ciftci (2011) conducted analyses on 1031 data samples including volcanic, sedimentary, metamorphic and plutonic rocks collected from the Kırşehir massif region of Central Anatolia. Values of crustal radiogenic heat production range from 0.62 $\mu W/m^3$ to 5.68 $\mu W/m^3$, with an average value of 2.16 $\mu W/m^3$ for the plutonic rocks, 1.68 $\mu W/m^3$ for volcanites, 1.25 $\mu W/m^3$

for sedimentary rocks, 1.20 μW/m^3 for metamorphic rocks and on the high side, 5.68 μW/m^3 for Neogene aged volcanic and volcano sedimentary deposits. For the given

Table 2. 10: Conductivity values of lithology samples in Turkey.

Location/Lithology	Conductivity, W/mºC		Reference
	Range	Mean	
Neogene clayey formations, Turkey		2.1	Tezcan [1979]
The Kirşehir Massif			
Plutonic rocks		2.5	Akın & Çiftçi [2011]
Metamorphic rocks		2.75	Akın & Çiftçi [2011]
Volcanic rocks		1.87	Akın & Çiftçi [2011]
Sedimentary rocks		2.06	Akın & Çiftçi [2011]
Western Anatolian extensional province	1.17 – 3.05	2.127	Yemen [1999; cited in Dolmaz et al. 2005]
Sampled from113 abandoned boreholes in Southern Marmara & the Aegean region			
Andesite		1.96	Erkan [2014]
Marl		1.73	Erkan [2014]
Sandstone		4.05	Erkan [2014]
Schist		2.42	Erkan [2014]
Mean value adopted for heat flux estimation		2.1	Erkan [2014]
Thrace region, Marmara & Aegean sea			
Oligocene strata [data from 4 oil wells]		2.3 ± 0.3	Pfister et al. [1998]
Eocene strata [1 oil well]		3.1 ± 0.2	Pfister et al. [1998]
Other 44 oil wells	1.5 ± 0.2 - 3.5 ± 0.6		Pfister et al. [1998]

range of crustal heat production, with D at 10 km, the DA corresponds to crustal contribution of 6.2 – 56.8 mW/m^2, and 16.8 mW/m^2 and 21.6 mW/m^2 for volcanic and plutonic rock values, respectively. Using the heat flow – heat production plot, they estimated 8.72 km as the thicknes of the crustal radiogenic layer and 57.22 mW/m^2 as the reduced heat flow. However, due to data scattering, a 10 km value was use for calcultions instead of 8.72 km value. Surface heat flux estimates varied between 50 - 110 mWm^{-2}, with an average of 72 mW/m^2. Crustal radiogenic heat source accounted for 8% - 40% and contributions from the lower crust and mantle in between 60% - 92% of the surface heat flow.

Similarly, based on the average concentration values of U, Th and K in Cenozoic (tertiary – quaternary) volcanic rocks obtained from Western Anatolia as provided by Ercan et al. (1985), Ilkisik (1995) used this data and calculated the mean radiogenic heat production as 3.73 $\mu W/m^3$, and between 3 – 4.5 $\mu W/m^3$ using seismological models. The assumed thickness value is between 13 – 15 km as the radiogenic zone (following Royer and Denis, 1988, estimates of similar terrains), the DA, an overall crustal contribution to surface heat flow is therefore between 50 – 60 mW/m^2.

3. DATA AND TECHNIQUES OF HEAT FLOW GENERATION

Two main data sources have been used for generating the deep geothermal gradient and deep-subsurface temperature distribution in Turkey. They are the Curie depth-temperature pair data and deep-well temperature measurement data obtained either or both from well logs and drill-stem tests (DST). The processes used in generating these data are discussed in the following sections.

3.1 Regeneration of Curie Depth Map of Turkey

There rarely exist direct temperature measurements at depths of 7 km and beyond. For this reason and for achieving the objective of this research, the most reliable, but indirect technique of Curie depth-temperature pair datum in the Earth was employed. First, the Curie-point depth (CPD) map of Turkey (Appendix B) prepared by MTA (2007) was digitized, gridded (grid spacing of 0.1×0.1 m or arc minutes) and remapped (Figure 3.1) using the Generic Mapping Tools (GMT) program, developed by Wessel and Smith (2013, version 4.5.9). The CPD values of the digitized data are between approximately 6000 m to 27500 m. Note that in Figure 3.1 the readings below 6000 meters (shallowest CPD) on the scale bar occurred because of the interpolation. The excess is about 400 meters and has very little or insignificant effect on the estimated temperature gradient values for the region.

The CPD within the Earth crust defines the point at which substances (rocks and/or minerals) passes from ferromagnetic state to paramagnetic state under the effect of increasing temperature. Its twin term, the Curie temperature, refers to the measure of temperature at which minerals loses their ferromagnetic properties (Beardsmore and Cull, 2001; Aydin et al, 2005; Şalk et al, 2005). The CPD is calculated to the basal (bottom) depth of the magnetized bodies. Secondly, it must be noted that CPD values of Figure 3.1 are given below the mean sea level datum. Therefore to obtain CPDs to ground level or from surface to the basal depths of the magnetized bodies, the CPD map was overlaid with the topography data of Turkey, shown in Figure 3.2. That is,

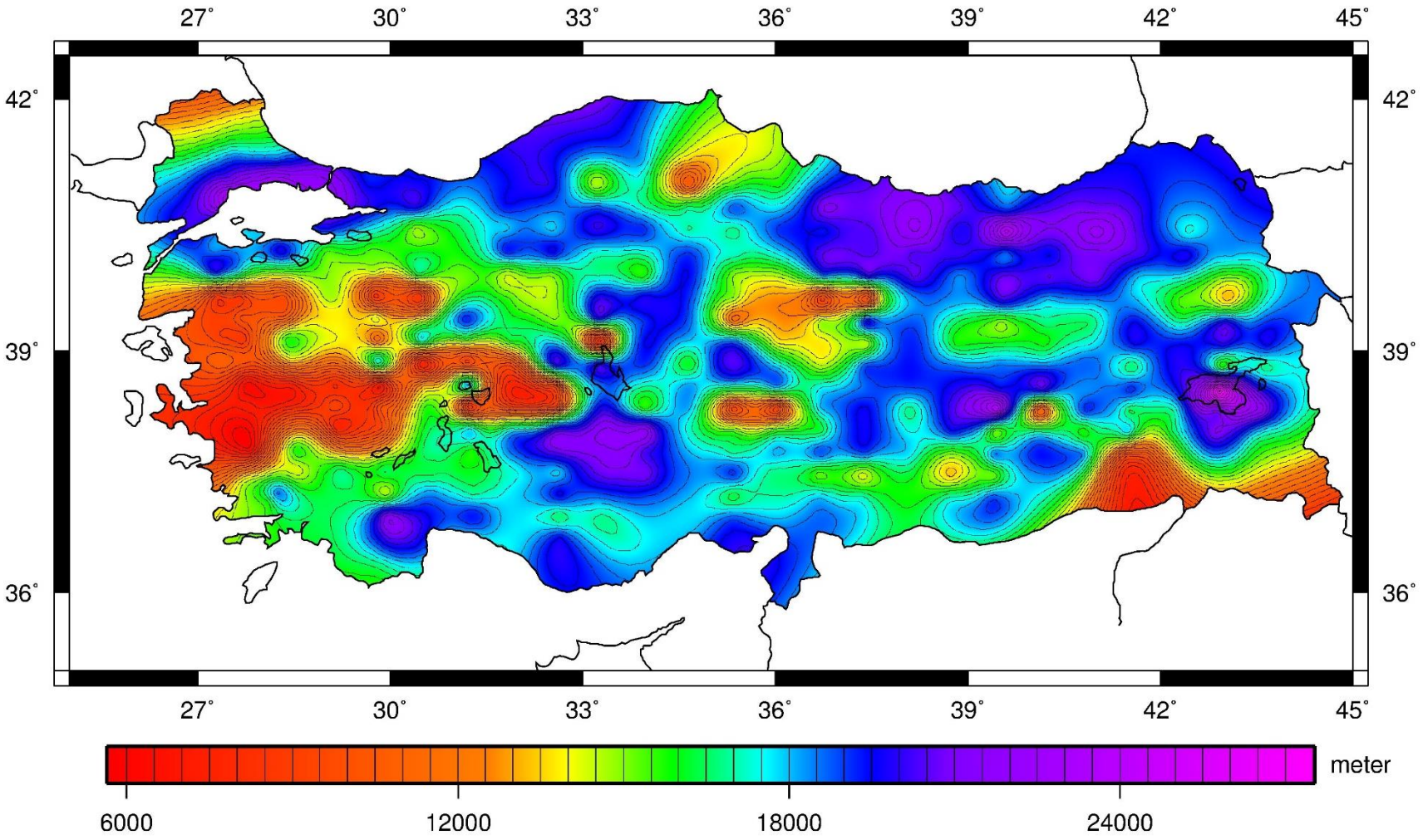

Figure 3. 1: Curie-point depth map of Turkey (modified after MTA, 2007).

the topography data was similarly gridded at the same grid spacing (0.1×0.1 m) to match the gidded CPD data coordinates and, then, added together to obtain the final CPDs to the surface.

After adding the two sets of data together, the minimum and maximum CPD range generated became approximately 6300 m (average value) to about 30 000 meters as shown in Figure 3.3. Note the wavy effect of topography data in the final CPD map of Figure 3.3. The topography map of Turkey (Figure 3.2) is produced from the digital elevation model topography data (grid spacing of 3×3 arc seconds) base of the USGS (U. S. Geological Survey) digital data series. The data is later resampled (grid spacing of 0.1×0.1 m), and then added to the CPD data (Figure 3.1) to produce the desired CPD data and map (Figure 3.4) from the surface to the bottom of the bodies responsible for causing magnetic anomalies. The highest peak in the topography data is about 5100 meters.

3.2 Re-evaluation of Deep Well Temperature Measurement Data

Mıhçakan et al. (2006) database for temperature measurement data, obtained mostly from deep oil and gas and some geothermal wells, is re-evaluated. The current data set is composed of 530 data points of measured temperatures in deep wells across Turkey. Few deep-well temperature data from Greek islands in the Northeast Aegean Sea are also included. The temperatures are between 18.9 ºC to 350 ºC at varying depths between 520 to about 5000 meters. Per the standard or criteria of this study, the data at depths less than 700 meters are eliminated. The remaining 520 data points are grouped in terms of depth. The first data set with 499 data points falls between 1000 and 5000 m, and the second data set with 21 data points falls between 700 and 999 m, most of which is above 800 m. Mıhçakan et al. (2006) also used the selected 520 data points to generate the subsurface geothermal gradient distribution map of Turkey, in Figure 3.5. The subsurface gradient distribution in the map ranges from 0.88 ºC/100 m to about 19 ºC/100 m, and the red lines indicate the various fault lines. However, for the peculiar nature of the current study, all offshore data (6 data points) are eliminated since the CPD data covers only the continental landmass of Turkey (except the Marmara Sea). Thus, limiting the study to the main continental landmass of Turkey implies a further reduction in data to 514 measured temperature points.

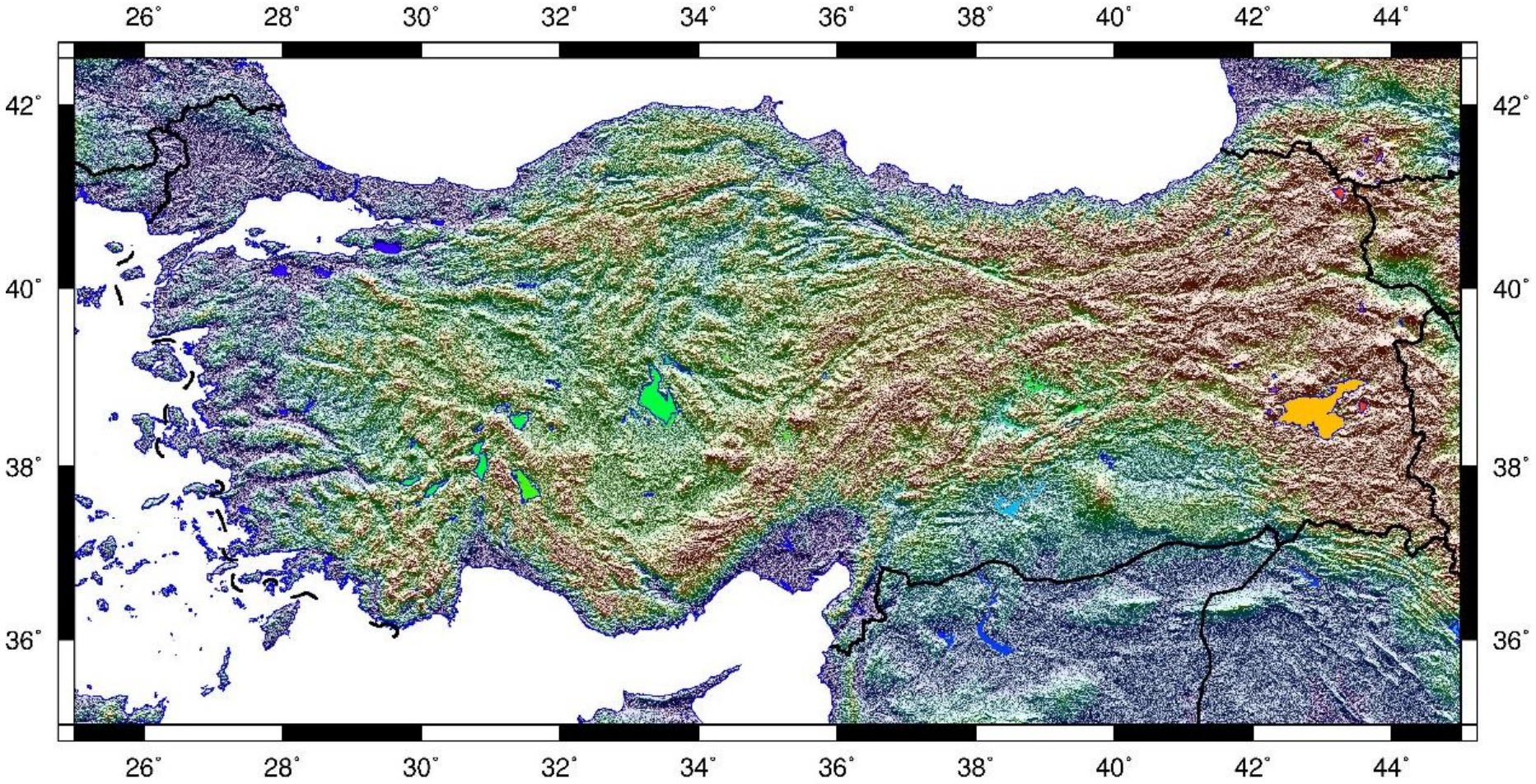

Figure 3. 2: Topography map of Turkey (digital elevetion model data taken from the USGS).

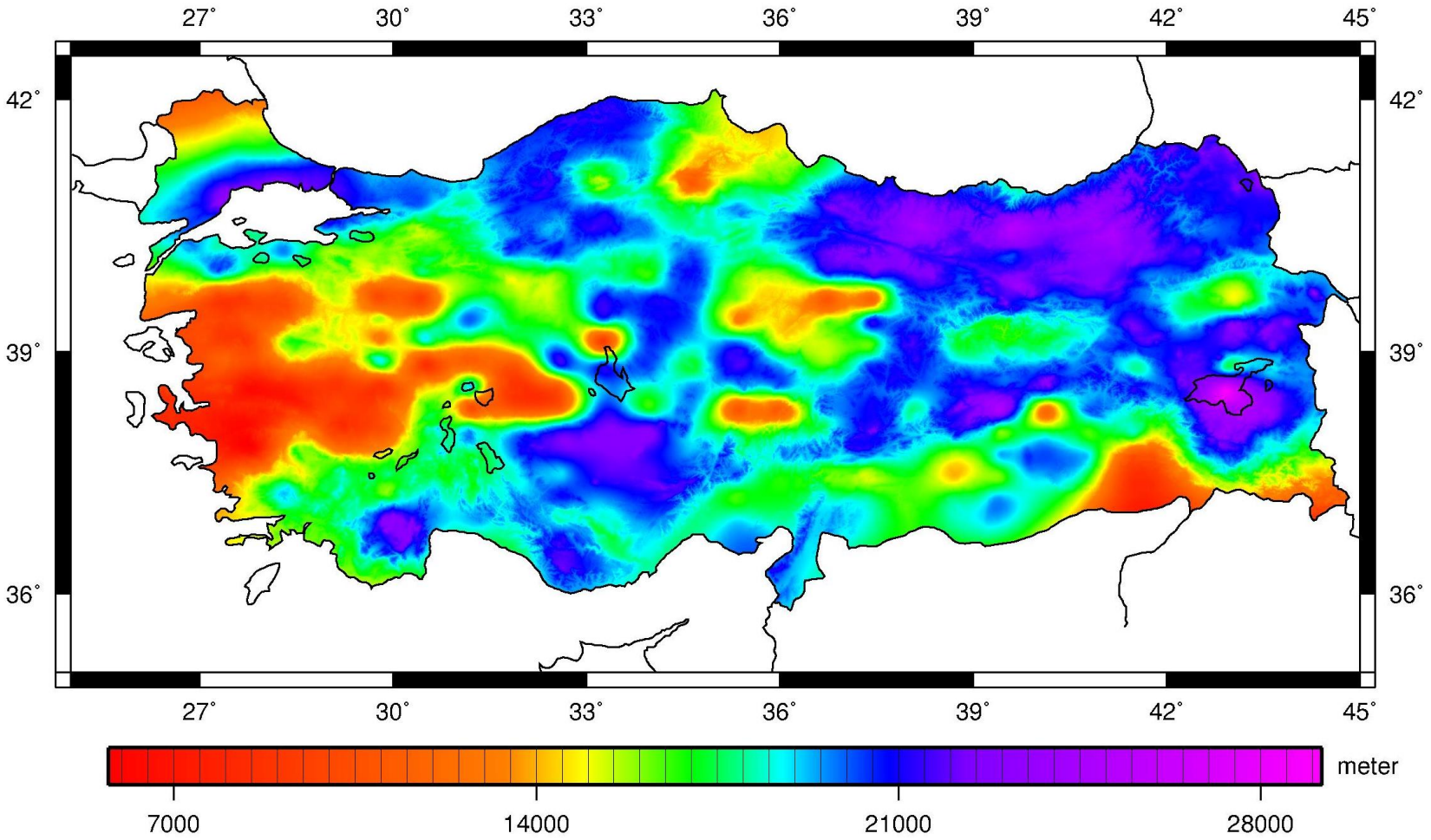

Figure 3. 3: CPD map of Turkey from ground level (modified after MTA, 2007).

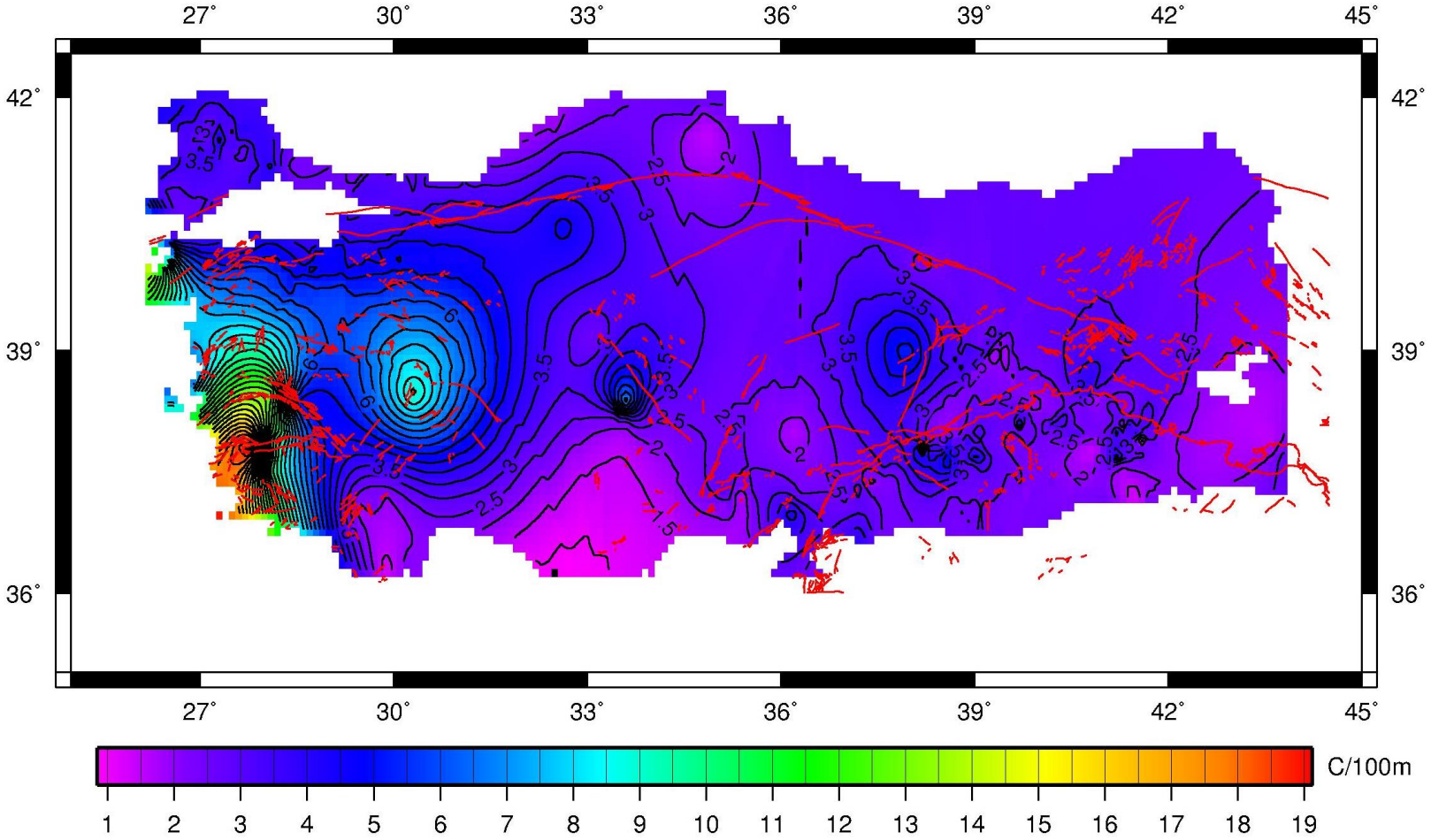

Figure 3. 4: Subsurface geothermal gradient map of Turkey to depth of ~5 km (modified after Mıhçakan et al, 2006).

These temperature data points are then grouped into fields or clusters, particularly, in areas of the Thrace part and the Southeastern border regions of Turkey, where data density is high. For a data point to belong to an oil and gas field the rule is arbitrarily set as it should not exceed a 5 km radius from the nearest neighbor or data point in the field. Data points, located exceedingly outside the fields and regions with single data point, are evaluated independently. By this process, data points affected by surface water circulation, topography, and drilling mud effects among other factors are identified and eliminated from the data set.

3.3 Deep-subsurface-thermal Gradient Estimation

As part of the correction process, unreliable temperature readings or measurements are identified based on the gradient plots analysis of data from each given field. This process 'cleans up' the data through the determination of the most appropriate best-fit line for the field. All data points, particularly those deemed to be in error in terms of temperature measurement are eliminated and the least disturbed data points (most stabilized temperature readings) chosen to represent the field. In general, data in the relatively high-density data areas are put into 51 fields (data within 5 km radius from the nearest data point) and their respective gradient plots made and then analyzed. Figure 3.5 (a) through to (h) are some examples of such gradient profiles. Figure 3.5 (a) is the gradient profile in Adıyaman field. Data distribution in terms of distance (or radius) from the nearest data points to the farthest data points is 0.5 km and 9 km, respectively. The 9 km data point qualifies to be part of the field because it falls outside the defined 5 km distance with respect to only two data points within the field whereas its distance to the rest of the data points is within the 5 km radius range. It is also expected that the temperature measurement of this data point should correlate with temperature measurements of points to which it is closer ($\leq$ 5 km) to within the field.

However, the data point A in Figure 3.5 (a), which falls within the range, has a high temperature recording that is uncharacteristic of the given area. It is believed that the high temperature value recorded for this data point may be a data entry error and the data point is therefore discarded. The point labeled B falls consistently ($\sim$ 85 km) outside the range to all data points and also has an unreliable temperature reading. In effect, two data points (indicated by thick black arrows) are chosen to represent the

Adıyaman field. Similarly, the Batı Raman field has the nearest and farthest distance as 0.3 km and 9 km (to 3 data points), respectively**.** Data points indicated with the thick black arrows are data chosen to represent the Batı Raman field. Data points C and D fall outside the 5 km distance. Most of the temperature measurements have perturbation effects due to insufficient equilibration time before the temperature measurements were taken. Three data points are chosen to represent this field and are shown by the thick black arrows. The temperature measurement taken at Soğuktepe field, Figure 3.5 (c), is data in the same well at two different depth intervals. The thick black arrows indicates all selected data points in the gradient profile analysis. The nearest and farthest points are between 0.5 – 2.8 km in Güney Karakuş field, 1.7 – 3.9 km in Güney Dinçer field, 0.03 – 0.8 km in Umurca field, 0.2 – 3 km in Çemberlitaş field, and 0.6 – 4.1 km in Hamitabat field. The data point marked red in the Çemberlitaş field has depth less than the cut off depth of 700 meters.

Upon the completion of the analysis, 318 data points are selected from the 514 deep-well temperature measurements. The selected data (318 data points) include the data from regions with single data points, which are also evaluated independently and used so. The exact CPDs beneath these data points or coordinates were obtained from the CPD data file (with topography) using the grdtrack command of the GMT software, and the deep subsurface temperature gradient distribution (Figures 3.6 and 3.7) is estimated using equation 3.1.

$$\frac{\Delta T}{\Delta Z} = \left[\frac{T_{CPD} - T_{DW}}{D_{CPD} - D_{DW}} \right] \qquad \textbf{(3.1)}$$

The parameters T_{CPD} and T_{DW} are the Curie-point depth temperature and deep well temperature, respectively. The T_{CPD} is the temperature at D_{CPD} (Curie-point depth of data point) and T_{DW} the temperature measured at D_{DW} (deep well depth at which temperature is measured).

For the purpose of this study, an average Curie isotherm of 560 ºC is chosen as the temperature at which the crustal rocks beneath Turkey loses permanent magnetic properties. Based on the 560 ºC value, the extracted CPD values, the deep well temperature measurements and the corresponding depth of measurements, a deep subsurface thermal gradient distribution of Turkey is estimated between 2.28 ºC/100 m to 11.10 ºC/100 m. Also, assuming a magnetite dominant magnetic crust, and at

the conventional Curie isotherm of 580 ºC (Curie temperature of pure Magnetite), the deep subsurface thermal gradient estimates are between 2.37 ºC/100 m to 11.56 ºC/100 m. Figures 3.6 and 3.7 below are the deep subsurface thermal gradient distribution maps based on Curie isotherms of 560 ºC and 580 ºC, respectively. The abbreviations AD refers to Ağrı dağı (Mount Ararat), whereas AL, AY, GH and SK refers to Alaşehir, Aydın, Gümüşhane, and Şırnak cities, respectively

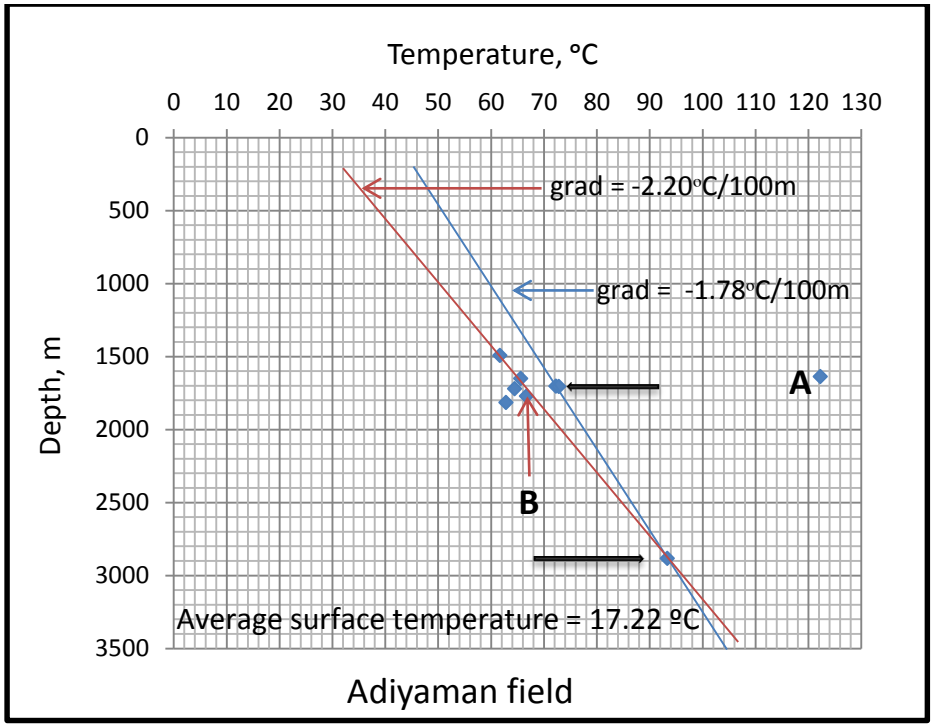

(a)

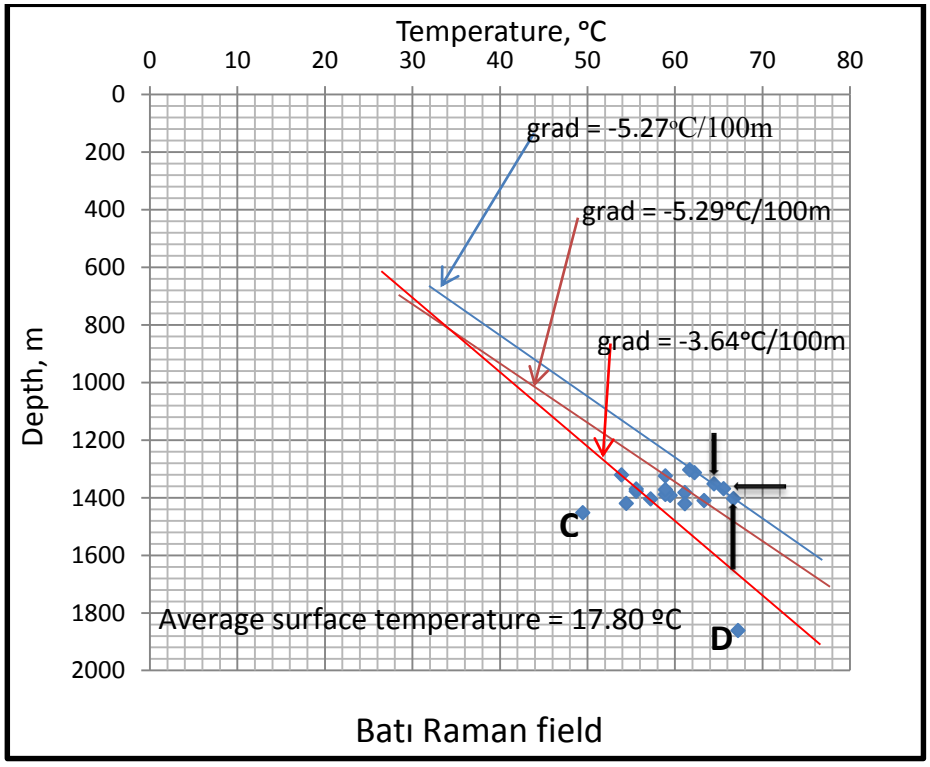

(b)

Figure 3. 5: Gradient profile analysis of field data.

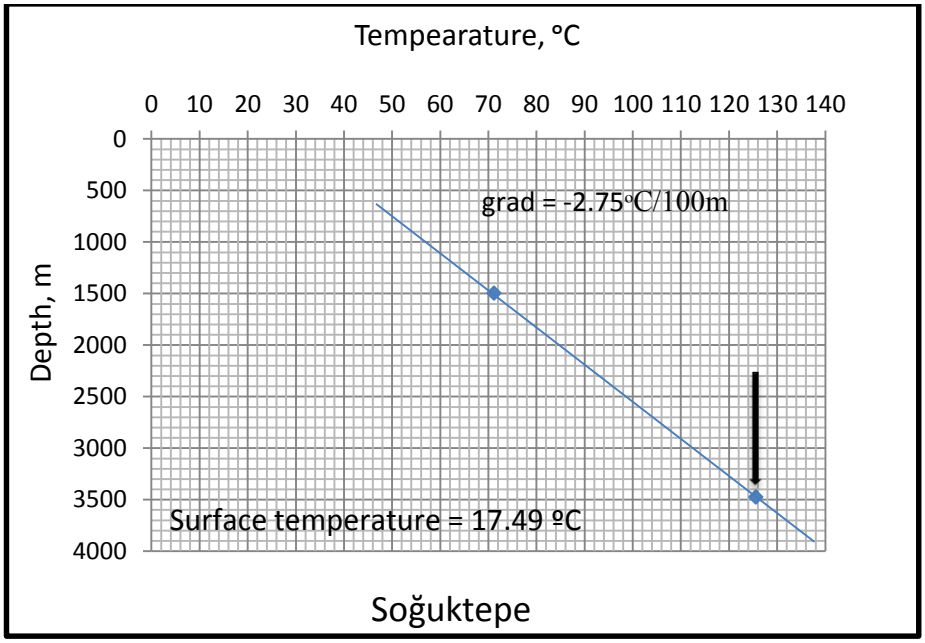

(c)

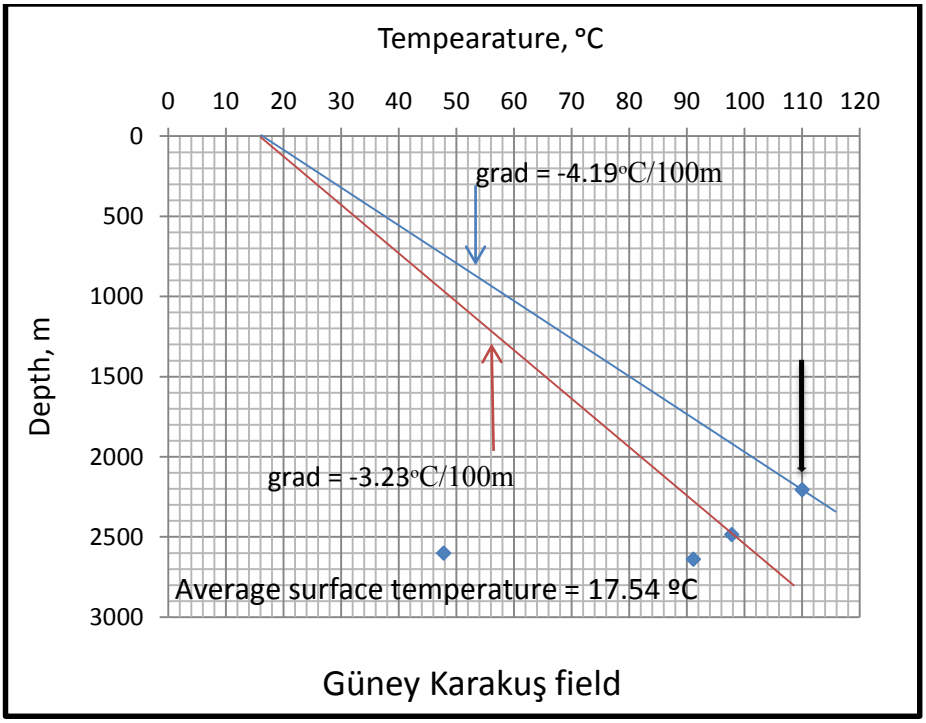

(d)

Figure 3.5 (continued): Gradient profile analysis of field data.

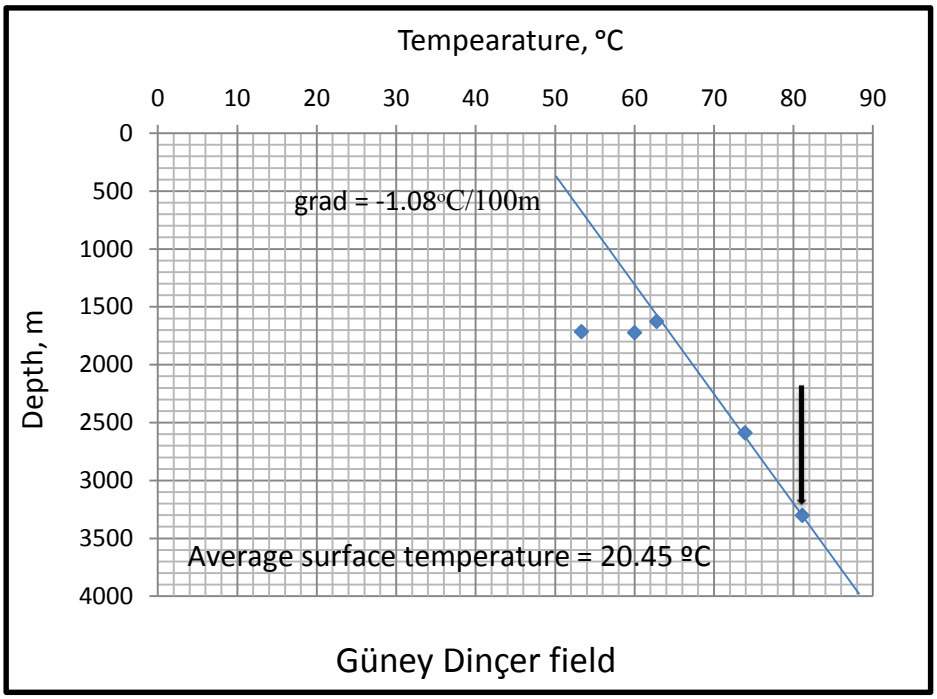

(e)

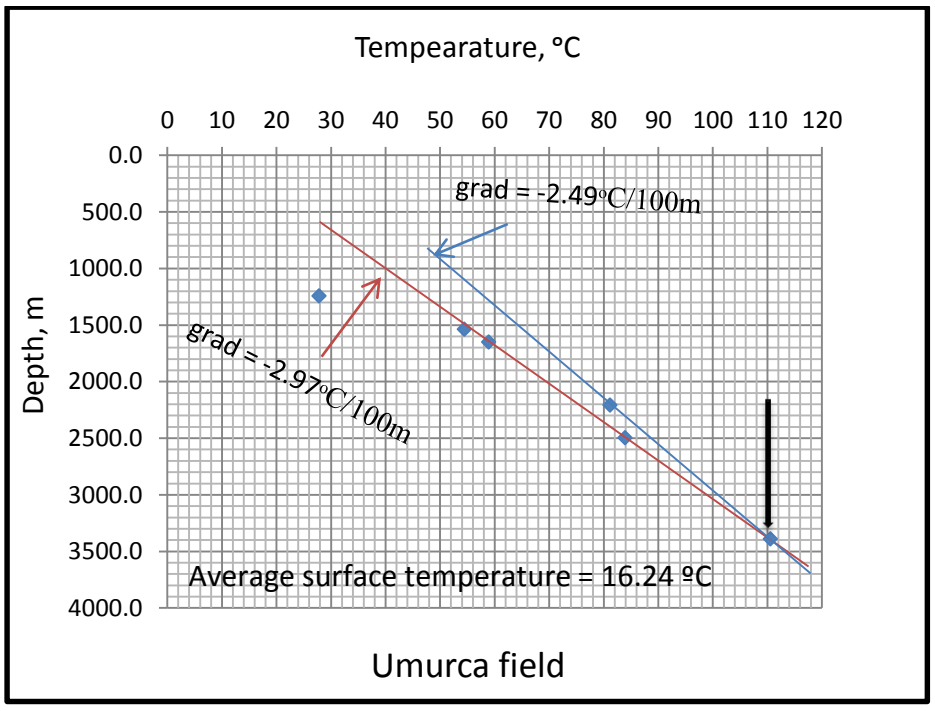

(f)

Figure 3.5 (continued): Gradient profile analysis of field data.

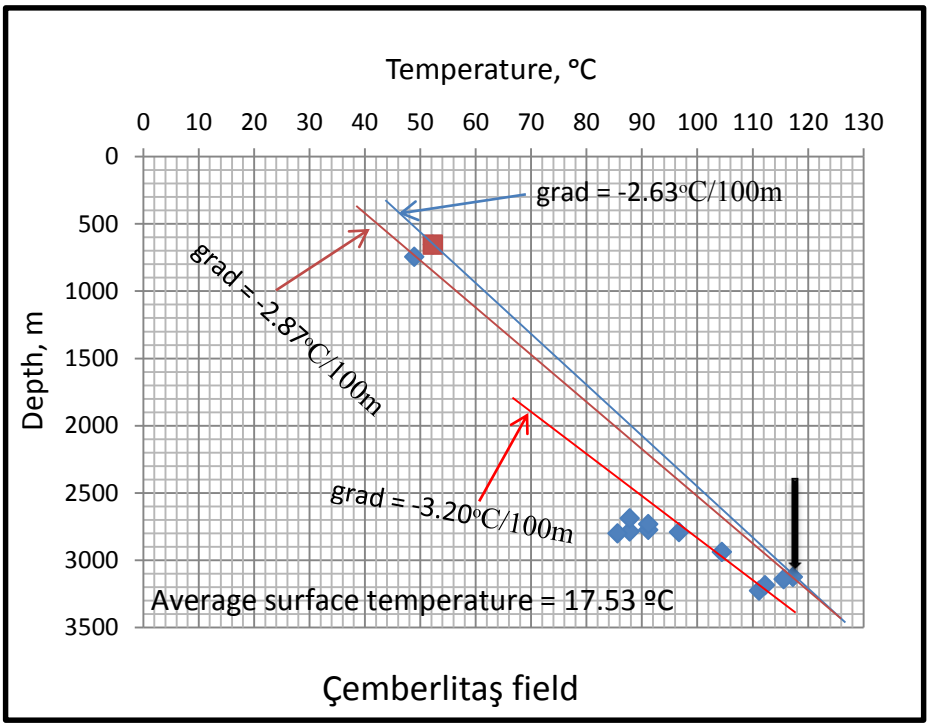

(g)

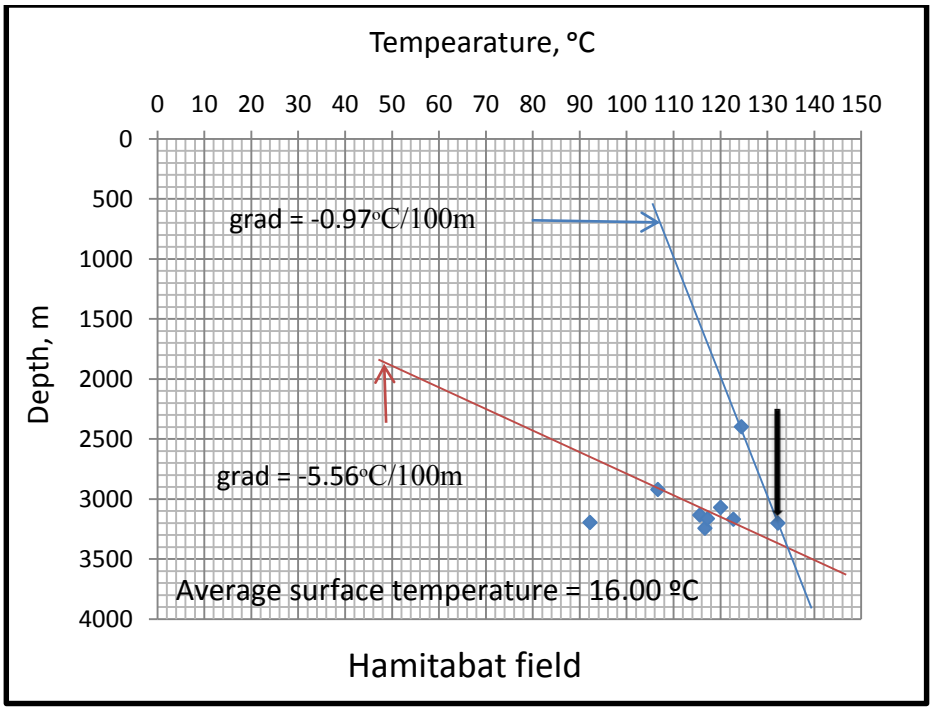

(h)

Figure 3.5 (continued): Gradient profile analysis of field data.

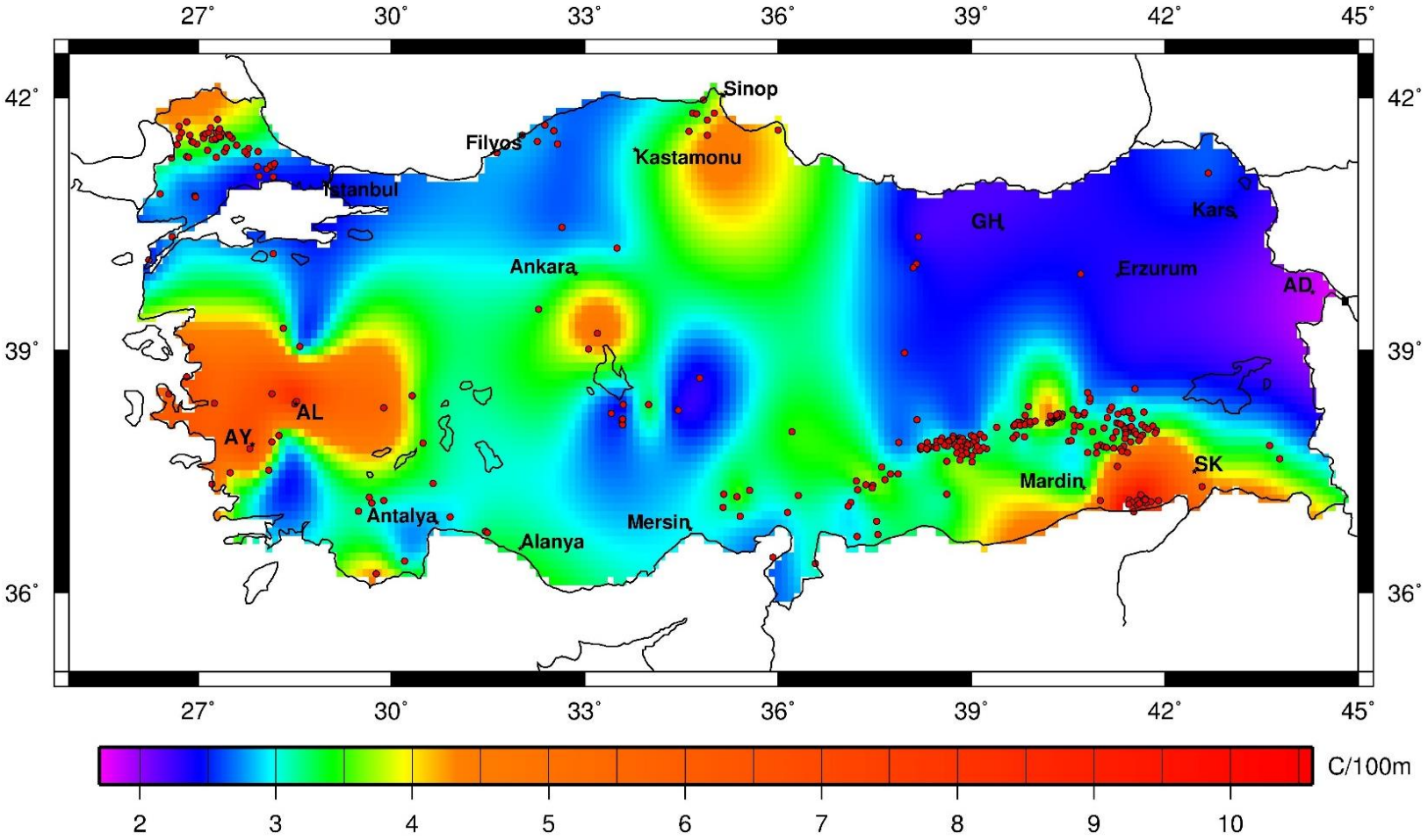

Figure 3. 6: Deep subsurface temperature gradient map of Turkey between depths of ~5 km to ~30 km for a Curie isotherm of 560 ºC.

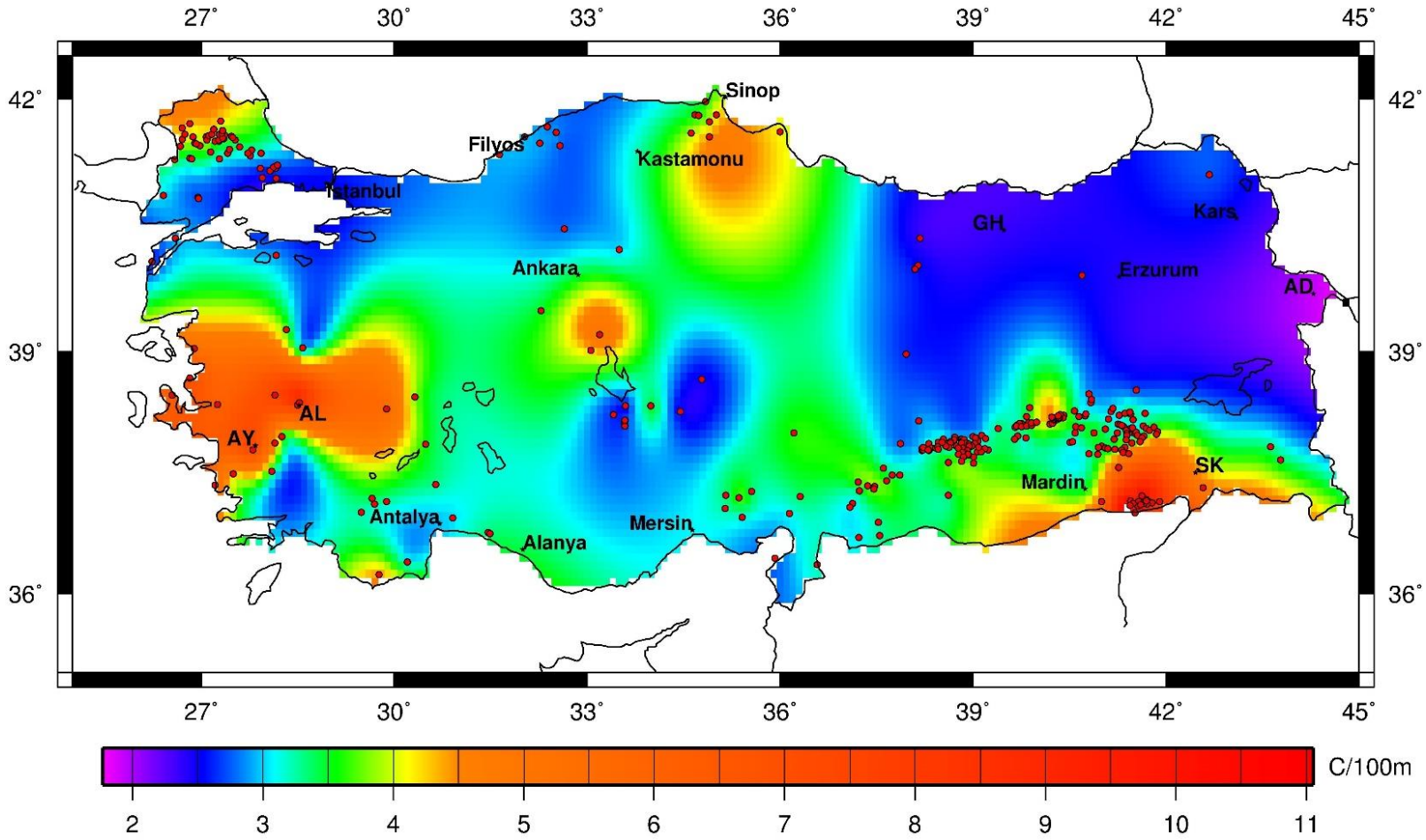

Figure 3. 7: Deep subsurface temperature gradient map of Turkey between depths of ~5 km to ~30 km for a Curie isotherm of 580 ºC.

3.4 Deep-subsurface Temperature Estimation

Subsurface temperature distribution may easily be estimated using the deep subsurface temperature gradient maps of Figures 3.6 and 3.7**,** and also, data such as the Mıhçakan et al.(2006) map of Figure 3.4. However, an initial attempt to estimate the subsurface temperature distribution at 2000 m (2 km) using the deep subsurface temperature gradient (T_g, ºC/m) data of Figure 3.6 and assuming a constant conductivity coefficient (λ) of 2.1W/mºC resulted in extremely very low and/or negative temperature values. In this attempt, heat flux (Q_c, W/m2ºC) is first determined using equation 3.2 (Fourier's law) and then the subsurface temeperature at 2000 m (T_{2000m},ºC) estimated using equation 3.4.

$$Q_C = \lambda T_g \qquad \textbf{(3.2)}$$

$$Q_C = \lambda\left[\frac{T_{CPD} - T_{2000m}}{\Delta D}\right] \qquad \textbf{(3.3)}$$

$$T_{2000m} = T_{CPD} - \frac{Q_C\left(D_{CPD} - 2000\right)}{\lambda} \qquad \textbf{(3.4)}$$

After examinig the the subsurface temeperature results at 2000 m using equation 3.4, it was realized that data points that produced either very low and/or negative temperature values had similar data distribution pattern. Firstly, these data points have their respective temperature measurement depth deeper than 2000 m, secondly, most of these data points (except two data points) have shallow Curie depth (average value of 7654 m) and are concentrated in the region between Mardin and Şırnak, and finally, the measured temperature values of these data points are relatively lower as compared to meaurements at similar depths in regions of similar Curie-point depth such as the West Anatolian region.

As a result of the above problem, a different methodology is devised to estimate the subsurface temperature distribution. In this approach, the CPD data, deep well data and surface temperature data for all the selected 318 data points obtained by the gradient profile analysis are plotted using the exponential fit graphs. The exponential function graphs produced the best results in the trial process as compared to other graphs of the various functions. However, it must be noted that most of the data

points did not generate good fits as shown by the blue trend line in Figures 3.8 (a) and (b). On the contrary, some data points also produced very good fits as shown in Figures 3.8 (c) and (d). A major reason for this misfit of some data points is that the available surface temperature data (measured at one meter depth beneath Turkey) is largely unreliable. A one-meter depth surface temperature would be greatly affected by climatic conditions and near-surface hydrothermal circulation. For this reason, a uniform approach is adopted, where by the exponential functions defined by the trend, T_a (shown by the red trendline), for the 318 data points are used for the subsurface temperature estimation. Equation 3.5 is the exponential function, where T (ºC) is the subsurface temperature distribution (valid between 1000 m to the CPD shown in Figure 3.3) and the depth, D (meters). The coefficients "a" and "b" of equation 3.5 are mapped and shown in Figure 3.9 and Figure 3.10, respectively.

$$T = a\ell^{bD} \quad \textbf{(3.5)}$$

Using the calculated values of coefficients "a" and "b" (Figure 3.9 and Figure 3.10), the subsurface temperature distribution beneath Turkey at depths of 2000 m (2 km) and 5000 m (5 km) are estimated and mapped as shown in Figure 3.11 and Figure 3.12, respectively. The subsurface temperature distribution at 2 km (Figure 3.11) vary between 20 ºC to 265 ºC, whereas that of 5 km (Figure 3.12) depth is between 40 ºC to 455 ºC. The highest subsurface temperature values are located in Western Anatolia.

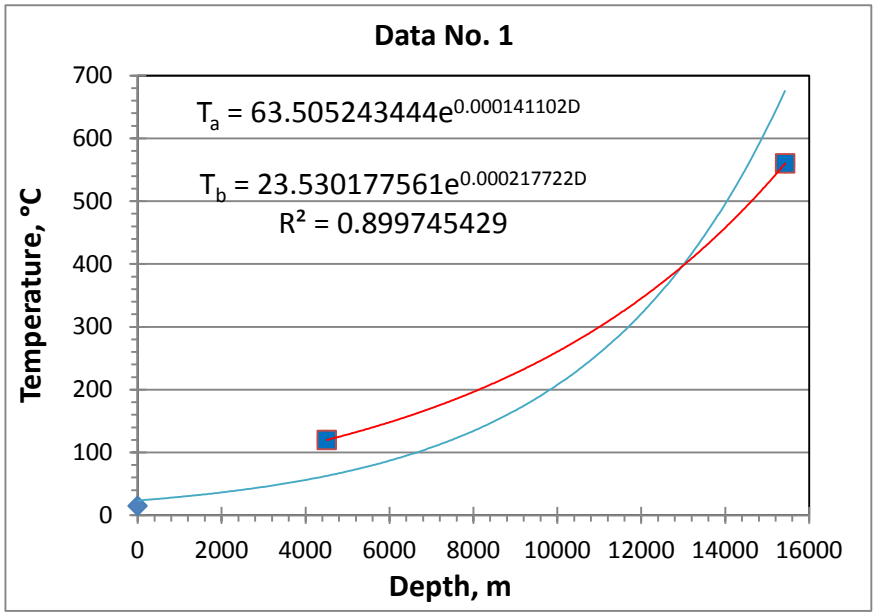

(a)

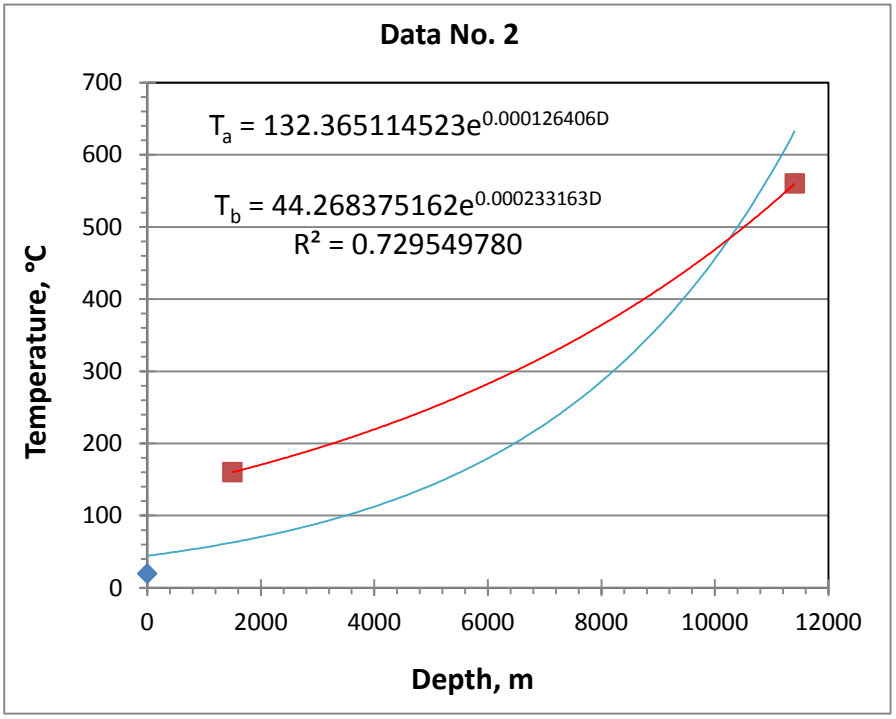

(b)

Figure 3. 8: Sample graphs of exponential function.

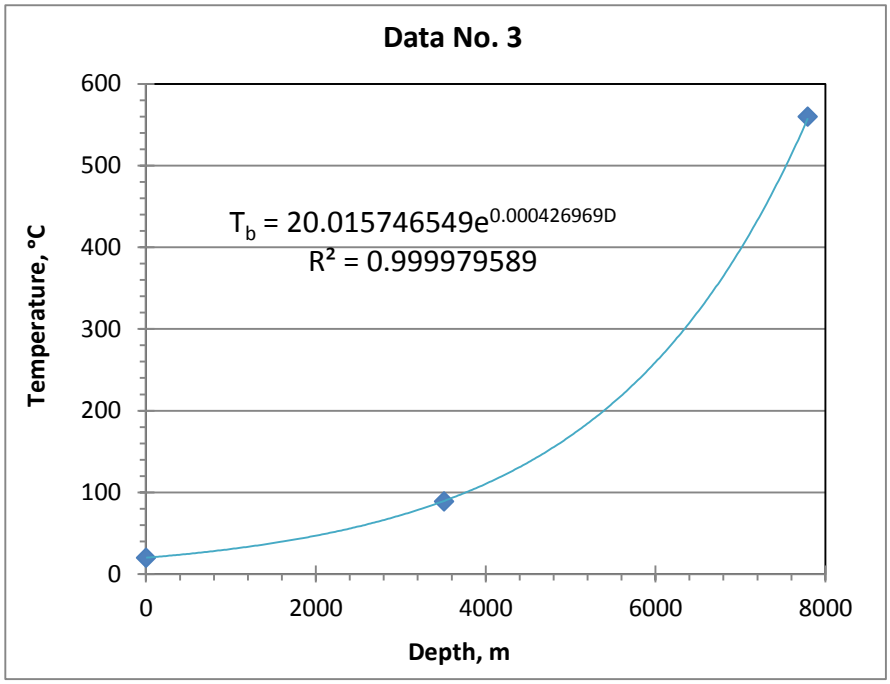

(c)

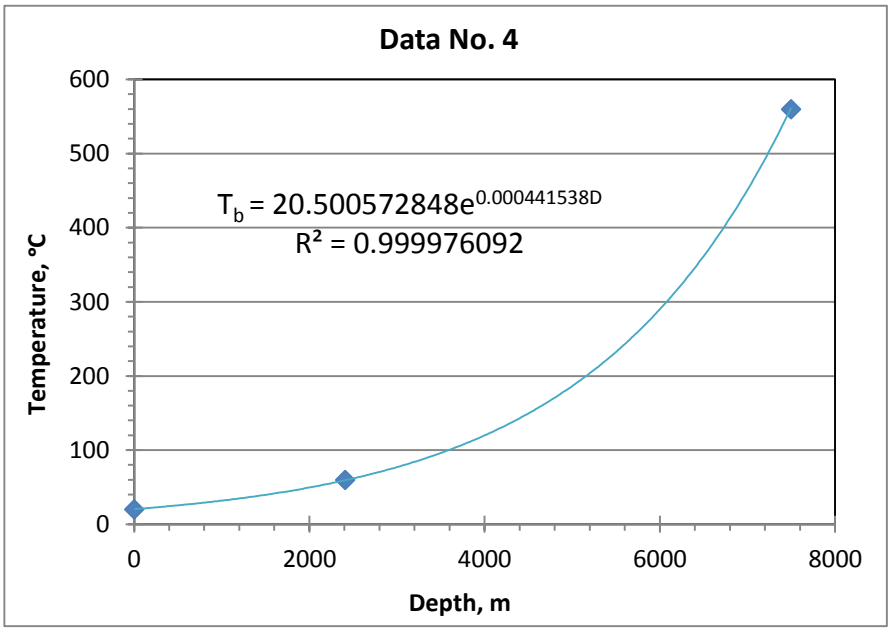

(d)

Figure 3.8 (continued): Sample graphs of exponential function.

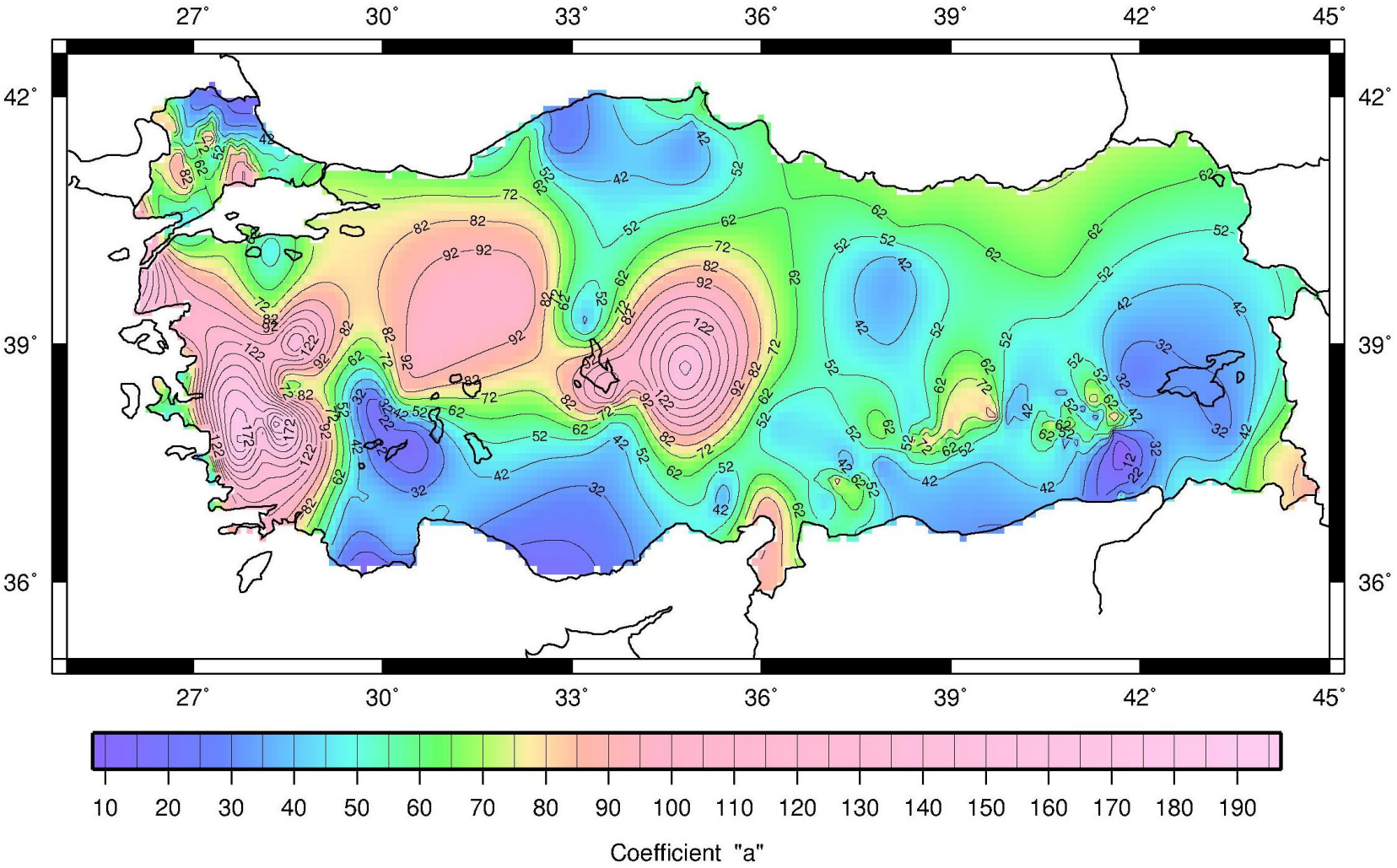

Figure 3. 9: Map of coefficient “a” distribution.

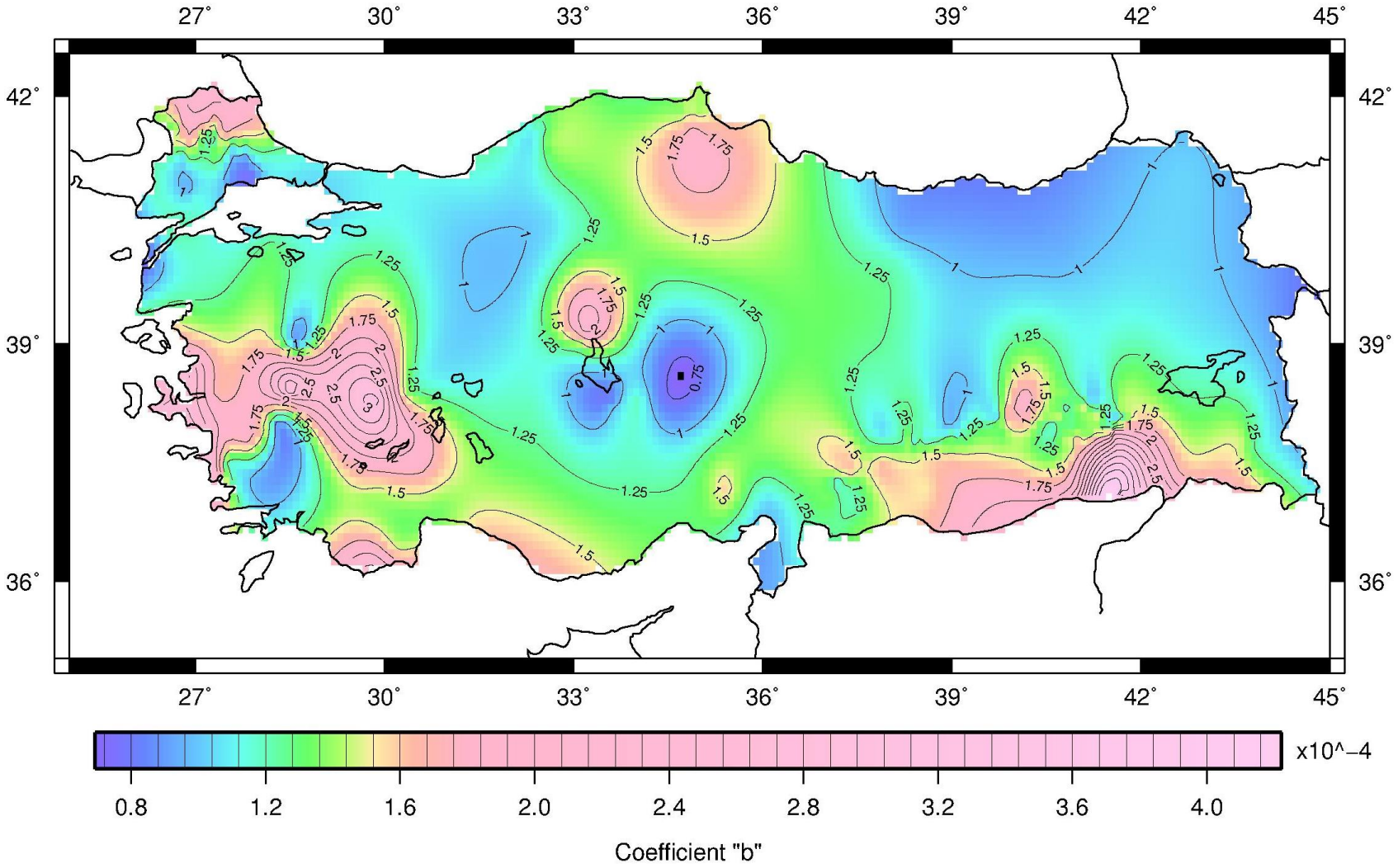

Figure 3. 10: Map of coefficient “b” distribution. .

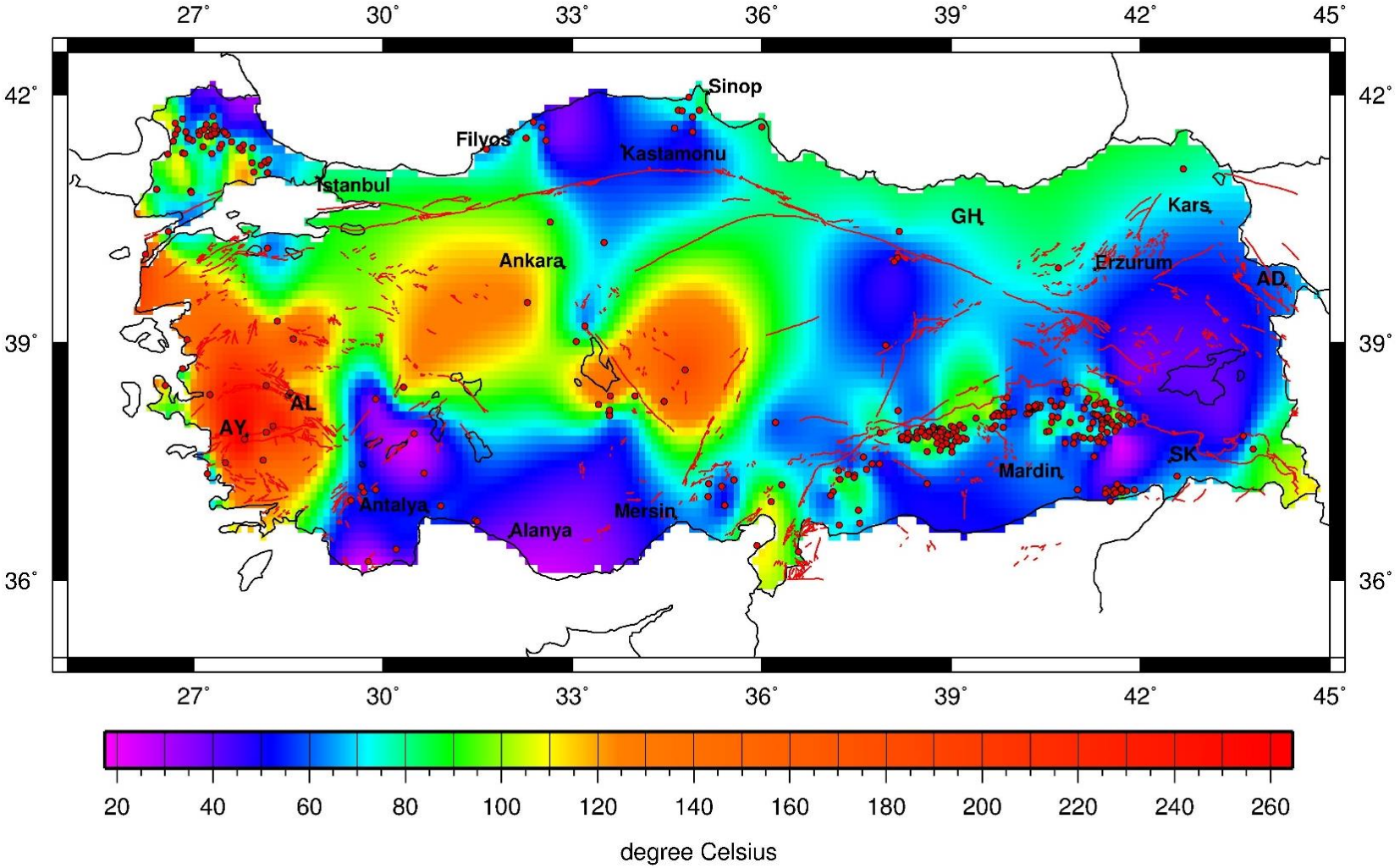

Figure 3. 11: Map of deep-subsurface temperature distribution beneath Turkey at 2 km depth.

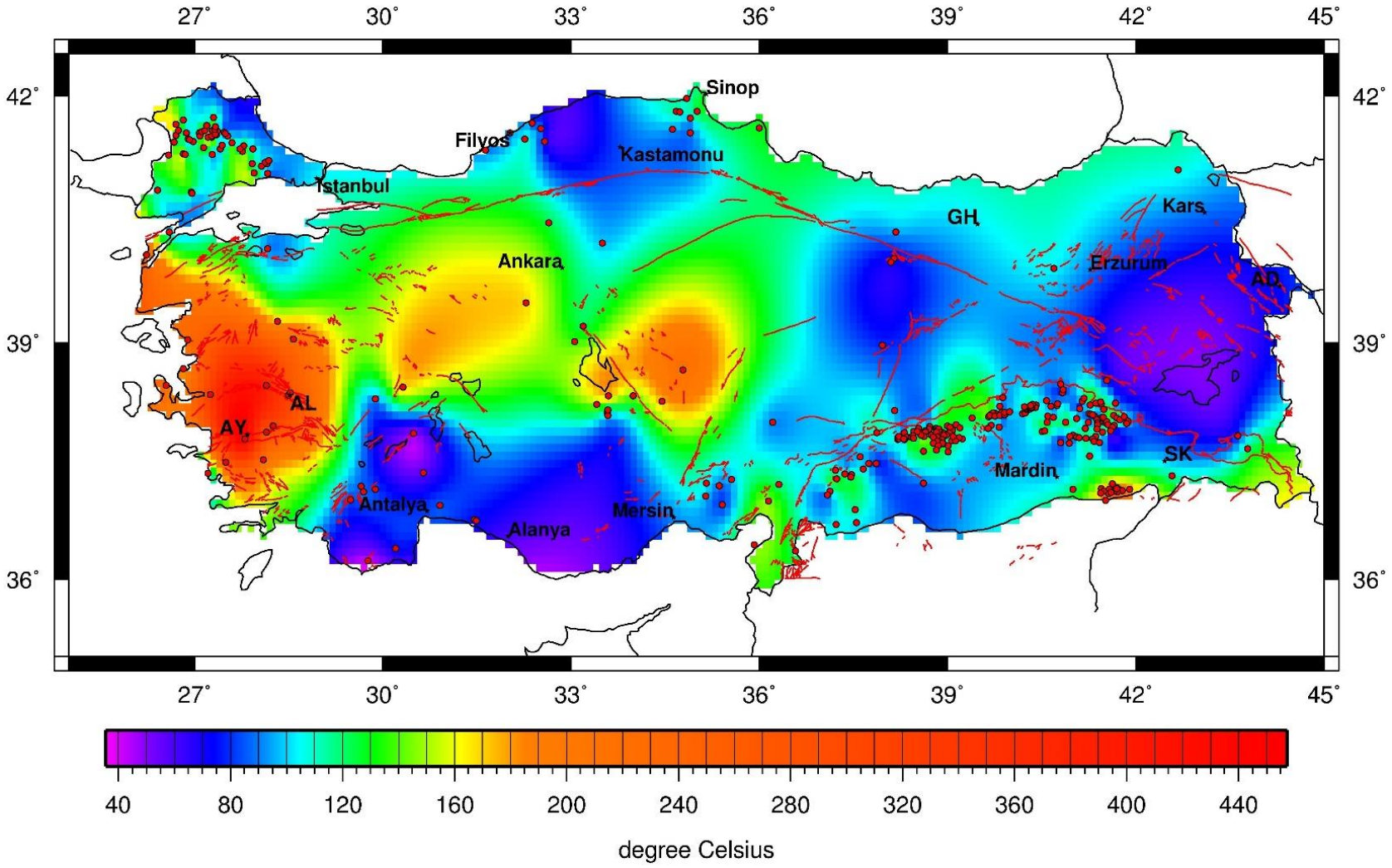

Figure 3. 12: Map of deep-subsurface temperature distribution beneath Turkey at 5 km depth.

4. DISCUSSION OF THE RESULTS

As observed in both Figure 3.6 and Figure 3.7 above, the 560 ºC and 580 ºC Curie isotherm based gradient distribution maps does not show much significant change in the extreme gradient values (that is, the calculated minimum and maximum values, and of course the gradient distribution). Therefore, a conservative value of 560 ºC is appropriate as confirmed by Şalk et al. (2005) estimate (560 ˚C Curie isotherm) for the region of Western Anatolia. In general, the gradient distribution shows an almost the same pattern as the CPD map of MTA (2007), however, some few areas do not coincide with the gradient distribution as was expected.

For instance, the highest and lowest thermal gradient does not coincide with the shallowest and deepest CPDs. The highest thermal gradient (> 8.33 ºC/100 to 11.10 ºC/100 m) corresponds to the hot spot located between Mardin and Şırnak, extending to the southern parts of Batman and Siirt. This hot region extends in both west and eastwards directions stretching to the southeastern corner in the region of Hakkari, Yüksekova and Şemdinli in the Turkish-Iraq-Iranian border and along the Turkish-Syrian border regions (Akçakale, Şuruç, Urfa, Şanlıurfa and Viranşehir areas, and the ragions of Kahramanmaras, Pazarcık, Akpınar, Samsat, Kırmacık and Bozova). Even though Western Anatolia has the shallowest CPD, the highest gradient in this region is about 8.33 ºC/100 m in the area around Alaşehir, Baklacı, Akkeçili and Erenköy. The highest gradients' distribtion perhaps reflect the Curie-point depth map of Turkey prepared by Aydın et al. (2005, Figure 4). In this map, two spots, namely the Menderes Massif region of Western Anatolia and the southeastern hot spot between Mardin and Şırnak are identified as the regions with the shallowest CPD value of 6000 m. Other high gradient regions include the area south of the Thrace basin (Kırklareli Lalapaşa Kofçaz Dereköy Erdırne and Süloğlu areas) and the Central Pontide region of Kastamonu, Sinop, Boyabat, Vezirköprü and Samsun.

The lowest gradient of about 2.28 ºC/100 m is located in the eastern Pontic Mountain regions around Şebinkarahisar, Reşadiye, Alurca and Gümüşhane (although the deepest CPD is located in south Van Lake region of southeastern Turkey). In general,

lower gradient regions include the southern or coastal areas of the Marmara Sea (Alipaşa, Çelkik and Silivri areas) of European Istanbul; the Konya area, including southern portions of Aksaray and Tuz gölü (Lake Tuz); the middle to upper northern section of eastern Turkey and little portions of Van Lake region. However, it is important to note that in the eastern border areas of Turkey, the regions of Ağrı Dağı (Mount Ararat volcanic cones) or the Ağrı Province, including the areas of Doğubayazıt, Iğdır, Kars and Erzurum boredering Armenia, Nakhichevan and Iran had almost no data. Therefore a value of below 2.ºC/100 m may not be representative of the area and must be used with caution. Furthermore, it is also important to indicate that temperature gradients in the farthermost region, north of the Thrace basin must be used with caution because of inadequate data representation in those regions.

The subsurface gradient distribution of Mıhçakan et al, (2006, Figure 3.4 above) determined from the deep well temperatures gives approximate CPDs, especially for regions with thermal gradients between 0.9 ºC/100 m to 11 ºC/100 m (with the exception of the high gradient region of the southwestern portion of Western Anatolia). The subsurface high gradients estimated for Western Anatolia (Figure 3.4) are understandable since these estimates are to approximate depths of about 5km. These gradients increase towards the coast and thus, reflect the high subsurface temperature values (maximum value of 350 ºC) obtained from the islands of the Aegean Sea.

Comparing the subsurface temperature distribtion of Figure 3.11 (2 km depth) and the Mıhçakan et al, (2006, Figure 3.4 above), the parttern of subsurface thermal distribution of the two maps is basically the same. Furthermore, it can be observed that in Figure 3.11, the shallow Curie-point depth region between Mardin and Şırnak has very low temperatures (average value of 58 ºC) at the 2 km depth. However, at the 5 km depth, the the subsurface temperatures increases to an average value of 193 ºC. At an average depth of 7654 m, the subsurface temperarture in the region is expected to reach 560 ºC. As shown in the two subsurface temperature distribution maps (Figures 3.11 and 3.12), the ative extensional region of Western Anatolia has the highest subsurface temperature estimates.

5. CONCLUSIONS AND FUTURE WORK

The study reveals a prodigious geothermal potential in terms of heat stored in hot dry rocks. These potentials are menifested in the high values of deep subsurface thermal gradient values in the southeastern corner of Turkey, Western Anatolia, portions of Central Turkey (north of Tuz Gölü), the Central Pontic belts of the NAFZ, and the region south.of the Thrace basin. The estimated deep-subsurface-temperature gradients are found to be varying from 2.28 to 11.10 °C/100m, based on the Curie isotherm of 560 °C, and varying from 2.37 to 11.56 °C/100m, based on the Curie isotherm of 580 °C. The highest values (> 8.33 to 11.10 °C/100m) of the deep-subsurface-temperature gradient are concentrated in the area between Mardin and Şırnak, in the Southeastern region of Turkey. On the other hand, the lowest values of the deep-subsurface-temperature gradient are located in the area of Şebinkarahisar, Reşadiye, Alurca and Gümüşhane, in the eastern Pontides Mountain regions. The highest value of the deep-subsurface-temperature gradient in Western Anatolia is about 8.33 ºC/100m, located in the area around Alaşehir, Baklacı, Akkeçili and Erenköy. These resources may also lie within reach of the current drilling technology and could be exploited to augment the energy budget of the country if the enhanced geothermal systems (EGS) technoloy is given serious attention.

The subsurface gradient distribution of Mıhçakan et al, (2006, Figure 3.4 above) determined from the deep well temperatures gives approximate CPDs, especially for regions with thermal gradients between 0.9 ºC/100 m to 11 ºC/100 m. This observation validates the data source and methodology used in the estimation of the deep subsurface thermal gradient distribution. Moreover, the deep-subsurface-temperature gradient map correlates very well with CPD map of Turkey, published by the MTA (2007, Figure B of Appendix B or Figure 3.1 above).

Subsurface temperatures estimates at 2 km depth using the exponential function produces similar subsurface thermal distribution pattern of the Mıhçakan et al, (2006) subsurface gradient map. At 2 km depth, temperature beneath Turkey varies

from 20 to 265 ºC, whereas that of 5 km depth is between 40 to 455 ºC. The ative extensional region of Western Anatolia has the highest subsurface temperature estimates. The Mardin-Şırnak region has very low temperatures (average value of 58 ºC) at the 2 km depth, but, at the 5 km depth, subsurface temperatures in the area increases to an average value of 193 ºC. At an average depth of 7654 m, the subsurface temperarture in the region is expected to reach 560 ºC. It may be said that the area (Mardin-Şırnak), has low temperatures to depths of about 4000 m but experience a high gradeint change at depths of 5 km and and beyond.

It must however be noted that with more deep well temperature data, very robust gradient estimates could be generated. Especially, for the regions of southeastern Turkey, Eastern part of central Turkey, farthermost north region of the Thrace basin, central part of the Anatolide-Tauride block around the Pamphylian suture (South of Cyprus), and the Istanbul zone and the Intra-Pontides suture regions. It is also very important to note that the southeastern hot spot, located between Mardin and Şırnak, coming out as the area with the highest deep-subsurface-temperature gradient estimates over the West Anatolian extensional province is unexpected. Therefore, a further regional base assessment of the regions' (the West Anatolian extensional province versus the southeastern Mardin-Şırnak area) deep-subsurface-temperature gradient is recommended. Thus, it is in this regard that future updates would be conducted to identify the subsurface hot spots (hot dry rock) of Turkey and accordingly produce very robust and reliable deep subsurface temperature distribution, and surface heat flow maps of Turkey.

REFERENCES

Akın, U. and Çiftçi, Y. (2011). Heat flow of the Kırşehir Massif and geological sources of the radiogenic heat production. Mineral Res. Expl. Bull., 143, 53-73.

Anderson, R. N. and Hobart, M. A. (1976). The relation between heat flow, sediment thickness, and age in the eastern Pacific. *Journal of Geophysical Research*, vol. 81, no.17, 2968-2989.

Angus, D. A., Wilson, D. C., Sandvol, E. and Ni, J. F. (2006). Lithospheric structure of the Arabian and Eurasian collision zone in eastern Turkey from S-wave receiver functions. *Geophysical Journal International*, 166, 1335-1346.

Arni, P. (1939). Tektonische Grundzuge Ostanatoliens und benachbarter Gebiete. *M.T.A. Publ.,* Ankara, série B, no. 4.

Arslan, S., Akin, U. and Alaca, A. (2010). Investigation of crustal structure of Turkey by means of gravity data. *Mineral Res. Expl. Bull*. 140, 55-71.

Artemmieva, I. M. (2011). The lithosphere: An interdisciplinary approach. U.S.A, New York, Cambridge University Press.

Ates, A., Bilim, F. and Buyuksarac, A. (2005). Curie point depth investigation of Central Anatolia, Turkey. *Pure appl. geophys*. 162, 357-371.

Ates, A., Bilim, F., Buyuksarac, A., Aydemir, A., Bektas, O. and Aslan, Y. (2012). Crustal structure of Turkey from aeromagnetic, gravity and deep seismic reflection data. *Sur. Geophys*. 33, 869-885.

Aydın, İ., Karat, H., İ. and Koçak, A. (2005). Curie-point depth map of Turkey. *Goephys. J. Int. 1*62, 633-640.

Barka, A. (1999). The 17 August 1999 Izmit earthquake. *Science*, 285, no. 5435, 1858-1859.

Basel, E. D. K., Serpen, U. and Satman, A. (2009). Assessment of Turkey geothermal resources: Proceeding, *Proceedings, Thirty-Fourth Workshop on Geothermal Reservoir Engineering*, Stanford University, Stanford, California, U.S.A., February 9 – 11.

Basel, E.D. K., Serpen, U., Satman, A. (2010). Turkey's geothermal energy potential: Updated results. *Thirty-Fifth Workshop on Geothermal Reservoir Engineering*, Stanford University, Stanford, California, February 1-3.

Başel, E. D.K., Serpen, U., Satman, A. (2010). Turkey geothermal resource assessment. *World Geothermal Congress, Bali, Indonesia, April* 25-29.

Beardsmore, G. R. and Cull, J. P. (2001). Crustal heat flow: A guide to measurement and modelling. Cambridge University press, United Kingdom.

Bektaş, Ö., Ravat, D., Büyüksaraç, A., Bilim, F. and Ateş, A. (2007). Regional geothermal characterization of East Anatolia from aeromagnetic, heat flow and gravity data. *Pure and Applied Geophysics*, 164, 975-998.

Bekler, T. and Gurbuz, C. (2008). Insight into the Crustal Structure of the eastern Marmara region, NW Turkey. *Pure and Applied Geophysics*, 165, 295-309.

Birch, F., Roy, R. F. and Decker, E. R. (1968). Heat flow and thermal history in New England and New York. In E-an Zen, White W. S., Hadley J. B., Thompson J. B. Jr. (eds.), *Studies of Appalachian Geology: Northern and Maritime*, New York, Wiley Interscience, 437–451.

Blumenthal, M. M. (1946). Die neue geologische Karte der Türkei und einige ihrer stratigraphisch-tektonischen Grundzüge. *Eclogae Geol. Helvetiae*, vol. 39, no. 2, 277 - 289.

Bozkurt, E. (2001). Neotectonics of Turkey - A synthesis. *Geodinamica Acta*, 14, no.1-3, 3-30.

Bozkurt, E. Park, R. G. and Winchester, J. A. (1993). Evidence against the core/cover interpretation of the southern sector of the Menderes Massif. *Tera Nova*, 5, no.5, 445-451.

Bozkurt, E. and Mittwede, S. K. (2001). Introduction to the geology of Turkey – A synthesis. *International Geology Review*, 43, 7, 578-594.

Bozkurt, E. and Oberhänsli, R. (2001). Menderes Massif (western Turkey): Structural, metamorphic, and magmatic evolution - A synthesis**.** *International Journal of Earth Sciences*, 89, no.4, 679-708.

Brune, J. N. (1968). Seismic moment, seismicity, and rate of slip along major fault zones. *Journal of Geophysical Research*, 73, no. 2, 777-784.

Brune, J. N., Henyey, T. L. and Roy, R. F. (1969). Heat flow, stress, and rate of slip along the San Andreas Fault, California. Journal of Geophysical Research, 74, no. 15, 3821-3827.

Candan, O., Dora, O., Çetinkaplan, M., Oberhänsli, R., Partzsch, J. H., Warkus, F. C. and Dürr, S. (2001). Pan-African high-pressure metamorphism in the Precambrian basement of the Menderes Massif, western Anatolia, Turkey. *International Journal of Earth Sciences*, 89, no.4, 793-811.

Chen, F., Siebel, W., Satır, M., Terzioğlu, M. N. and Saka, K. (2000). Geochronogy of the Karadere basement (NW Turkey) and implications for the geological evolution of the Istanbul zone. *International Journal of Earth Sciences (Geol. Rundsch)*, 91, 469-481.

Çakır, Ö. and Erduran, M. (2011). On the P and S receiver functions used for inverting the one-dimensional upper mantle shear-wave velocities. *Surveys in Geophysics*, 32, no. 1, 71-98.

Çağlayan, M. A., İnal, R. N., Şengün, M. and Yurtsever, A. (1984). Structural setting of the Bitlis Massif. Editors Tekeli, O. and Göncüoğlu, M. C., *Geology of the Taurus Belt*, Mineral Research and Exploration Institute of Turkey, Ankara, Turkey, 245-254.

Çiner, A., Deynoux, M., Ricou, S. and Kosun, E. (1996). Cyclicity in the Middle Eocene Çayraz carbonate formation, Haymana basin, central Anatolia, Turkey. *Palaeogeography, Palaeclımatology, Palaeoecology*, 121, no. 3-4, 313-329.

Dam, A. T. and Khrebtov, A. I. (1970). The Menderes Massif geothermal province. In *U. N. Symposium on the Development and Utilization of Geothermal Resources, Geothermics,* Special Issue 2.

Davies, G. F. (1980). Review of oceanic and global heat flow estimates. *Reviews of Geophysics and Space Physics*, 18, no.3, 718-722.

Davies, J. H. and Davies, D. R. (2010). Earth's surface heat flow. *Solid Earth*, 1, 5-24.

Delaloye, M. and Bingöl, E. (2000). Granatoids from western and northwestern Anatolia: Geochemistry and modelling of geodynamic evolution. International Geology Review, 42, no.3, 241-268.

Dean, W. T., Monod, O., Rickards, R. B., Demir, O. and Bultynck, P. (2000). Lower Paleozoic stratigraphy and Paleontology, Karadere-Zirze area, Pontus mountains, northern Turkey. *Geological Magazine*, 137, no.5, 555-582.

DOE. (2008). An evaluation of enhanced geothermal systems technology. U.S. Department of Energy. Energy Efficiency and Renewable Energy.

Dolmaz, M. N., Hisarli, Z. M., Ustaömer, T. and Orbay, N. (2005). Curie point depths based on spectrum analysis of aeromagnetic data, West Anatolian extensional province, Turkey. *Pure appl. geophys*., 162, 571-590.

Drury, M. J. (1989). The heat flow – heat generation relationship: Implications for the nature of continental crust. Editors Çermak, V., Rybach, L. and Decker, E. R., Heat Flow and the Lithosphere Structure, *Tectonophysics*, 164, 93-106.

Dunlop, D. and Özdemir, Ö. (2001). Rock magnetism: Fundamentals and frontiers. Cambridge, U.K, Cambridge Univ. Press.

Erdogan, B. (1990). Stratigraphic features and tectonic evolution of the Izmir-Ankara Zone in the region between Izmir and Seferihisar. *Turkish Association of Petroleum Geologists Bulletin*, 2, 1-20 (in Turkish with English abstract).

Erdoğan, B., Altıner, D., Güngör, T. and Özer, S. (1990). Stratigraphy of the Karaburun Peninsula. *Bulletin of the Mineral Research and Exploration of Turkey,* 111, 1-20.

Egeran, N. (1947). Tectonique de la Turquie et relations entre les unités tectoniques et les gîtes métallifères de la Turquie. Impr. George Thomas, Nancy.

Ercan, T., Satır, M., Kreuzer, H., Türkecan, A., Günay, E., Çevikbaş, A., et al. (1985). Batı Anadolu Senozoik volkanitlerine ait yeni kimyasal, izotopik ve radyometrik verilerin yorumu. *Turk. Jeol. Kurumu Bült*., 28, 121-136.

Erkan, K. (2014). Crustal heat measurement in western Anatolia from borehole equilibrium temperatures. *Solid Earth Discuss*, 6, 403-426.

Flecker, R. M., Robertson, A. H. F., Poisson, A. and Müller, C. (1995). Facies and tectonic significance of two contrasting Miocene basins in south coastal Turkey. *Terra Nova*, 7, no.2, 221-232.

Fourier, J. (1955). The analytical theory of heat. Dover Publications, New York, N. Y, U.S.A.

Frost, B R. and Shive, P. N. (1986). Magnetic mineralogy of the lower continental crust. *Journal of Geophysical Research*, 91, no.B6, 6513-6521.

Gasparini, P., Mantovani, M. S. M., Corrado, G. and Rapolla, A. (1979). Depth of Curie temperature in continental shields: A compositional boundary? *Nature*, 278, 845-846.

Gök, R. Pasyanos, M. E. and Zor, E. (2007). Lithospheric structure of the continent–continent collision zone: Eastern Turkey. *Geophysical Journal International*, 169, 1079-1088.

Göktürkler, G., Salk, M. and Sari, C. (2003). Numerical modelling of conductive heat transfer in Western Anatolia. . *Journal of Balkan Geophysical Society*, 6, no.1, 1-15.

Göncüoğlu, M. C. (2010). Introduction to the geology of Turkey: Geodynamic evolution of the pre-Alpine and Alpine terranes. *MTA Monogr, Ser*, 66, ISBN 978-605-4075-74.

Göncüoğlu, M. C. and Turhan, N. (1984). Geology of the Bitlis metamorphic belt. Editors Tekeli, O. and Göncüoğlu, M. C., *Geology of the Taurus Belt*, Mineral Research and Exploration Institute of Turkey, Ankara, 237-244.

Göncüoglu, M. C. and Erendil, M. (1990). Pre-Late Cretaceous tectonic units of the Armutlu Peninsula. *Proceedings of the 8th Petroleum Congress of Turkey*, 161-168.

Göncüoglu, M. C. Dirik, K. and Kozlu, H. (1997). Pre-Alpine and Alpine terrenes in Turkey: Explanatory notes to the terrane map of Turkey. Annales Géologiques des Pays Helléniques, 37, 515-536.

Göncüoglu, M. C., Turhan, N., Sentürk, K., Özcan, A., Uysal, S. and Yaliniz, M. K. (2000). A geotraverse across northwestern Turkey: Tectonic units of the Central Sakarya region and their tectonic evolution. Editors Bozkurt, E., Winchester, J. A. and Piper, J. D. A., Tectonics and Magmatism in Turkey and the Surrounding Area, Special Publication, Geological Society, London, U.K., 173, 139-161.

Görür, N. and Okay, A. I. (1996). A fore-arc origin for Thrace basin, NW Turkey. Geologisches Rundschau, 85, no. 4, 662-668.

Görür, N., Monod, O., Okay, A. I., Şengör, A. M. C., Tüysüz, O., Yiğitbaş, E., et al. (1997). Paleogeographic and tectonic position of the Carboniferous rocks of the Western Pontides (Turkey) in the frame of the Variscan belt. Bulletin Societe Geologique de France, France, 168, 197-205.

Görür, N., Tüysüz, O. and Şengör, A. M. C (1998). Tectonic evolution of the Central Anatolian basins. *International Geology Review*, 40, no. 9, 831-850.

Gürsu, S. Göncüoğlu, M. C. and Bayhan, H. (2004). Geology and geochemistry of pre-Early Cambrian rocks in Sandikli area: Implications for the Pan-African evolution in NW Gondwanaland, *Gondwana Research*, 7, no.4, 923-935.

Haggerty, S. E. (1978). Mineralogical constraints on Curie isotherms in deep crustal magnetic anomalies. *Geophysical Research Letters*, 5, no.2, 105-108.

Harris, N. B. W., Kelly, S. and Okay, A. I. (1994). Post collisional magmatism and tectonics in northwest Anatolia. Contributions to Mineralogy and Petrology, 117, 241-252.

Hayward, A. B. (1984). Miocene clastic sedimentation related to the emplacement of the Lycian nappes and Antalya complex, SW Turkey. Editors J. E Dixon and A. H. F. Robertson, The Geological Evolution of the Eastern Mediterranean, Special Publication, *Geological Society*, London, U.K., 17, 287-300.

Helvaci, C., Inci, U., Yagmurlu, F. and Yilmaz, H. (1989). Geology and Neogene trona deposits of the Beypazari region, Turkey. *Doga, Turkish Journal of Engineering and Environmental Sciences*, 13, 245-256.

Hisarli, Z. M., Dolmaz, N., Okyar, M., Etiz, A. and Orbay, N. (2012). Investigation into the regional thermal structure of the Thrace region, NW Turkey, from aeromagnetic and borehole data. *Inst. Geophys*. AS CR, Prague. *Stud. Geopys. Geod.*, 56, 269-291.

Ilkışık, O. M. (1995). Regional heat flow in Western Anatolia using silica temeperature estimates from thermal springs. Tectonophysics, 244, 175-184.

İnci, U. (1991). Miocene alluvial fan-alkaline playa lignite-trona bearing deposits from an inverted basin in Anatolia. Sedimentology and tectonic controls on deposition. *Sedimentary Geology*, 71, no. 1-2, 73-97.

Jackson, J. and McKenzie, D. P. (1984). Active tectonics of the Alpine-Himalayan belt between western Turkey and Pakistan. *Goephys. J. R. astr. Soc*. 77, 185-264.

Jackson, J. and McKenzie, D. P. (1988). The relationship between plate motions and seismic moment tensors, and the rates of active deformation in the Mediterranean and Middle East. *Geophysical Journal*, 93, 45-73.

Jaupart, C. and Mareschal, J.-C. (2003). Constraints on crustal heat production from heat flow data. In Rudnick, R. l. (Ed.), Treatise on Geochemistry: *The Crust*, 3, 65-84.

Jaupart, C., Labrosse, S., Mareschal, J.-C. (2007). Temperatures, heat and energy in the mantle of the Earth. *Treatise on Geophysics*, 7, 253-303.

Jaupart, C. and Mareschal, J-C. (2011). Heat generation and transport in the earth. U.S.A, New York, Cambridge University Press.

Karabiyikoğlu, M., Çiner, A., Monod, O., Deynoux, M., Tuzcu, S. and Örçen, S. (2000). Tectonosedimentary evolution of the Miocene Manavgat basin, western Taurides, Turkey. Editors Bozkurt, E., Winchester, J. A. and Piper, J. D. A., Tectonics and Magmatism in Turkey the Surrounding Area, Special Publication, Geological Society, London,U.K., 173, 271-294.

Karabulut, H., Paul, A., Ergün, T. A., Hatzfeld, D. Childs, D. M. and Aktar, M. (2013). Long-wavelength undulations of the seismic Moho beneath the strongly stretched Western Anatolia. *Geophysical Journal International*, *194*, no.1, 450-464.

Kaymakçi, N., White, S. H. and Van Dijk, P. M. (2000). Palaeostress inversions in a multiphase deformed area: Kinematic and structural evolution of the Çankırı basin (central Turkey), Part 1- northern area. Editors Bozkurt, E., Winchester, J. A. and Piper, J. D .A., Tectonics and Magmatism in Turkey and the Surrounding Area, Special Publication, Geological Society, London, U.K., 173, 295-323.

Kennedy, G. C. (1959). The origin of the continents, mountain ranges, and ocean basins. *American Scientist*, 47, no.4, 491-504.

Keskin, M., Pearce, J. A. and Mitchell, J. G. (1998). Volcano-stratigraphy and geochemistry of collision-related volcanism on the Erzurum-Kars plateau, northeastern Turkey. *Journal of Volcanology and Geothermal Research*, 85, 355-404.

Ketin I. (1966). Tectonic units of Anatolia (Asia Minor). *Maden Tekik ve Arama Bulletin*, 66, 23-34.

Kraskowski, S. A. (1961). On the thermal field in old shields. Izvestia Akademic Nauk, SSSR, Ser. Geophys., no.3, 247-250 (EnglishTranslation).

Lachenbruch A. H. (1970). Preliminary geothermal model of the Sierra Nevada. *Journal of Geophysical Research*, no.73, 6977– 6989.

Le Pennec, J. L., Bourdier, J. L., Froger, J. L., Temel, A., Camus, G. and Gourgaud, A. (1994). Neogene ignimbrites of the Nevsehir plateau (Central Turkey) – stratigraphy, distribution and source constraints. *Journal of Volcanology and Geothermal Research*, 63, 59-87.

Lee, W.H.K. and Uyeda, S. (1965). Review of heat flow data. In Lee W. H. K. (ed.), Terrestrial Heat Flow, Monograph 8, Washington DC, *American Geophysical Union*, 87-190.

Maden, N. (2009). Crustal thermal properties of the Central Pontides (Northern Turkey) deduced from spectral analysis of magnetic data. *Turkish Journal of Earth Sciences*, 18, 383-392.

Maden, N. (2010). Curie-point from spectral analysis of magnetic data in Erciyes stratovolcano (Central Turkey). *Pure and Applied Geophysics*, 167, 349-358.

Malamud, B. D. and Turcotte, D. L. (1999). How many plumes are there? *Earth and Planetary Science Letters*, 174, 113-124.

Mayhew, M. A. (1982). Application of satellite magnetic anomaly data to Curie isotherm mapping. Journal of Geophysical Research, 87, no.B6, 4846-4854.

McClusky, S. Balassanian, S., Barka, A., Demir, C., Ergintav, S., Georgiev, I., et al. (2000). Global positioning system constraints on plate kinematics and dynamics in the eastern Mediterranean and Caucasus. *Journal of Geophysical Research*, 105, no.B3, 5695-5719.

McKenzie, D. P. (1970). Plate tectonics of the Mediterranean region. *Nature*, 226 no.5242, 239-243.

McKenzie, D. P. (1972). Active tectonics of the Mediterranean region. *Geophys. J. R. astr. Soc*. 30, 109-185.

Mihcakan, M., Onur, M., Ercelebi, S. G., Okay, A. and Yilmazer, M. (2006). Map of subsurface temperature gradient distribution of Turkey using deep well temperatures and variogram analysis. TUBİTAK, Report No: YDABCAG-100Y040, November.

Mertoglu, O., Simsek, S., Dagistan, H., Bakir, N. and Dogu, N. (2010). Geothermal contry update report of Turkey (2005-2010). *Proceedings, World Geothermal Congress* 2010, Bali, Indonesia, 25-29 April.

Moix, P., Beccaleto, L., Kozur, H. W., Hochard, C., Rosselet, F. and Stampfli, G. M. (2008). A new classification of the Turkish terranes and sutures and its implication for the paleotectonic history of the region. *Tectonophysics*, 451, 7-39.

MTA. (2007). Curie-point depth map of Turkey.

Necioğlu, A., Maddison, B. and Türkelli, N. (1981). A study of crustal and upper mantle structure of northwestern Turkey. *Geophysical Research Letters*, 8, no.1, 33-35.

Ocakoğlu, F. (2001). Repetitive subtidal-to-coastal Sabkha cycles from a Lower-Middle Miocene marine sequence, eastern Sivas basin. Turkish *Journal of Earth Sciences*, 10, no.1, 17-34.

Okay, A. I. (1984). Distribution and characteristics of the northwest Turkish blueschists. Editors Dixon, J. E. and Robertson, A. H. F., The Geological Evolution of the Eastern Mediterranean, Special Publication, Geological Society, London, U.K., 17, 455-466.

Okay, A. I. (1989). An exotic eclogitic/blueschist slice in a Barrovian-style metamorphic terrain, Alanya nappes, southern Turkey. *Journal of Petrology*, 30, 107-132.

Okay, A. I. (1996). Granulite facies gneisses from the Pulur region, Eastern Pontides. *Turkish Journal of Earth Sciences*, 5, 55-61.

Okay, A. I. (1986). High-pressure/low temperature metamorphic rocks of Turkey. Editors Evans, B. W. and Brown, E. H., *Blueschists and Eclogites, Geological Society of America Memoir*, no.164, 333-347.

Okay A. I. (2008). Geology of Turkey: A synopsis. Anschnitt, 21, 19-42.

Okay, A. I. and Özgül, N. (1984). HP/LT metamorphism and the structure of the Alanya Massif, southern Turkey: An allochthonous composite tectonic

sheet. Editors Dixon, J. E. and Robertson, A. H. F. (Eds.), The Geological Evolution of the Eastern Mediterranean, Special Publication, Geological Society, London, U.K., 17, 429-439.

Okay, A. I. and Leven, E. J. (1996). Stratigraphy and paleontology of the Upper Paleozoic sequences in the Pulur (Bayburt) region, eastern Pontides. *Turkish Journal of Earth Sciences*, 5, 145-155.

Okay, A. I., Satir, M., Maluski, H., Siyako, M., Monie, P., Metzger, R. and Akyüz, S. (1996). Paleo- and Neo-Tethyan events in northwest Turkey: Geological and geochronological constraints. In Yin, A. and Harrison, M. (Eds.), *Tectonics of Asia*, Cambridge University Press, 420-441.

Okay, A. I., Harris, N. B. W. and Kelley, S. P. (1998). Exhumation of blueschists along a Tethyan suture in northwest Turkey. *Tectonophysics*, 285, 275-299.

Okay, A. I. and Tüysüz, O. (1999). Tethyan sutures of northern Turkey. Editors Durand, B., Jolivet, L., Horvath, D. and Serrene, M., The Mediterranean Basins: Tertiary extensions within the Alpine orogeny, Special Publications, Geological Society, London, U.K., 156, 475-515.

Okay, A. I., and Satir, M. (2000a). Upper Cretaceous eclogite facies metamorphic rocks from the Biga Peninsula, northwest Turkey. *Turkish Journal of Earth Sciences*, 9, 47-56.

Okay, A. I. and Satir, M. (2000b). Coeval plutonism and metamorphism in a latest Oligocene metamorphic core complex in northwest Turkey. *Geological Magazine*, 137, 495-516.

Okay, A. I., Harris, N. B. W. and Kelley, S. P. (1998). Blueschist exhumation along a Tethyan suture in northwest Turkey. *Tectonophysics*, 285, 275-299.

Okay, A. I., Satir, M., Tüysüz, O., Akyüz, S. and Chen, F. (2001). The tectonics of the Strandja Massif: Variscan and mid-Mesozoic deformation and metamorphism in the northern Aegean. *International Journal of Earth Siences* (Geolgische Rundschau), 90, 217-233**.**

Okay, A. I., Monod, O. and Monié, P. (2002). Triassic blueschists and eclogites from northwest Turkey: Vestiges of the Paleo-Tethyan subduction. *Lithos*., 64, 155-178.

Okay, A. I., Satir, M. and Siebel, W. (2006). Pre-Alpine orogenic events in the eastern Mediterranean region (European Lithosphere Dynamics). Geological Society, London, U.K., Memoirs, 32, 389-405.

Okubo, Y., Graf, R. J., Hansen, R. O., Ogawa, K. and Tsu, H. (1985). Curie point depths of the island of Kyushu and surrounding areas, Japan. *Geophysics*, 50, 481–494.

Özgül, N. (1984). Stratigraphy and tectonic evolution of the Central Taurides. Editors Tekeli, O. and Göncüoğlu, M. C., Geology of the Taurus Belt, *Mineral Research and Exploration Institute of Turkey*, Ankara, 77-90.

Özcan, A., Göncüoglu, M. C., Turan, N., Uysal, S., Sentürk, K. and Isik, A. (1988). Late Palaeozoic evolution of the Kütahya-Bolkardag belt. *METU Journal of Pure and Applied Science*, 21, 211-220.

Parlaktuna, M., Mertoglu, O., Simsek, S., Paksoy, H. and Basarir, N. (2013). Geothermal country update report of Turkey (2010-2013), *European Geothermal Congress 2013*, Pisa, Italy, June 3-7.

Pasquaré, G., Poli, S., Vezzolli, L. and Zanchi, A. (1988). Continental arc volcanism and tectonic volcanism in Central Anatolia, Turkey. Tectonophysics, 146, 217-230.

Pasquale, V., **Verdoya, M. and Chozzi, P**. (2014). Geothermics: Heat flow in the lithosphere. Springer Briefs in Earth Science.

Pfister, M., Rybach, L. and Simsek, S. (1998). Geothermal reconnaissance of the Marmara Sea region (NW Turkey): Surface heat flow density in an area of active continental extension. *Tectonophysics*, 291, 77-89.

Pollack, H.N. (1982). The heat flow from the continents. Ann. Rev. *Earth Planet Sci*., 10:459-81.

Pollack, H. N. and Chapman, D. S. (1977a). On the regional variation of heat flow, geotherms, and lithospheric thickness. *Tectonophysics*, 38, 279-296.

Pollack, H. N. and Chapman, D. S. (1977b). Mantle heat flow. *Earth and Planetary Science Letters*, 34, 174-184.

Pollack, H. N., Hurter, S. J. and Johnson, J. R. (1993). Heat flow from the Earth's inerior: Analysis of the global data set. *Reviews of Geophysics*, 31(3), 267-280.

Polyak, B. G. and Smirnov, Ya. B. (1968). Relationship between terrestrial heat flow and the tectonics of continents. *Geotectonics*, 4, 205-213.

Robertson, A. H. F. (2000). Mesozoic-Tertiary tectono-sedimentary evolution of a south Tethyan oceanic basin and its margin in southern Turkey. In Bozkurt, E., Winchester, J. A. and Piper, J. D. A. (Eds.), Tectonics and Magmatism in Turkey and the surrounding area. *Geological Society, London, Special Publication*, 173, 97-138.

Robertson, A. H. F., Clift, P. D., Degnan, P. and Jones, G. (1991). Palaeogeographic and paleotectonic evolution of eastern Mediterranean region. *Palaeogeography, Palaeoclimatology, Palaeoecology*, 87, 289-344.

Ross, H. E., Blakely, R. J. and Zoback, M. D. (2006). Testing the use of aeromagnetic data for the determination of Curie depth in California. *Geophysics*, 71, no.5, L51−L59.

Roy, R. F., Blackwell, D. D. and Birch, F. (1968). Heat generation of plutonics rocks and continental heat flow provinces. *Earth and Planetary Science Letters*, 5, 1-12.

Royer, J .J. and Danis, M. (1988). Steady state geothermal model of the crust and the problem of the boundary conditions: Application to a rift system, the southern Rhine graben. *Tectonophysics*, 156, 239-255.

Saunders, P., Priestley, K., Taymaz, T. (1998). Variations in the crustal structure beneath western Turkey. *Geophysical Journal International*, 134, 373-389.

Schats, J. F. **and Simmons, G.** (1972). Thermal conductivity of the Earth materials at high temperatures. *Journal of Geophysical Research*, 77, no.35, 6966-6983.

Schumacher, R. and Mues-Schmacher, U. (1996). The Kizilkaya ignimbrite – an unusual low-aspect-ratio ignimbrite from Cappadocia, Central Turkey. *Journal of Volcanology and Geothermal Research*, 70, 107-121.

Sherlock, S. C., Kelley, S. P., Inger, S., Harris, N. and Okay, A. I. (1999). ^{40}Ar-^{39}Ar and Rb-Sr geochronology of high pressure metamorphism and exhumation history of the Tavsanli zone, NW Turkey. Contributions to Mineralogy and Petrology, 137, 46-58.

Sclater, J. G. and Francheteau, J. (1970). The implications of terrestrial heat flow observations on current tectonic and geochemical models of the crust and upper mantle of the Earth. Geophys. J. astr. Soc., 20, 509-542.

Sclater, J. G., Jaupart, C. and Galson, D. (1980). The heat flow through oceanic and continental crust and the heat loss of the Earth. Review of Geophysics and Space Physics, 18, no.1, 269-311.

Schilinger, C. M. (1985). Magnetism of lower crust and interpretation of regional anomalies: Examples from Lofoten and Vesteralen, Norway. Journal of Geophysical Research, 90, no.B13, 11,484-11,504.

Schön, J. H. (1998). Physical properties of rocks: Fundamentals and principles of petrophysics (Handbook of Geophysical Exploration: Seismic Exploration), 18, Pergamon Press.

Smith, P.J. (1973). Topics in Geophysics. The MIT Press, Cambridge, Massachusetts.

Spector, A. and Grant, F. S. (1970). Statistical models for interpreting aeromagnetic data. *Geophysics*, 35, 293–302.

Sunal, G., Natal'in, Satır, M. and Toraman, G. (2006). Paleozoic magmatic events in the Strandja Massif, NW Turkey. Geodinamica Acta, 19, no.5, 283-300.

Stein, C. A. and Stein, S. (1994). Constraints on hydrothermal heat flux through the oceanic lithosphere from global heat flow. Journal of Geophysical Research, 99, no.B2, 3081-3095.

Stein, C. A. (1995). Heat flow of the Earth. In Ahrens, T. J (Ed.), Global Physics: A Hand Book of Physical Constants, AGU Reference shelf 1, *American Geophysical Union*, 144-158.

Şalk, M., Pamukçu, O. and Kaftan, I. (2005). Determination of the Curie point depth and heat flow from Magsat data of Western Anatolia. *Journal of Balkan Geophysical Society*, 8, no.4, 149-160.

Şengör, A. M. C. and Yilmaz, Y. (1981). Tethyan evolution of Turkey: A plate tectonic approach. *Tectonophysics*, 75, 181-241.

Şengör, A. M. C., Satir, M. and Akkök, R.: (1984). Timing of tectonic events in the Menderes Massif, western Turkey: Implications for tectonic evolution and evidence for Pan-African basement in Turkey. *Tectonics*, 3, 693-707.

Şengör, A. M. C., Görür, N. and Saroğlu, F. (1985). Strike-slip faulting and related basin formation in zones of tectonic escape: Turkey as a case study. In Biddle, K. T. and Christie-Blick, N. (Eds.), Strike-Slip Deformation, Basin Formation, and Sedimentation (SP37), *Society of Economic Paleontologists and Mineralogists, Special Publication*, 37, 227-264.

Tanaka, A., Okuba, Y. and Matsubayashi, O. (1999). Curie point depth based on spectrum analysis of the magnetic anomaly data in East and Southeast Asia. *Tectonophysics*, 306, 461-470.

Tankut, A., Wilson, M. and Yihunie, T. (1998). Geochemistry and tectonic setting of Tertiary volcanism in the Güven area, Anatolia, Tuerkey. *Journal of Volcanology and Geothermal Research*, 85, 285-301.

Tchalenko, J. S. (1977). A reconnaissance of the seismicity and tectonics at the northern border of the Arabian plate (Lake Van region). *Revue de Géographie Physique et de Géologie Dynamique*, 19, 189-208.

Temel, A., Gündoğdu, N., Gourgaud, A. and Le Pennec, J.-L. (1998). Ignimbrites of Cappadocia (Central Anatolia, Turkey): Petrology and Geochemistry. Journal of Volcanology and Geothermal Research, 85, 447-472.

Tezcan, A. K. (1979). Geothermal studies, their present status and contribution to heat flow contouring in Turkey. Editors Cermak, V. and Rybach, L., *Terrestrial Heat Flow in Europe*, Springer-Verlag, Berlin, 283–292.

Tezcan, A. K. (1995). Geothermal explorations and heat flow in Turkey. Editors Gupta, M. L. and Yamano, M., *Terrestrial Heat Flow and Geothermal Energy in Asia*. Oxford and IBH Publishing Co. Pvt. Ltd., New Delhi, India, 23−42.

Tezel, T., Erduran, M. and Alptekin, O. (2007). Crustal shear wave velocity structure of Turkey by surface wave analysis. *Annals of Geophysics*, 50, no.2, 177-190.

Tezel, T., Shibutani, T. and Kaypak, B. (2010). Crustal structure variation in Western Turkey inferred from the receiver function analysis. *Tectonophysics*, 492, 240-252.

Tezel, T., Shibutani, T. and Kaypak, B. (2013). Crustal thickness of Turkey determined by receiver function. *Journal of Asian Earth Sciences*, 75, 36-45.

Topal, T. and Sözmen, B. (2001). Characteristics of the weathering zones developed within the tuffs of Midas monument. *Turkish Journal of Earth Sciences*, 10, 83-91.

Topuz, G., Altherr, R., Kalt, A., Satır, M., Werner, O. and Schwartz, W. H. (2004). Aluminous granulites from the Pulur Complex, NE Turkey: A case of partial melting, efficient melt extraction and crystallisation. *Lithos*, vol. 72, no.3-4, 183-207.

Topuz, G., Altherr, R., Schwarz, W. H., Dokuz, A. and Mayer, H.-P. (2007). Variscan amphiobolites-facies rocks from the Kurtoğlu metamorphic complex (Gümüşhane area, Eastern Pontides, Turkey). International Journal of Earth Sciences, 96, 861-873.

Tureyen, Ö. İ., Satman, A. (2013). Multiple licence holders in the same area: An expected risk to geothermal development in Turkey. Thirty-Eight Workshop on Geothermal Reservoir Engineering, Stanford University, Stanford, California, February 11-13.

UNESCO. (2003). Geothermal energy: Utilization and technology. Editors Dickson, M. H., and Fanelli, M., *Renewable Energy Series*.

Url-1 <http://dds.cr.usgs.gov/srtm/version1/Eurasia/> data retrieved 23.10.2014.

Ustaömer, P. A. and Rogers, G. (1999). The Bolu Massif: Remnant of a pre-Early Ordovician active margin in the west Pontides, northern Turkey. *Geological Magazine*, 136, no.5, 579-592.

Ustaömer, P. A., Mundil, R. and Renne, P. R. (2005). U/Pb and Pb/Pb zircon ages for arc related intrusions of the Bolu Massif (W Pontides, NW Turkey): Evidence for Late Precambrian (Cadomian) age. *Terra Nova*, 17, 215-223.

Vitorello, I. and Pollack, H. N. (1980). On the variation of continental heat flow with age and the thermal evolution of continents. *Journal of Geophysical Research*, 85, no. B2, 983-995.

Wasilewski, P. and Fountain, D. M. (1982). The Ivrea zone as a model for the distribution of magnetism in the continental crust. *Geophysical Research Letters*, 9, no.4, 333-336.

Wasilewski, P. and Mayhew, M. A. (1982). Crustal xenolith magnetic properties and long wavelength anomaly source requirements. *Geophysical Research Letters*, vol. 9, no.4, 3 29-332.

Wessel, P. and Smith, W. H. F. (2013). GMT (Generic Mapping Tools) software, version 4.5.9. School of Ocean and Earth Science and Tech., University of Hawai'i at Mānoa.

Williams, G. D., Ünlügenç, U. C., Kelling, G. and Demirkol, C. (1995). Tectonic controls on stratigraphic evolution of the Adana basin, Turkey. *Journal of the Geological Society of London*, 152, 873-882.

Williams, M. C., Shive, P. N., Fountain, D. M. and Frost, B. R. (1985). Magnetic properties of exposed deep crustal rocks from the Superior Province of Manitoba. *Earth and Planetary Science Letters*, 76, 176-184.

Williams, D. L. and Von Herzen, R. P. (1974). Heat loss from the Earth: New estimate. Geology, 2, no.7, 327-328.

Wilson, M., Tankut, A. and Güleç, N. (1997). Tertiary volcanism of the Galatia province, north-west Central Anatolia, Turkey. *Lithos*. 42, 105-121.

Yemen, H. (1999). Heat-flow Distribution of Aegean Region of Turkey. M.Sc. Thesis, Suleyman Demirel University Science Institute, Isparta, Turkey (in Turkish).

Yetiş, C., Kelling, G., Gökçen, S. L. and Baroz, F. (1995). A revised stratigraphic framework for later Cenozoic sequence in the northeast Mediterranean region. *Geologisches Rundschau*, 84, no.4, 794-812.

Yiğitbaş, E., Elmas, A. and Yilmaz, Y. (1999). Pre-Cenozoic tectono-stratigraphic components of the western Pontides and their geological evolution. *Geological Journal*, 34, 55-74.

Yiğitbaş, E., Kerrick, R. Yılmaz, Y., Elmas, A. and Xie, O. L. (2004). Characteristics and geochemistry of Precambrian ophiolites and related volcanics from the Istanbuil-Zonguldak unit, northernwestern Anatolia, Turkey: Following the missing chain of the Precambrian south European suture zone to the east. *Precambrian Research*, 132, 179-206.

Zhoa, C., Hobbs, B. E. and Ord, A. (2008). Convective and advective heat transfer in geological systems. Springer-Verlag Berlin Heidelberg.

Zhu, L., Mitchell, B.J., Akyol, N., Cemen, I. and Kekovali, K. (2006). Crustal thickness variations in the Aegean region and implications for the extension of continental crust. *Journal of Geophysical Research*, 111, B01301.

Zor, E., Özalaybey, S. and Gürbüz, C. (2006). The crustal structure of the Eastern Marmara Region (Turkey) by teleseismic receiver functions. *Geophysical Journal International*, 167, 213-222.

Zor, E., Sandvol, E., Gurbuz, C., Turkelli, N., Seber, D., Barazangi, M. (2003). The crustal structure of the east Anatolian plateau (Turkey) from receiver functions. *Geophysical Research Letters*, 30, no. 24, 8044. TUR 7-1 – TUR 7-4.

APPENDICES

APPENDIX A: The maps for the tectonic regions, major sutures, and continental blocks, in addition to the different basement types and accretionary complexes in Turkey.

APPENDIX B: Curie-point depth map of Turkey (MTA, 2007).

APPENDIX A

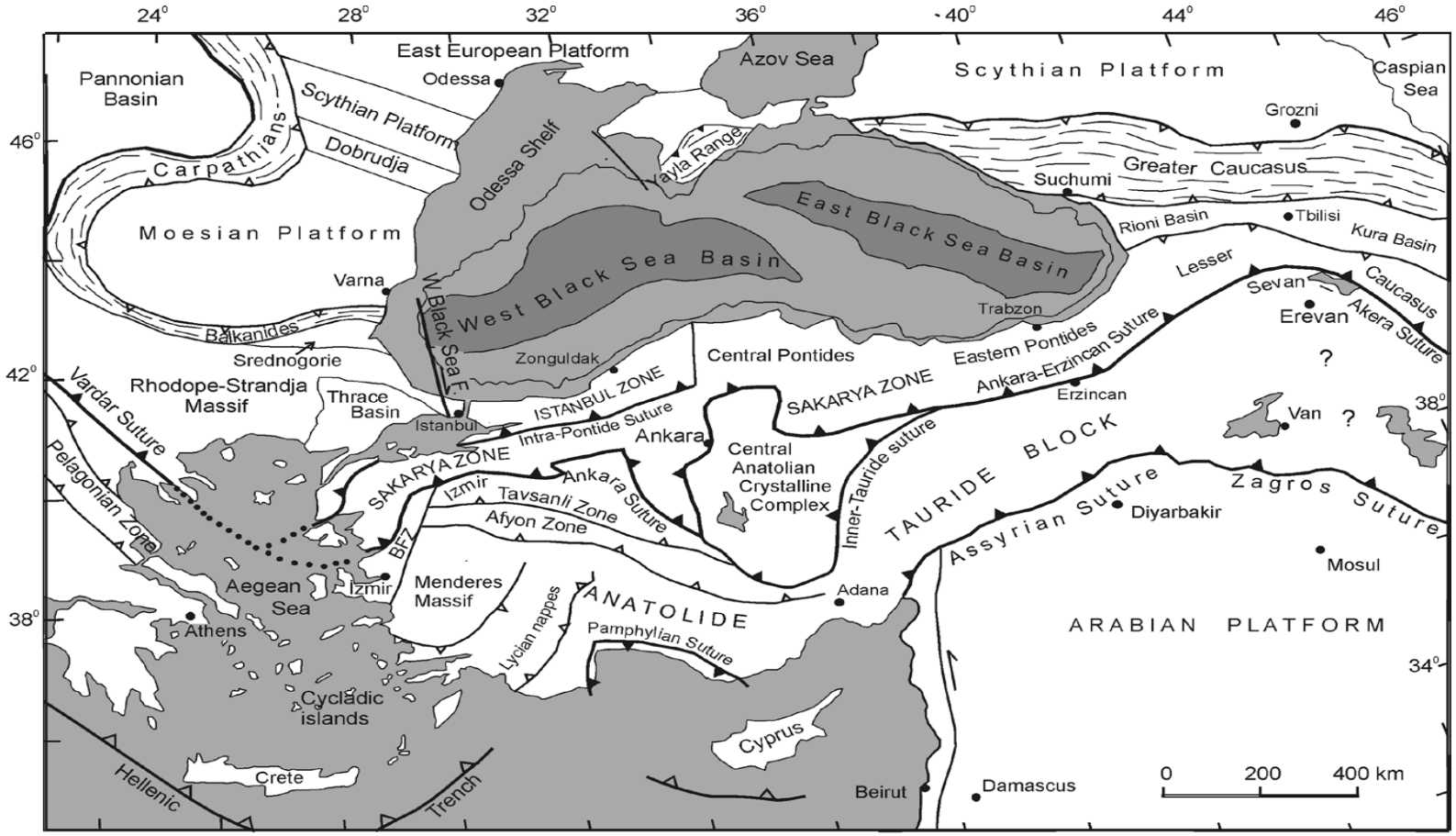

Figure A. 1: Tectonic map of North-eastern Mediterranean region showing the major sutures and continental blocks (Okay, 2008). Solid triangles on heavy lines indicate the polarity of former subduction zones; hollow triangles on heavy lines represent active subduction zones; the darker grey shaded area is the Late Cretaceous oceanic crust in the Black Sea; and small-size hollow triangles on lighter lines indicate the vergence of the major fold and thrust belts. BFZ in Western Anatolia denotes the Bornova Flysch Zone.

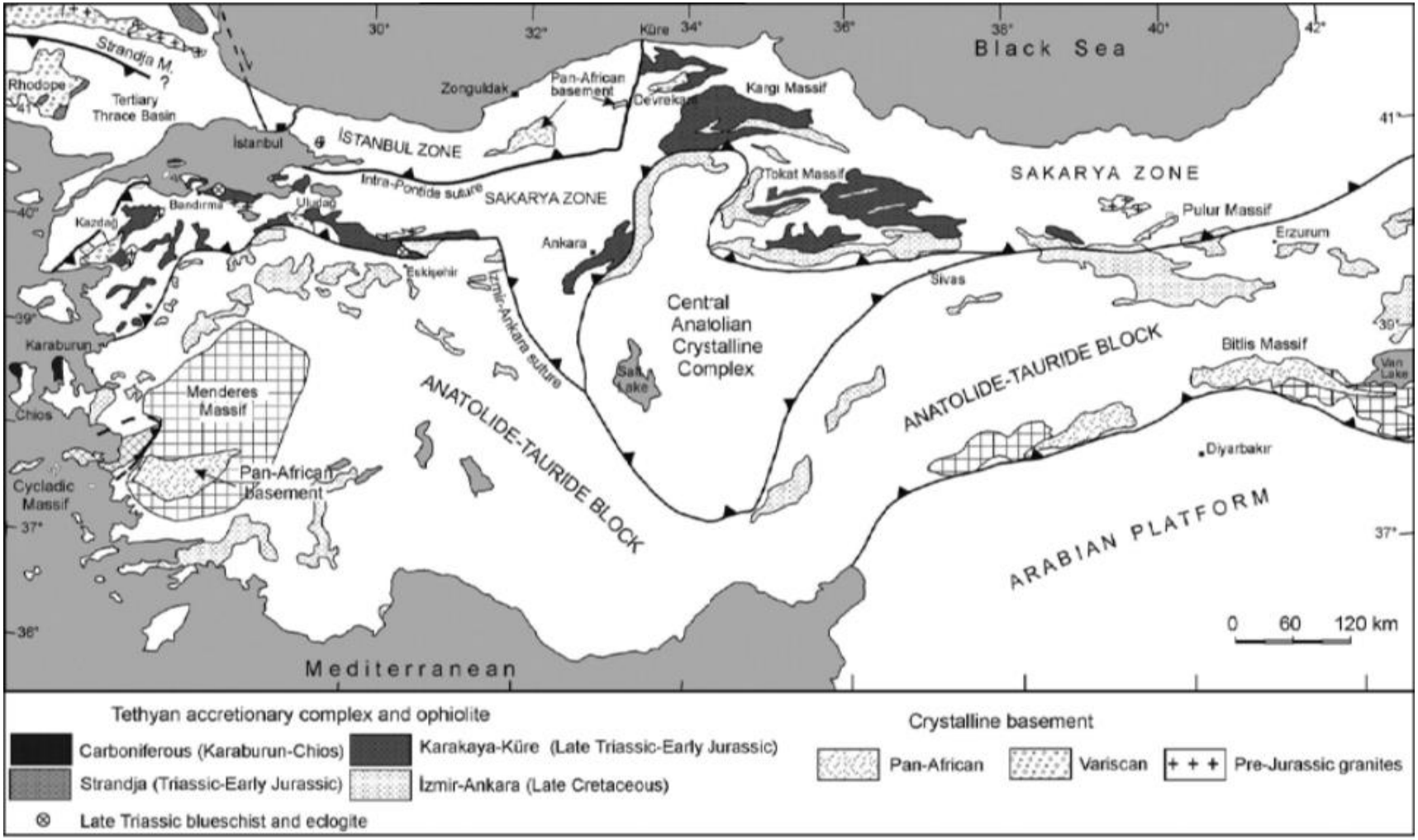

Figure A. 2: Distribution of different basement types and accretionary complexes in Turkey (Okay, 2008).

APPENDIX B

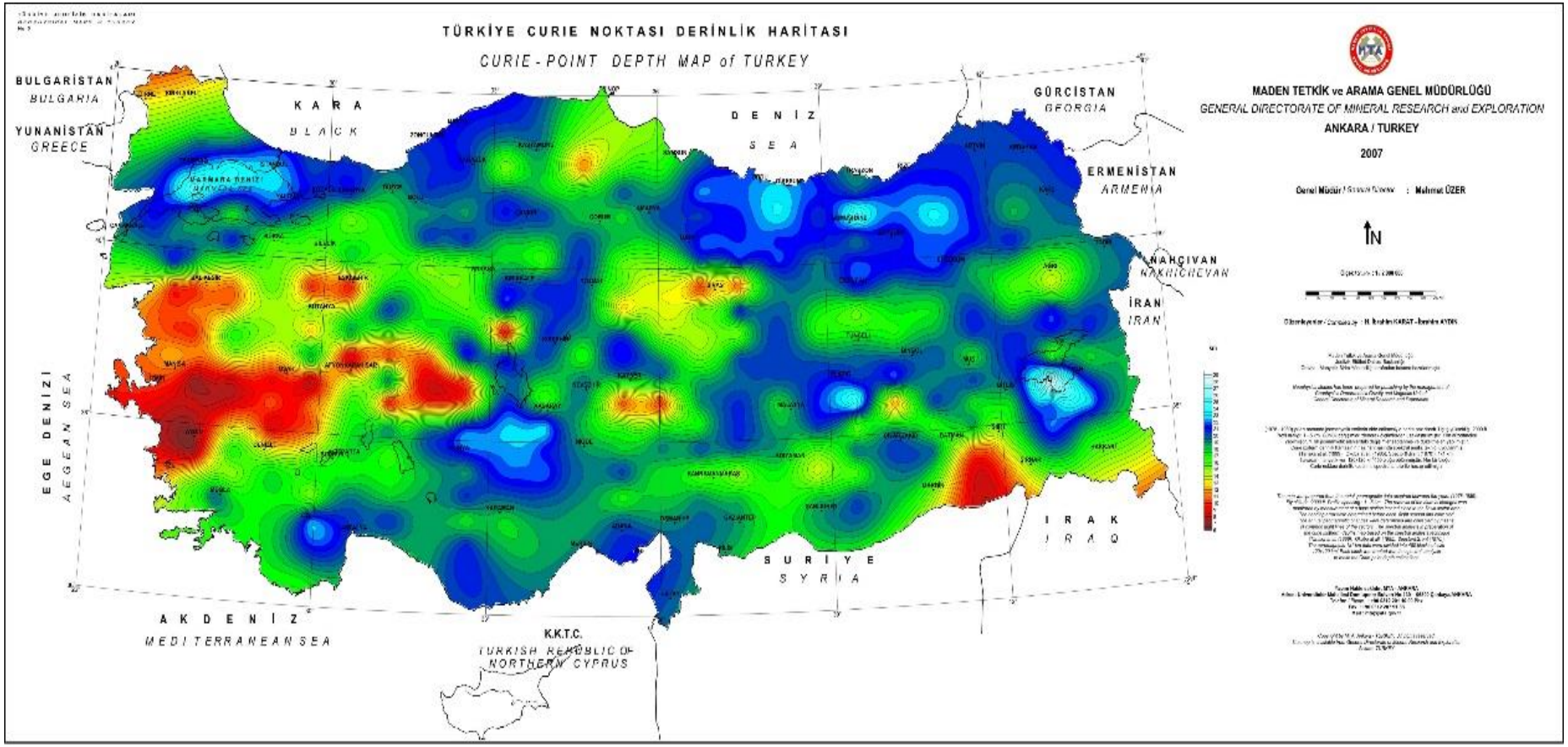

Figure B: Curie-point depth map of Turkey (MTA, 2007).

CURRICULUM VITAE

Name Surname: Daniel Nlimah NJOLNBI

Place and Date of Birth: Saboba (Ghana), 17th December 1985

Address: C/o E. P. Church, P. O. Box 10, Ghana, Saboba N/R, Ghana.

E-Mail: aliki_09@yahoo.com

B.Sc.: Land Economy

Professional Experience and Rewards:

Ghana Government Scholarship 2010 – 2015.

Turkish Government Scholarship 2010 – 2015